EXPERIMENTAL INVESTIGATION OF THE INTERACTION OF A DETONATION WAVE WITH A BOUNDARY GAS

Thesis for the Degree of Ph. D.
MICHIGAN STATE UNIVERSITY
TIM GARDINER ADAMS
1972

This is to certify that the

thesis entitled

Experimental Investigation of the Interaction of a Detonation with a Boundary Gas

presented by

Tim G. Adams

has been accepted towards fulfillment
of the requirements for

PH.D. degree in Mechanical Engineering

MC Smith

Major professor

Date July 24, 1972

O-7639

ABSTRACT

EXPERIMENTAL INVESTIGATION OF THE INTERACTION
OF A DETONATION WAVE WITH A BOUNDARY GAS

by

Tim Gardiner Adams

An experimental study has been conducted to determine the influence of a low density boundary gas on the propagation velocity of a gaseous detonation wave. The interaction of a detonation wave with a boundary gas results in a lateral shock wave moving into the boundary. The theoretical analysis has shown that this shock may be a weak oblique shock or it may develop as a detached shock in certain explosive-boundary combinations. Previous experimenters found that when an explosive-boundary combination was used that produced a detached shock, the velocity of the detonation wave was about 50% of the Chapman-Jouget value. This low velocity "detonation wave" gave rise to speculation that a weak detonation wave might exist. This study was performed using explosive-boundary combinations that did not have an oblique shock solution so that a sub-Chapman-Jouget wave would result.

The study of a detonation wave travelling through a mixture composed of 30% CH_4 - 70% O_2 with a helium boundary was made. A shock wave was formed in the boundary gas that ran out ahead of the detonation wave and resulted in an oblique shock forming in the explosive mixture. Quenching of the detonation wave occurred and the complex series of shock waves formed were found to decay to an acoustic pulse travelling at the sound speed of the boundary gas.

The propagation of a detonation wave in a H_2 - O_2 mixture with either a hydrogen or helium boundary resulted in a decrease of the wave velocity by about 17% within the limits of the test section. This was interpreted as being indicative of the onset of quenching. The addition of some air to the hydrogen-oxygen mixture in the test section resulted in positive quenching of the detonation wave. Again, the complex series of shock waves formed were found to decay to an acoustic pulse moving at the sound speed commensurate with the higher sound speed gas.

In all of the experimental work, the explosive mixture was separated from the boundary gas by a very thin (< 900Å) nitrocellulose film to minimize diffusion. Although some diffusion was noted, it was small and did not influence the results.

No evidence was found in this research to support suppositions relative to the existence of a weak detonation wave.

EXPERIMENTAL INVESTIGATION OF THE INTERACTION OF A DETONATION WAVE WITH A BOUNDARY GAS

by

Tim Gardiner Adams

A THESIS

Submitted to
Michigan State University
in partial fulfillment of the requirements
for the degree of

DOCTOR OF PHILOSOPHY

Department of Mechanical Engineering

1972

ACKNOWLEDGMENTS

It has been the author's privilege to have had the following gentlemen serve on his doctoral committee:

Professor Mahlon C. Smith, Chairman

Professor Martin C. Hawley

Professor Joachim E. Lay

Professor Edward A. Nordhaus

The author is particularly indebted to Wayne H. Buell, President, and Mordica M. Ryan, Dean of Academic Affairs, (retired), of Lawrence Institute of Technology, for providing the facilities and the equipment needed to carry out this research. Appreciation is also extended to these gentlemen as well as to Professors Hans G. Erneman and Henry W. Nace for their letters of recommendation which helped me to obtain a National Science Foundation Science Faculty Fellowship under which this research was begun.

Special recognition is due my children Michelle, Jennifer, Gardiner, and Douglas for their tolerance of the demands a doctoral program places on a father's time and disposition. And to my wife, Leah, where words are truly inadequate to express my appreciation for her continual encouragement and understanding.

TABLE OF CONTENTS

LIST OF TABLES

LIST OF FIGURES

NOMENCLATURE

A	area
$\mathring{A}$	angstrom units 10^{-8}cm
A_f	area covered by film
a	speed of sound
C_p	specific heat at constant pressure
C-J	Chapman-Jouget condition
e	internal energy per unit mass
F	function defined in Equation (2.34)
f	function defined in Equation (2.35)
f	function defined in Equation (2.56)
h	enthalpy per unit mass
M	Mach number
m	molecular weight
m_v	mass of nitrocellulose per unit volume
n	number of drops
n_v	number of drops per unit volume
P	pressure
q	specific heat release
$\overline{R}$	Universal gas constant
s	specific entropy
T	temperature
t	time
t_f	thickness of film
u	velocity
V_c	volumetric concentration of collodion in amyl acetate
V_e	flow velocity of explosive mixture
V_i	interface or contact surface velocity

v	specific volume
w	piston velocity
$\overline{X}$	reaction length
Y	distance into test section
β	shock angle
β_{max}	shock detachment angle
γ	ratio of specific heats
ϵ	coefficient defined in Equation (2.39)
θ	interface angle
ν	Prandtl-Meyer function
ξ	fractional area increase defined by Equation (2.36)
ρ	density
ρ_f	density of nitrocellulose

Subscripts

1	condition ahead of wave
2	condition behind wave
3	condition behind wave after expansion
e	explosive
i	boundary
max	maximum
t	stagnation conditons

CHAPTER I

INTRODUCTION

The phenomenon known as combustion commences with the occurrence of a self-supporting exothermic reaction which may proceed as either a deflagration or a detonation wave. Deflagration is a process which is governed by diffusion, thermal action and molecular transport and the resulting flame velocity is relatively slow, e.g., 0.3 to 30 ft/sec. A detonation wave is a supersonic process which displays a flame front velocity several orders of magnitude greater, e.g., 6,000 to 12,000 ft/sec. The transport processes governing the propagation of a simple flame are insufficiently rapid to cause the detonation process and reaction in this case is caused by a supersonic pressure wave. This shock wave serves to heat the gas and initiate the chemical reaction, which in turn provides the driving force for the shock. If the energy release provided by the exothermic chemical reaction is not maintained, the shock is normally accompanied by an expansion wave which results in the decay of the pressure wave until it returns to the ambient state.

1.1 Summary of Gaseous Detonation Research

The number of studies and consequently the level of understanding of gaseous detonation waves have increased rapidly since the initial identification of their supersonic nature by Berthelot and Vielle (1) and independently by Mallard and LeChatelier (2). Shortly thereafter, Chapman (3) and Jouget (4) formulated the hydrodynamic theory to explain most of the experimentally observed characteristics of gaseous detonation waves. The hydrodynamic approach was responsible for identifying a detonation wave as a shock wave followed closely by an extremely rapid exothermic chemical reaction. This identification seems to have been a stimulus for many investigators as the results of many studies began to appear. Most of the early work, both analytical and experimental is summarized in books by Jost and Croft (5), and Lewis and von Elbe (6). Also, excellent bibliographies of research during the 1950's and the early 1960's are contained in the reviews of Morrison, et al (7), Evans and Ablow (8), and Oppenheim, et al (9), and have been summarized in the recent book by Strehlow (10).

In the study of deflagration, experimentalists have had the decided advantage of stabilized flames created by the use of Bunsen flames, flat low pressure flames, diffusion flames and flameholder anchored flames. The experimentalist in detonation has been handicapped by the necessity of trying to make measurements on very thin reaction zones propagating at

Mach numbers upwards to about M = 10 for some explosives such as ether-oxygen mixtures.

These experiments always resulted in a seemingly stable detonation wave corresponding to the Chapman-Jouget state. Since the detonation always appeared in this stable state it seemed that there might be many advantages from the generation of a stationary detonation wave. If this were accomplished, then many more measurements might be made such as pressure, temperature, ionization, and composition. It was also conceivable that detonation waves might be generated which were different from the Chapman-Jouget type. Several experimenters were successful in producing a standing detonation wave. It was concluded: "strong as well as C-J detonations can be stabilized in an open jet facility, provided the proper levels of stagnation pressure are maintained commensurate with the mixture ratio employed." (11)

About the same time, Voitsekhovskii (12, 13) reported that a detonation wave had been maintained in an annulus with the front moving in the tangential direction. The detonation was maintained for a duration of 1 to1.5 seconds by exhausting gas through one side and replenishing the annulus with the explosive gas from the other side. The relative positions of the maintained detonation fronts are shown in Figure 1. Of particular interest was the report of a steady detonation velocity that propagated at half the C-J velocity in this annular channel with side relief. This

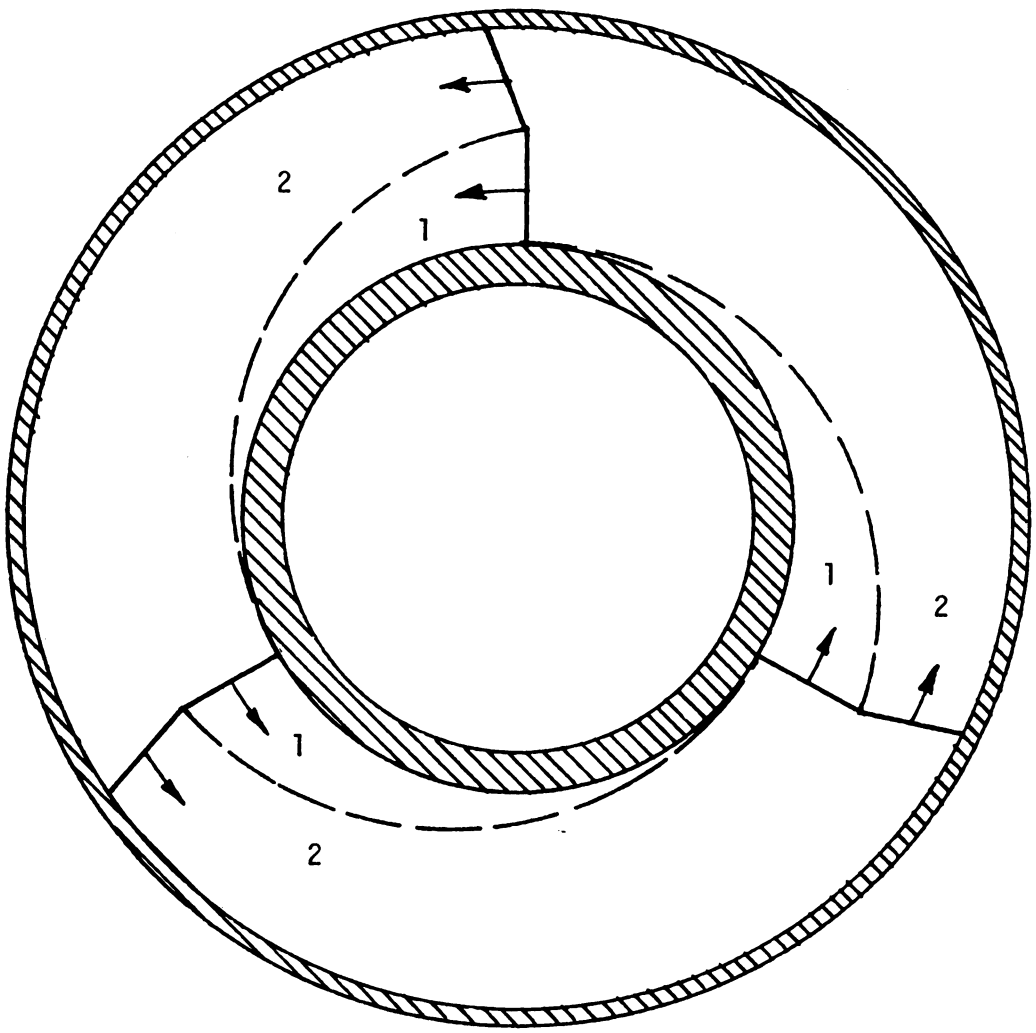

FIGURE 1. Location of the maintained detonation fronts (12):
1) original mixture;
2) detonation products

appeared to be a new mode of propagation of a detonation wave that was contrary to any previously reported results. Earlier experiments by Brochet, et al (14, 15, 16), on self-sustained detonation waves yielded a definite conclusion that, in general, there exists a small (0.3 to 1%) deviation in the propagation velocity from that calculated using the Chapman-Jouget theory. These deviations were attributed to an uncertainty in some numerical data used, the departure in the behavior of the burned gas from that of a perfect gas mixture, or from the spin of the detonation wave. These results, however, were obtained from measurements of wave propagation in long tubes and did not constitute a model of the maintained detonation in an annulus.

During this same period Sommers (17) was investigating the interaction between a condensed explosive (i.e., liquid or solid) detonation wave and the explosive container. A gaseous model was used in which the explosive was bounded by an inert gas. The boundary gas was to behave as the explosive container, i.e., the container would become compressible under the influence of the detonation pressure. This experimental configuration did provide a model of the maintained detonation in a circular track in that it presented side relief for an explosive mixture which was bounded by an inert gas. Although some of the experimental runs did show a change in the propagation velocity of the detonation wave others did not. When a velocity change was

noticeable, it was generally small and did not compare to the 50% reduction noted by Voitsekhovskii (12, 13). It was concluded however, that

> The interaction of a gaseous detonation wave with an inert gaseous boundary causes a lateral shock wave to exist in the boundary. It was found that this shock wave could be either a weak oblique shock or a detached shock, depending upon the Mach number of the detonation wave and the thermodynamic properties of the explosive and boundary (17).

Subsequently, Dabora, et al (18) investigated the velocity decrement of a gaseous detonation wave propagating through a channel bounded by a compressible, non-reacting gas. It was found that if the density of the boundary gas was much lower than that of the explosive a detached shock would develop. The preliminary experiments indicated that the reaction zone would propagate at about half the theoretical C-J velocity. It was also noted that there was some uncertainty as to whether the wave was steady (continuing to propagate at this lower velocity) or quenched; thereby exhibiting this velocity only in the transient state of decaying to a deflagration.

Several years later, while investigating H_2-CO-O_2 reactions, Lu (19) made a limited effort to determine whether or not these sub-Chapman-Jouget waves were steady. Using an explosive mixture composed of 75% H_2 and 25% O_2, by volume, and hydrogen or helium as the boundary gas, he found that the velocities measured from streak pictures were considerably lower than that predicted by the C-J theory. The wave speeds when bounded by hydrogen were 60 - 70% of the C-J velocity while the propagation velocity was 50 - 60% of

the theoretical value when bounded by helium. The wave speeds apparently were steady.

1.2 The Purpose of this Investigation

The existence of detonation waves above the C-J speed has been noted to exist (see, for example, References 20, 21, and 22) only if they are overdriven. When the piston effect is removed, they decay rapidly to a constant velocity which corresponds to the theory that the only stable detonation state is one which progresses at the C-J speed.

It has been postulated (23) that weak and slow moving detonation waves might exist. Indeed, the work of Voitsekhovskii (12, 13), Dabora, et al., (18) and Lu (19) would certainly indicate the possible existence of a form of detonation which has a propagation velocity considerably less than the C-J velocity. If this is true, then it would certainly be a significant factor in the design of a gaseous fuel powered rotating detonation wave rocket engine such as the one described in a feasibility study by Nicholls and Cullen (24) or even on the performance of the recently patented continuous detonation wave reaction engine (25).

Therefore, the purpose of this investigation is to study further the boundary interaction between a gaseous detonation wave and a low density boundary gas. The results of the previous studies will be extended in order to determine whether a sub-Chapman-Jouget wave does exist. Although Sichel (26) was successful in

providing a hydrodynamic theory for the interaction of a gaseous detonation wave with a compressible boundary, it was applicable only for cases in which the sound speed was less in the inert than in the explosive. For the case considered here, the acoustic velocity will be greater in the boundary gas than in the explosive. The interface flow will be more complex due to possible shock detachment and resulting refracted and/or reflected shocks in the explosive mixture. This produces a very complex flow pattern and does not lend itself to the construction of an analytical model. Instead, the primary concern will be in experimentally examining the interaction in an attempt to determine the existence of a sub-Chapman-Jouget detonation wave.

CHAPTER II

CHARACTERISTICS OF GASEOUS DETONATION WAVES

In a survey of recent work on the structure of detonation waves Edwards (27) concludes:

> It has now been indisputably established experimentally that the wave front of all self-sustaining detonation waves is three dimensional. Ample evidence exists that an adequate description of the gross wave properties of near plane detonation waves propagating in tubes, is provided by the simple one-dimensional structure envisaged in the ZND model. Acceptance of this model in a limiting situation does not impute any special significance to the C-J hypothesis as it is normally interpreted from stability arguments. However, if this hypothesis is defined in a generalized form as stated by White, as requiring the lowest possible wave velocity which is compatible with the conservation laws, including dissipation effects, then the objections which arise through an over idealization of structure are removed. That the C-J hypothesis is successful in predicting wave velocities is irrefutable and this is all it purports to do.

Based on the above conclusion, a simplified model will be treated in order to determine the characteristics of a gaseous detonation wave.

2.1 One-Dimensional Analysis

Consider, as shown in Figure 2, a stationary exothermic wave existing in a constant area duct. The combustible material flows from left to right with the free stream conditions (unburned gas) denoted by (1) and the final conditions (burned gas) denoted by (2). Assuming the steady flow of an inviscid

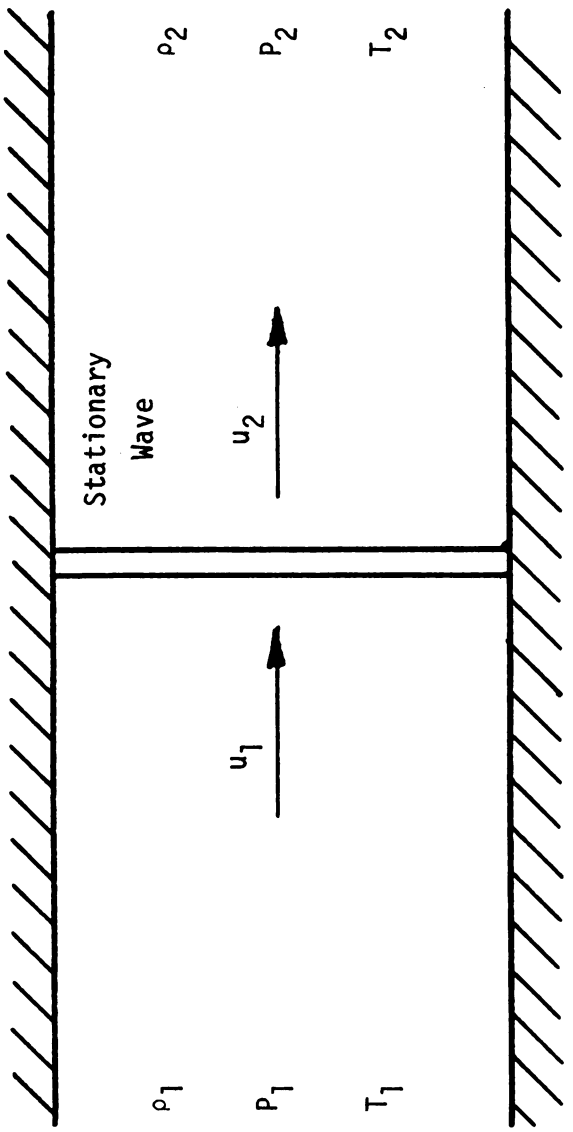

FIGURE 2. One-Dimensional Detonation Wave

fluid and that the wave can be represented as a planar discontinuity having uniform conditions along the wave, then the conservation equations may be written as follows:

a. Conservation of mass

$$\rho_1 u_1 = \rho_2 u_2 \tag{2.1}$$

b. Conservation of momentum

$$P_1 + \rho_1 u_1^2 = P_2 + \rho_2 u_2^2 \tag{2.2}$$

c. Conservation of energy

$$q + h_1 + \frac{u_1^2}{2} = h_2 + \frac{u_2^2}{2} \tag{2.3}$$

where q is the enthalpy of reaction per unit mass.

A realistic representation of the combustion process requires that the gases ahead and behind the wave have different specific heats as well as different molecular weights. However, in order to preserve the simplified analysis the gases will be assumed to be both thermally and calorically perfect. This allows the equation of state to be expressed as

$$P = \rho \frac{\bar{R}}{m} T \tag{2.4}$$

and the enthalpy as

$$h = C_p T = \frac{\gamma}{\gamma - 1} \frac{\bar{R}}{m} T$$

$$= \frac{\gamma}{\gamma - 1} \frac{P}{\rho} = \frac{\gamma}{\gamma - 1} Pv \tag{2.5}$$

Combining Equations (2.1) and (2.2) gives

$$(\rho_1 u_1)^2 = (\rho_2 u_2)^2 = \frac{P_2 - P_1}{v_1 - v_2} \tag{2.6}$$

The left side of Equation (2.6) is always positive which means that the signs of the numerator and denominator of the term on the right side must be identical. When Equation (2.6) is plotted on a P-v diagram, it will be seen as a straight line with a negative slope. This is called the Rayleigh line.

If Equation (2.6) is used to eliminate the velocity terms in Equation (2.3), the resulting equation is

$$q + h_1 - h_2 = \frac{1}{2}(P_1 - P_2)(v_1 + v_2) \tag{2.7}$$

which is known as the Hugoniot equation.

2.2 Representation of Detonation on a Hugoniot Curve

The classical treatment of detonation has centered around a Hugoniot curve representation of detonative combustion. If the kinetic terms are eliminated in favor of the thermodynamic variables, as was done in Equation (2.7), it leads to a convenient means of classifying exothermic waves.

Equation (2.7) can be further rearranged by combining it with the enthalpy relation of Equation (2.5) to give the Hugoniot equation in the form

$$\left(\frac{2q}{P_1 v_1} + \frac{\gamma_1 + 1}{\gamma_1 - 1} - \frac{\gamma_2 - 1}{\gamma_2 + 1}\right)\left(\frac{\gamma_2 - 1}{\gamma_2 + 1}\right) = \left(\frac{P_2}{P_1} + \frac{\gamma_2 - 1}{\gamma_2 + 1}\right)\left(\frac{v_2}{v_1} - \frac{\gamma_2 - 1}{\gamma_2 + 1}\right) \tag{2.8}$$

which would plot as a family of hyperbolas, with q and the γ's as a parameter, on a P-v diagram.

Figure 3 is a schematic plot of Equation (2.6) and Equation (2.8) for both the adiabatic case and for two cases with heat release. The adiabatic (q=o) Hugoniot line passes through the point (P_1,v_1) whereas the curves that represent an exothermic reaction system, in which chemical equilibrium is attained, must include the energy liberated by the reaction. The effect of this is to displace the Hugoniot curves to higher values of P and v so they do not pass through (P_1,v_1).

Also, the Hugoniot curves do not pass through the area upward and to the right of the section bounded by the lines P_1 and v_1 since, from Equation (2.6), this would correspond to an imaginary velocity. Thus, there are two quite separate regions: the upper one corresponding to $P_2 > P_1$, $v_2 < v_1$ and the lower to $P_2 < P_1$, $v_2 > v_1$.

The curves in the lower region of Figure 3 represent a condition in which the combustion wave is subsonic. The pressure and density decrease across the transition and the gas leaves it at a greater velocity than that at which it enters. This portion of the curve corresponds to a deflagration wave and is not relevant to this study.

Points on the curves in the upper left of Figure 3 lead to velocities greater than the acoustical velocity. Hence this portion describes the detonation process. The Rayleigh line,

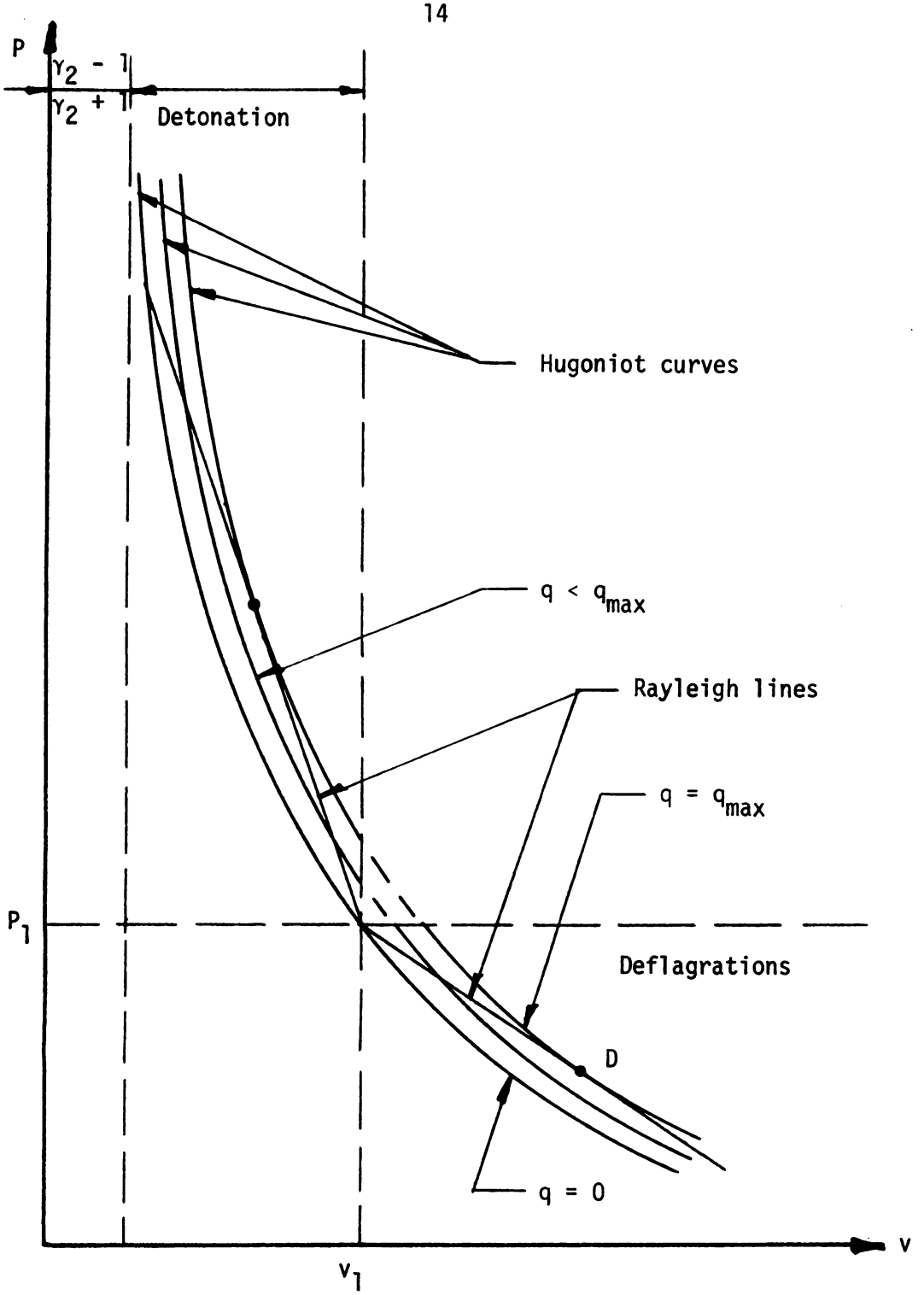

FIGURE 3. Hugoniot-Rayleigh Representation of Combustion Processes.

drawn from (P_1,v_1), will in general intersect a Hugoniot curve at two points which represents the simultaneous solution of Equations (2.6) and (2.7) or (2.8).

A Rayleight line drawn from (P_1,v_1) which makes a tangent to the curve at the C-J (the Chapman-Jouget point) has a slope (as has the tangent through point D):

$$\left(\frac{dP_2}{dv_2}\right)_{C\text{-}J} = \frac{P_2 - P_1}{v_2 - v_1} \quad . \tag{2.9}$$

From the first law of thermodynamics,

$$Tds = dh - vdP \tag{2.10}$$

and the adiabatic form of Equation (2.6) combined with Equation (2.10) shows that

$$ds = 0 \tag{2.11}$$

at point C-J. This is equivalent to

$$\left(\frac{dP_2}{dv_2}\right)_{C\text{-}J} = - \rho_2^2 \, a_2^2 \quad . \tag{2.12}$$

Using Equation (2.12) in (2.6) shows that

$$u_2 = a_2 \quad . \tag{2.13}$$

This indicates that for a Chapman-Jouget wave the velocity of the burned gas immediately behind the wave travels at the local acoustical velocity with respect to the wave.

Points to the left of the C-J state correspond to over-driven detonations, that is where the detonation gains additional energy apart from that provided by the chemical reaction. Such detonations will occur if they are initiated by a strong shock wave but, unless supported by a piston following the detonation, they are unstable and will decay to the C-J velocity.

Points to the right of the C-J state between C-J and (P_1, v_1) are classified as weak detonations and are thermodynamically improbable. This may be shown from Equation (2.6) considering differentiation to correspond to infinitesimal changes. Thus,

$$dP_2 + (\rho_2 u_2)^2 \, dv_2 = (v_1 - v_2) \, d(\rho_2 u_2)^2 \quad . \tag{2.14}$$

The adiabatic form of Equation (2.3) may be written as

$$h_1 + \tfrac{1}{2}(\rho_1 u_1)^2 \, v_1^2 = h_2 + \tfrac{1}{2}(\rho_2 u_2)^2 \, v_2^2 \tag{2.15}$$

and differentiated, yields:

$$dh_2 + (\rho_2 u_2)^2 \, v_2 dv_2 = \tfrac{1}{2}(v_1^2 - v_2^2) \, d(\rho_2 u_2)^2 \quad . \tag{2.16}$$

As a result of the first law of thermodynamics

$$dh_2 = T_2 ds_2 + v_2 dP_2 \tag{2.17}$$

Substituting this into Equation (2.16) and combining with Equation (2.14) gives

$$T_2 ds_2 = \frac{1}{2}(v_1 - v_2)^2 \, d(\rho_2 u_2)^2 \quad . \tag{2.18}$$

Since $(v_1 - v_2)^2$ and T_2 must be positive,

$$\frac{ds_2}{d(\rho_2 u_2)^2} > 0 \quad . \tag{2.19}$$

Some important conclusions result from the consideration of Equation (2.19). Since $(\rho_2 u_2)^2$ increases in either direction from the C-J point, so must the entropy s_2. Therefore, the C-J point is a point of minimum entropy for the detonation products.

A recapitulation of the divisions of the upper and lower branches of the Hugoniot curve allows that they may be characterized as follows:

strong detonation	M_1 supersonic	M_2 subsonic
C-J detonation	M_1 supersonic	M_2 sonic
weak detonation	M_1 supersonic	M_2 supersonic
weak deflagration	M_1 subsonic	M_2 subsonic
C-J deflagration	M_1 subsonic	M_2 sonic
strong deflagration	M_1 subsonic	M_2 supersonic

2.3 Chapman-Jouget Detonation Relationships for Ideal Gases

In order to gain a better insight as to the structure of gaseous detonation waves it is instructive to examine their properties. Treating the reactants and the products as ideal gases makes it possible to obtain several useful equations to relate the properties across a detonation wave.

Dividing the conservation of momentum (Equation 2.2) equation through by P_1 and rearranging gives the pressure ratio across the discontinuity.

$$\frac{P_2}{P_1} = 1 + \frac{\rho_1 u_1^2}{P_1} - \frac{\rho_2 u_2^2}{P_1}$$

$$= 1 + \frac{\rho_1 u_1^2}{P_1}\left(1 - \frac{v_2}{v_1}\right) \quad . \tag{2.20}$$

Defining the Mach number as $M = u/a$ where

$$a^2 = \frac{\gamma \bar{R} T}{m} = \frac{P\gamma}{\rho} \tag{2.21}$$

and substituting (2.21) into Equation (2.20) allows the pressure ratio to be expressed in terms of the Mach number as

$$\frac{P_2}{P_1} = 1 + \gamma_1 M_1^2\left(1 - \frac{v_2}{v_1}\right) \quad . \tag{2.22}$$

If Equation (2.2) is again used with (2.21) and the Chapman-Jouget condition is specified ($u_2 = a_2$), then

$$\frac{P_2}{P_1} = \frac{1 + \gamma_1 M_1^2}{1 + \gamma_2} \quad . \tag{2.23}$$

Furthermore, since the gases behind a Chapman-Jouget detonation wave move at the local acoustic velocity relative to the front, Equation (2.4) may be written as

$$\gamma_1 M_1^2 = \frac{1 - P_2/P_1}{v_2/v_1 - 1} \quad . \tag{2.24}$$

The temperature ratio across the discontinuity may be specified as

$$\frac{T_2}{T_1} = \frac{m_2 P_2 v_2}{m_1 P_1 v_1} \tag{2.25}$$

where m_1 and m_2 are the average molecular weight upstream and downstream of the detonation wave. Introducing the expression for the pressure ratio Equation (2.26) into (2.25), one obtains:

$$\frac{T_2}{T_1} = \frac{m_2}{m_1} \frac{\gamma_2}{\gamma_1} \frac{(1 + \gamma_1 M_1^2)^2}{M_1^2 (1 + \gamma_2)^2} \quad . \tag{2.26}$$

The specific volume ratio may be found by incorporating Equations (2.23) and (2.25) into Equation (2.26) to obtain:

$$\frac{v_2}{v_1} = \frac{\gamma_2}{\gamma_1} \frac{(1 + \gamma_1 M_1^2)}{M_1^2 (1 + \gamma_2)} \quad . \tag{2.27}$$

If the enthalpy base is considered to be zero when the temperature equals zero and the specific heats C_{p1} and C_{p2}, are assumed constant, the conservation of energy equation becomes:

$$q + C_{p1}T_1 + \frac{u_1^2}{2} = C_{p2}T_2 + \frac{u_2^2}{2} \quad . \tag{2.28}$$

Since $C_p = \frac{\gamma \bar{R}}{(\gamma - 1)m}$; $a^2 = \frac{\gamma \bar{R} T}{m}$; $M = \frac{u}{a}$

and for a Chapman-Jouget wave, $M_2 = 1.0$, it follows that

$$\frac{T_2}{T_1} = \frac{\frac{1}{\gamma_1 - 1} + \frac{M_1^2}{2} + \frac{q}{a_1^2}}{\frac{\gamma_2}{2\gamma_1}\left(\frac{\gamma_2 + 1}{\gamma_2 - 1}\right)} \quad . \tag{2.29}$$

From the foregoing equations it is apparent that if the initial thermodynamic properties, the value of the heat release (q) and the specific heat ratio of the burned gas (γ_2) are known, then the detonation velocity can be found. However, finding q and γ_2 generally requires a trial and error solution that involves chemical equilibrium behind the wave. Solutions to this problem have been obtained for many combustible mixtures by Lewis and von Elbe (6), Dunn and Wolfson (28), Eisen, et al. (29), Gealer and Churchill (30), Moyle (31), and Zeleznik and Gordon (32).

2.4 Classification of Detonation Waves

Detonation waves are usually classified relative to the Chapman-Jouget wave; a weak detonation wave would have a final

Mach number greater than 1; a Chapman-Jouget wave has a final Mach number equal to 1; and a strong or over-driven detonation wave has a final Mach number less than 1, where in each case, the final Mach number refers to the Mach number after the wave and is measured relative to the wave. It has always been a problem to classify the detonation waves mathematically such that the previously noted distinctions are simply represented. Adamson (33) proposes the following which are presented here without derivation.

a. Pressure ratio

$$\frac{P_2 - P_1}{P_1} = \frac{\gamma_1 F}{\gamma_2 + 1} \left(M_1^2 - \frac{\gamma_2}{\gamma_1}\right) ; \tag{2.30}$$

b. Density ratio

$$\frac{\rho_2}{\rho_1} = \frac{1}{1 - \frac{F}{(\gamma_2 - 1)} \left(M_1^2 - \frac{\gamma_2}{\gamma_1}\right) \frac{1}{M_1^2}} ; \tag{2.31}$$

c. Temperature ratio

$$\frac{T_2}{T_1} = \frac{m_2}{m_1} \left[1 - \frac{1}{M_1^2} \frac{F}{(\gamma_2 - 1)} \left(M_1^2 - \frac{\gamma_2}{\gamma_1}\right)\right] \times \left[1 + \frac{\gamma_1 F}{(\gamma_2 - 1)} \left(M_1^2 - \frac{\gamma_2}{\gamma_1}\right)\right] ; \tag{2.32}$$

d. The Mach number behind the wave

$$M_2 = \left[\frac{\gamma_1}{\gamma_2} \left\{\frac{(\gamma_2 + 1 - F)\left(M_1^2 - \frac{\gamma_2}{\gamma_1}\right) + \left(\frac{\gamma_2}{\gamma_1}\right)(\gamma_2 + 1)}{\gamma_1 F\left(M_1^2 - \frac{\gamma_2}{\gamma_1}\right) + (\gamma_2 + 1)}\right\}\right]^{1/2} \tag{2.33}$$

where

$$F = 1 \pm \sqrt{1 - f} \tag{2.34}$$

and

$$f = \frac{2(\gamma_2^2 - 1)}{(\gamma_1 - 1)} \frac{M_1^2}{(M_1^2 - \frac{\gamma_2}{\gamma_1})^2} \left[\frac{q}{C_{p1}T_1} - \frac{\gamma_1 - \gamma_2}{\gamma_1(\gamma_2 - 1)}\right] . \tag{2.35}$$

Compared with normal shock theory, the definition of F implies the following:

$F = 2$	corresponds to an adiabatic shock wave (when $\gamma_1 = \gamma_2$)
$1 < F < 2$	corresponds to a strong detonation wave
$F = 1$	corresponds to a C-J detonation wave.

Adamson (33) also suggests that $f > 1$ corresponds to a weak detonation wave. This case requires the heat added to be sufficient to bring the Mach number behind the detonation wave to a supersonic value. Based on the previous equations, this would represent an impossible solution since the value of f would be imaginary.

The Chapman-Jouget detonation wave requires that $M_2 = 1$, which allows the propagation Mach number of a detonation wave to be found from Equation (2.34). It should be noted that a solution for q and γ_2 must be obtained by trial and error as noted in the previous section.

2.5 Interaction of a Gaseous Detonation Wave with an Inert Boundary.

The study of the interaction of a detonation wave with an inert boundary gas is believed to have been investigated first by Doering and Burkhart (34) and more recently by Sommers (17), Dabora, et al. (18), and Lu (19). Since a similar technique will be used in this study, a brief description of the interaction will be given.

When a plane detonation wave propagates through a column of gaseous explosive material which is bounded by an inert gas, an oblique shock will be induced into the boundary gas. This results from the expansion of the burned gas behind the shock front. It should also be noted that the reaction is not instantaneous as was suggested by Figure 2. Instead, it will be assumed after Zeldovich (35), von Neumann (36), and Doering (37) that the detonation consists of a shock wave followed by combustion. Since the combustion cannot be instantaneous neither can the heat release. This requires the Chapman-Jouget plane, which represents the limiting value of the heat release, to trail the shock front by some finite distance which is known as the reaction length. The ZND (Zeldovich, von Neumann, and Doering) model is shown in Figure 4; the reaction length is denoted as $\bar{X}$.

For a detonation wave that propagates in a solid tube, the C-J plane would have the same area as the shock front. However, if the detonation experiences side relief, the gas following the shock front, being at a higher pressure than the inert, will undergo a lateral expansion. This causes the

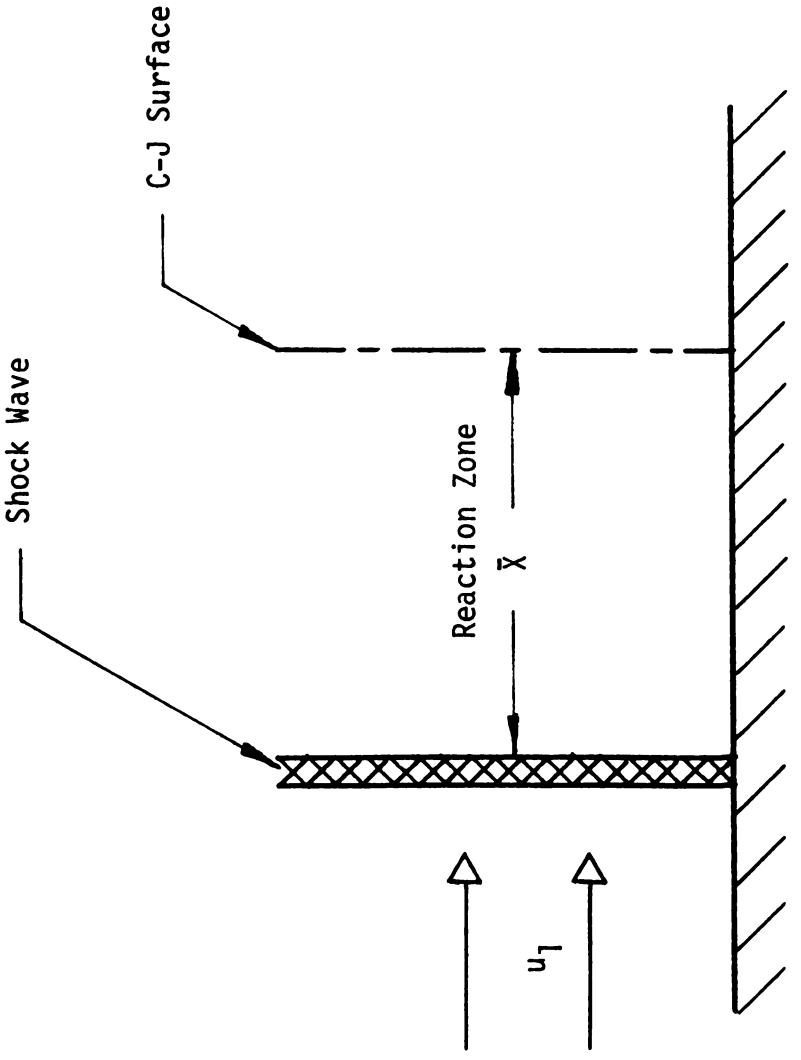

FIGURE 4. ZND Model of a Gaseous Detonation.

C-J plane to have a larger area than the shock front. The effect of side relief on the reaction includes both subsonic and supersonic flow regimes and is further complicated by the chemical reaction. Also, experiments have shown that adjustments in the flow behind the shock front cause some slight curvature of the wave. Sichel (26) postulates that the flow at the edge of the interaction zone is as shown in Figure 5.

A detonation wave bounded by an inert gas poses a problem in that the deflection experienced by the interface will cause each stream tube, originating at the front of the detonation wave, to experience an area increase at the C-J plane. How this area increase effects the flow velocity was investigated by Dabora, et al. (18), and is briefly summarized since the results have a direct bearing on this study.

2.5.1 Effect of Area Change on Propagation Velocity.

To find the influence of side relief on the propagation velocity of a detonation wave, Dabora, et al. (18), assumed an idealized flow model similar to that shown in Figure 6. If the shock front area is denoted as A_1 and the area at the C-J plane is specified as A_2, then

$$\frac{A_2}{A_1} = 1 + \xi \tag{2.36}$$

where ξ is the average fractional change in the area of each stream tube. The conservation equations for mass and momentum

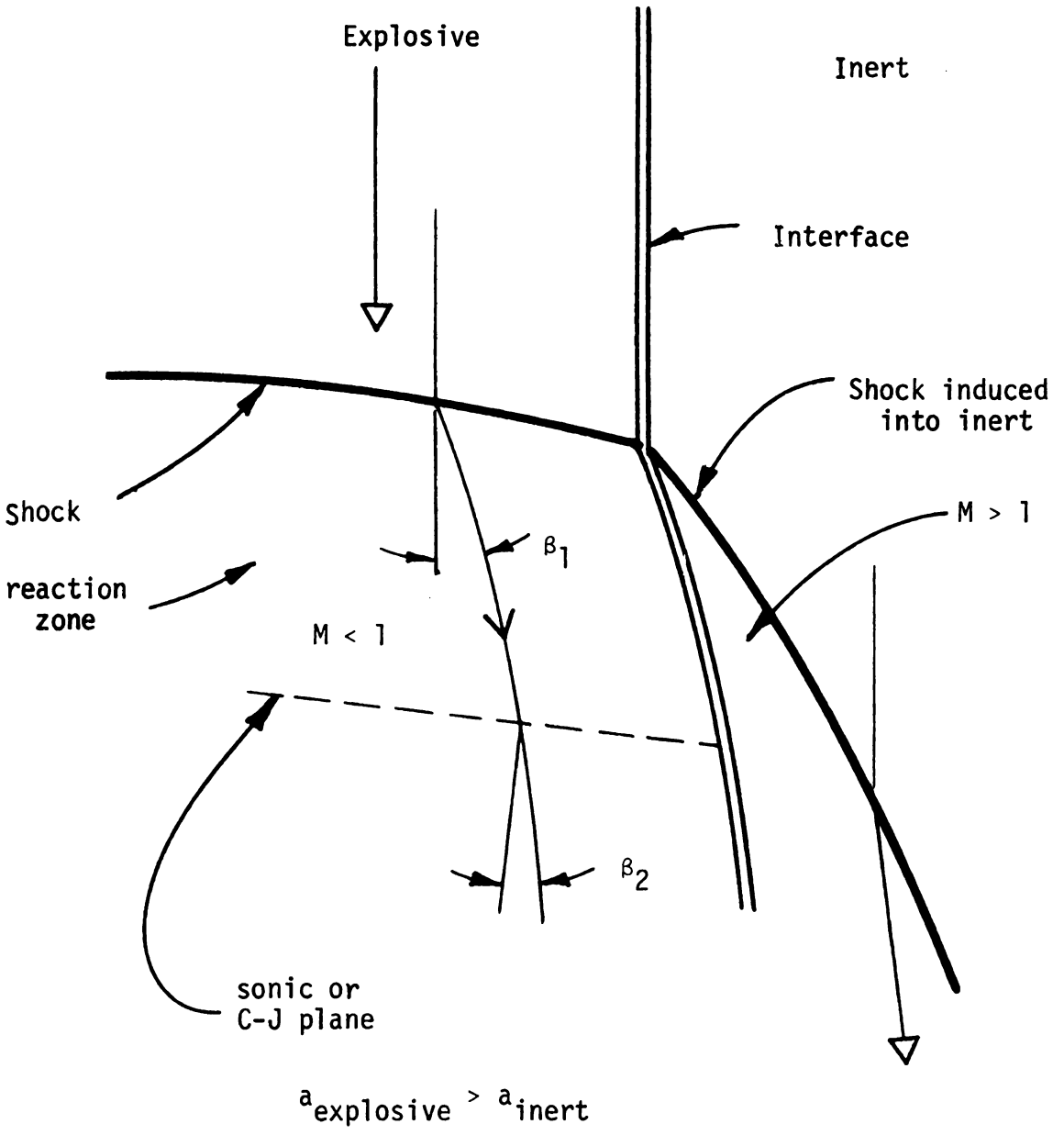

FIGURE 5. Postulated Flow at the Edge of the Interaction Zone (26).

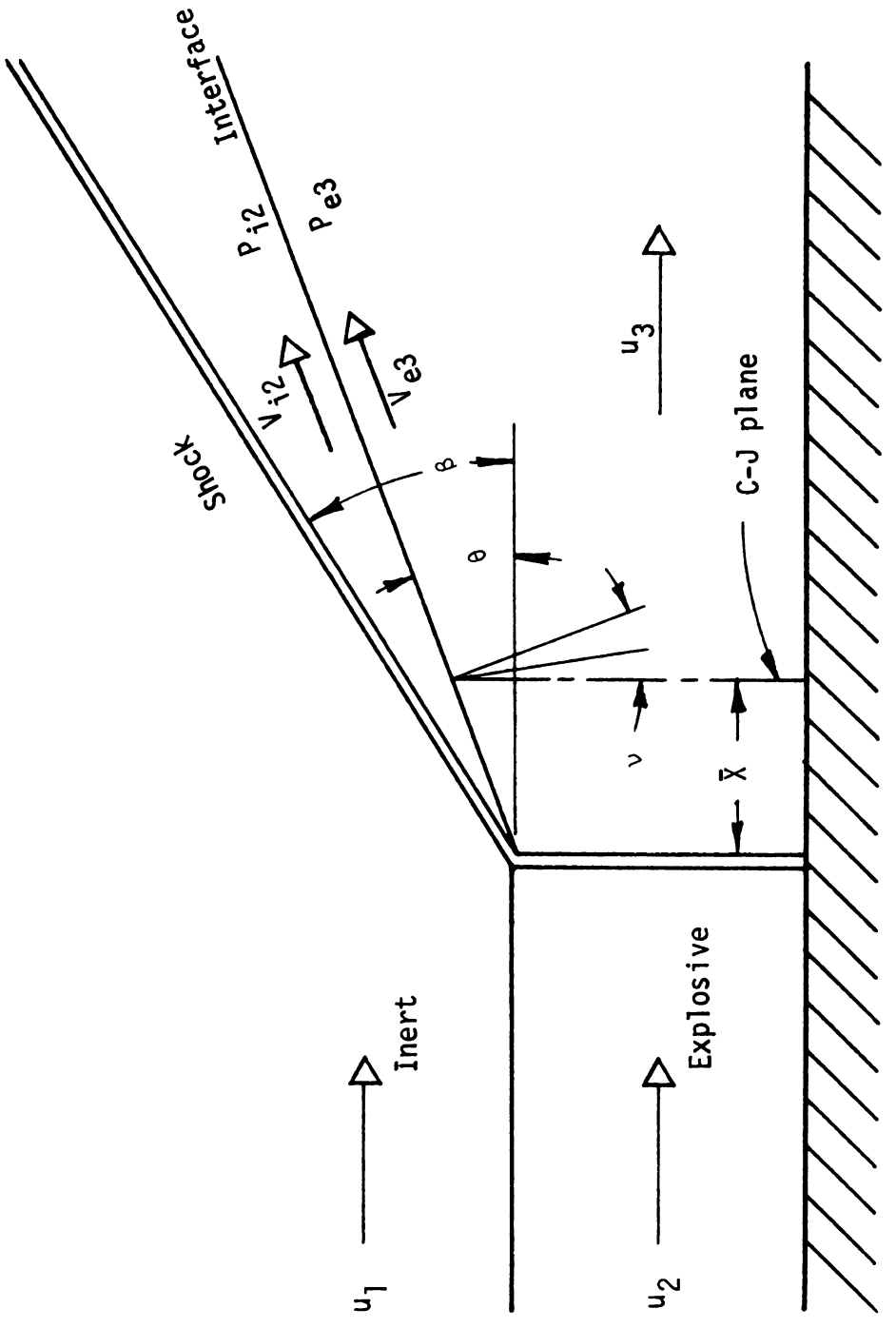

FIGURE 6. Idealized Model of Detonation Wave-Boundary Interaction. (Flow is assumed quasi one-dimensional in the reaction zone and two-dimensional behind the C-J plane).

may be written, respectively, as

$$\rho_1 u_1 = \rho_2 u_2 (1 + \xi) \tag{2.37}$$

$$P_1 + \rho_1 u_1^2 = (P_2 + \rho_2 u_2^2)(1 + \xi) - \int_0^{\xi} P d\xi \tag{2.38}$$

The conservation of energy equation will remain the same as Equation (2.3). The evaluation of the integral of Equation (2.38) requires a detailed knowledge of the variation of the pressure along the interface between the shock front and the C-J plane. However, the integral was defined by Dabora, et al. (18), as

$$\int_0^{\xi} P d\xi = P_2 \varepsilon \xi \tag{2.39}$$

Equation (2.30) suggests that for Mach numbers that are large, compared to unity, the value of $P_2 = 2P_1$ for a shock and $P_2 = P_1$ for a C-J detonation wave. This implies that $1 < \varepsilon < 2$. Assuming the specific heat ratios and the molecular weight change across the wave; both the explosive and inert gases are thermally and calorically perfect; the heat release remains the same whether there is an area change or not; and if $M_1 >> 1$, Dabora, et al. (18), concluded that the fractional decrease in the velocity or Mach number could be expressed as

$$\frac{\Delta M_1}{M_1(\xi=0)} = 1 - \left\{\frac{\left[1 - \frac{\varepsilon}{1+\gamma_2}\frac{\xi}{1+\xi}\right]^2}{\left[1 - \frac{\varepsilon}{1+\gamma_2}\frac{\xi}{1+\xi}\right]^2 + \gamma_2\left[2\frac{\varepsilon}{1+\gamma_2}\frac{\xi}{1+\xi} - \left(\frac{\varepsilon}{1+\gamma_2}\right)^2\left(\frac{\xi}{1+\xi}\right)^2\right]}\right\}^{1/2} \tag{2.40}$$

Also, it was stated (18):

> For an estimate of ε, the pressure distribution within the reaction zone of a detonation wave with an irreversible unimolecular reaction calculated by Hirschfelder and Curtiss was used and a value of 1.13 was obtained.

The effect of side relief on propagation velocity is easily seen if Equation (2.40) is plotted. Using a value of $\gamma_2 = 1.2$, which is a reasonably typical value for the ratio of specific heats as will be seen in a later section, and $\varepsilon = 1.13$, the plot shown in Figure 7 was obtained.

Figure 7 illustrates the effect an area change at the C-J plane has on the detonation velocity. Since this study deals with the determination of the existence of weak detonation waves that propagate at half the Chapman-Jouget value, it is necessary to determine the deflection angle so that ξ can be estimated.

2.5.2 Determination of Shock and Interface Angles.

To determine the shock and interface angles, the idealized model shown in Figure 6 will be used. The solution for the shock angle β and the interface angle θ is made possible by the fact that along the interface the pressure and the flow direction in

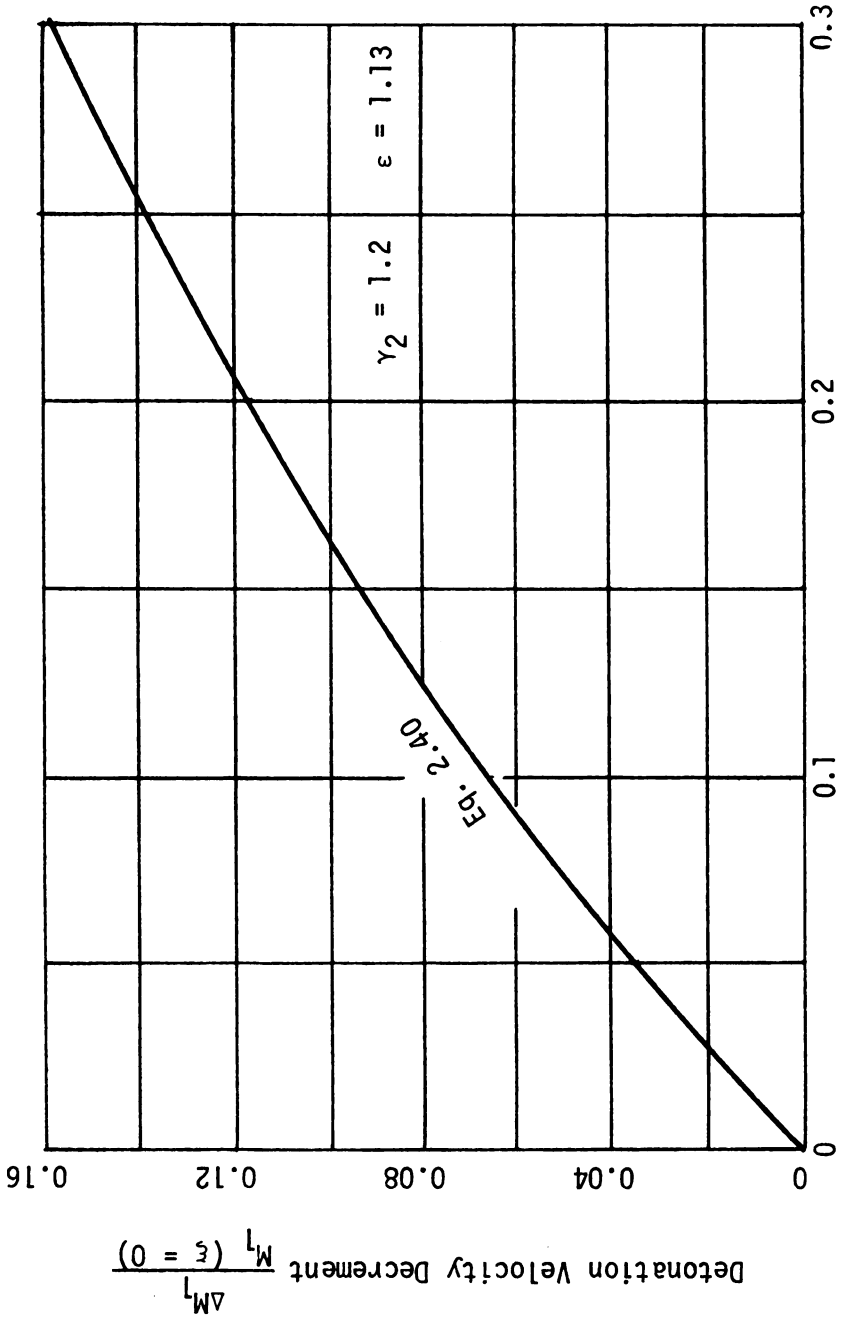

FIGURE 7. Fractional Change in Detonation Wave Propagation vs. the Average Fractional Area Change.

the reaction zone and in the supersonic region behind the induced shock must match. Therefore, a trial and error solution is suggested in which the conditions in the boundary gas are matched with conditions behind the C-J plane.

To perform the calculations requires prior knowledge of u_1, the detonation velocity; m_i and m_e, which are the molecular weights of the boundary gas and the explosive gas respectively; and the specific heat ratios, γ_{i1}, γ_{e1} and γ_{e2}; and the initial temperature T_1.

The acoustic velocity is computed for both the explosive and boundary gas. Using Equation (2.21)

$$a_{e1}^2 = \frac{\gamma_{e1}\bar{R}T_1}{m_{e1}} \tag{2.41}$$

$$a_{i1}^2 = \frac{\gamma_{i1}\bar{R}T_1}{m_{i1}} \quad . \tag{2.42}$$

Since the detonation velocity, u_1, is known, the flow Mach numbers are

$$M_{e1} = \frac{u_1}{a_{e1}} \quad \text{and} \quad M_{i1} = \frac{u_1}{a_{i1}} \tag{2.43}$$

where

$$M_{e1} = M_1 \quad .$$

Although the propagation velocity, u_1, is the same for both the explosive and boundary gas, the difference in their respective acoustic velocities will cause a noticeable difference

in their respective Mach numbers. Calculations of the Mach number for the explosive-boundary gas combinations are given in Table 1.

A comparison of the idealized model of the detonation wave-boundary interaction of Figure 6, with that of supersonic flow over a wedge reveals a similarity. If the interface angle θ can be considered to correspond to the wedge angle and the shock angle β corresponds to the oblique shock angle, then a solution of the flow over a wedge would be an analogue of a propagating detonation wave with a gaseous boundary.

The relationship between the shock and deflection angle for a given Mach number in the boundary gas is (38)

$$\tan \theta = 2 \cot \beta \frac{M_1^2 \sin^2 \beta - 1}{M_1^2 (\gamma_1 + \cos 2\beta) + 2} \quad . \tag{2.44}$$

The maximum detachment angle, β_{max}, may be found by differentiating Equation (2.44) and setting the result equal to zero. Therefore,

$$\sin^2 \beta_{max} = \frac{1}{\gamma_{i1} M_{i1}^2} \left[\left(\frac{\gamma_{i1} + 1}{4} \right) M_{i1}^2 - 1 + \sqrt{(\gamma_{i1} + 1)\left(1 + \frac{\gamma_{i1} - 1}{2} M_{i1}^2 + \frac{\gamma_{i1} + 1}{16} M_{i1}^4\right)} \right] \tag{2.45}$$

Using the Mach number of the boundary gas as determined from Equation (2.43) together with Equation (2.45) allows one to

TABLE 1

FLOW MACH NUMBERS OF VARIOUS EXPLOSIVE MIXTURES AND GASEOUS BOUNDARIES

Explosive	Boundary	u_1 ft/sec	$T_1 = 530°R$					
			γ_{el}	γ_{il}	m_{el}	m_{il}	M_{el}	M_{il}
Hydrogen and Oxygen								
50% H_2 - 50% O_2	Helium	7550	1.4	1.66	17.0	4	5.12	2.28
45% H_2 - 55% O_2	Helium	7240	1.4	1.66	18.5	4	5.12	2.19
35% H_2 - 65% O_2	Helium	6350	1.4	1.66	21.5	4	4.85	1.92
30% H_2 - 70% O_2	Air	6140	1.4	1.4	23.0	29	4.85	5.44
35% H_2 - 65% O_2	78%H_2 - 22%O_2	6350	1.4	1.4	21.5	8.6	4.85	3.06
50% H_2 - 50% O_2	35%H_2 - 65%O_2	7550	1.4	1.4	17.0	21.5	5.12	5.76
50% H_2 - 50% O_2	Hydrogen	7550	1.4	1.4	17.0	2	5.12	1.76
50% H_2 - 50% O_2	Nitrogen	7550	1.4	1.4	17.0	28	5.12	6.69
30% H_2 - 70% O_2	Air	6140	1.4	1.4	23.0	29	4.85	5.44
Methane and Oxygen								
30% CH_4 - 70% O_2	Helium	7550	1.4	1.4	27.2	4	6.48	2.28
30% CH_4 - 70% O_2	78%H_2 - 22% O_2	7550	1.4	1.4	27.2	8.6	6.48	3.64
30% CH_4 - 70% O_2	Air	7550	1.4	1.4	27.2	29	6.48	6.69
Butane and Oxygen								
13.4%C_4H_{10}-86.6%O_2	Helium	7250	1.4	1.66	35.5	4	7.11	2.19

compute the maximum possible shock angle. If an oblique shock solution exists, the shock angle β must be less than, or equal to the value of β_{max}. For the specific heat ratios of the boundary gases considered in this study, the maximum shock angle was computed for the different Mach numbers and the results are plotted in Figure 8.

As the products of combustion leave the C-J plane they are assumed to turn through a centered expansion wave until the flow is parallel to the interface. This requires the Prandtl-Meyer function ν to equal the interface angle θ. As a result of passing through the expansion fan, the gas is accelerated to a high Mach number which is related to the turning angle by the expression (38):

$$\nu = \sqrt{\frac{\gamma_{e2} + 1}{\gamma_{e2} - 1}} \tan^{-1} \sqrt{\frac{\gamma_{e2} - 1}{\gamma_{e2} + 1} (M_{e3}^2 - 1)} - \tan^{-1} \sqrt{M_{e3}^2 - 1} \tag{2.46}$$

Equation (2.46) gives the value of ν in radians and assumes γ_{e2} remains constant during the expansion process.

The numerical value of γ_{e2} must be determined for each explosive mixture and is a function of the temperature, pressure and composition of the products. For the calculations used in this study, γ_{e2} was determined in two different ways depending upon whether the fuel used was hydrogen or a hydrocarbon.

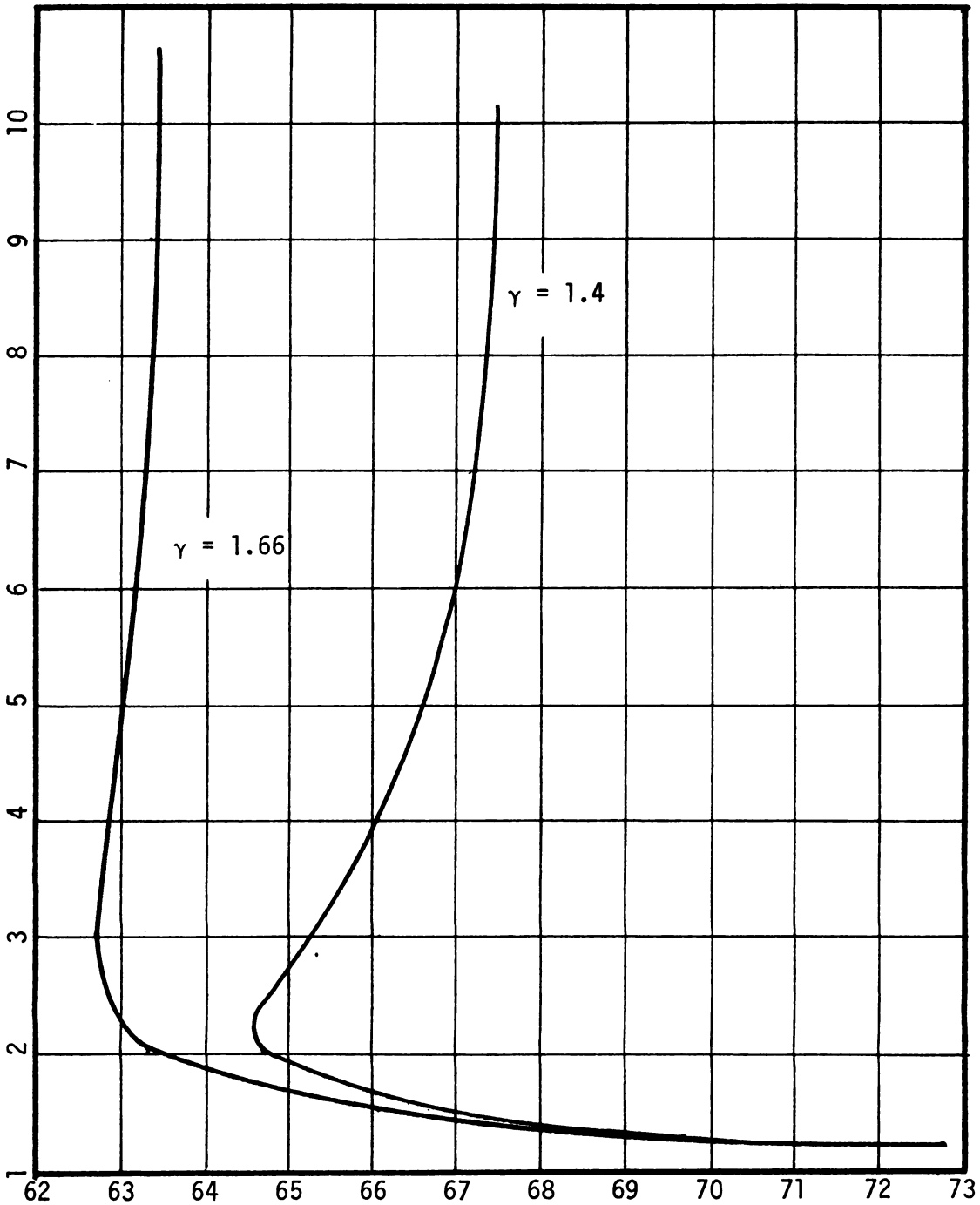

FIGURE 8. Boundary Gas Mach Number versus Shock Angle as a Function of the Specific Heat Ratio.

The method of determining γ_{e2} for hydrogen-oxygen mixtures was facilitated by Moyle's (31) study in which he determined the ratio of specific volumes (v_{e1}/v_{e2}) across a C-J detonation wave for different mole fractions of hydrogen. Using Moyle's results and Equation (2.22) one is able to solve for the pressure ratio across the detonation wave.

$$\frac{P_{e2}}{P_{e1}} = 1 + \gamma_{e1} M_{e1}^2 \left(1 - \frac{v_{e2}}{v_{e1}}\right) \quad . \tag{2.47}$$

Knowing P_{e2}/P_{e1}, Equation (2.23) may then be solve for γ_{e2} .

$$\gamma_{e2} = \frac{P_{e1}}{P_{e2}} \left(1 + \gamma_{e1} M_{e1}^2\right) - 1 \quad . \tag{2.48}$$

The value of γ_{e2} for hydrocarbon fuels was estimated from the work of Eisen, et al., (29). It is interesting to note that for hydrogen-oxygen mixtures and for the hydrocarbon fuel-oxygen mixtures used in this study $\gamma_{e2} \doteq 1.2$.

The ratio of the local stagnation pressure to the static pressure at the end of the Prandtl-Meyer expansion is

$$\left(\frac{P_{et}}{P_e}\right)_3 = \left(1 + \frac{\gamma_{e2} - 1}{2} M_{e3}^2\right)^{\gamma_{e2}/\gamma_{e2} - 1} \quad . \tag{2.49}$$

At the C-J plane, the ratio of stagnation to static pressure is

$$\left(\frac{P_{et}}{P_e}\right)_2 = \left(1 + \frac{\gamma_{e2} - 1}{2}\right)^{\gamma_{e2}/\gamma_{e2} - 1} \quad . \tag{2.50}$$

Although the Prandtl-Meyer expansion process is ideally a reversible, adiabatic process, the results will not be significantly changed since the heat transfer and viscous effects are vanishingly small. This allows the pressure ratio at the C-J plane to equal that at the end of the expansion. Consequently, the static pressure ratio across the entire process undergone by the explosive gas may be determined.

$$\frac{P_{e3}}{P_{e1}} = \left(\frac{P_{e2}}{P_{e1}}\right)\left(\frac{P_{et}}{P_{e}}\right)_2\left(\frac{P_{e}}{P_{et}}\right)_3 \quad . \tag{2.51}$$

One of the original criteria for the solution of the shock and interface angles was that the pressure ratios on each side of the interface must be equal. Using Equation (2.30), a value of F = 2 for an adiabatic shock and $\gamma_1 = \gamma_2$, allows the pressure ratio across the oblique shock in the boundary gas to be written as

$$\frac{P_{i2}}{P_{i1}} = 1 + \frac{2\gamma_{i1}}{\gamma_{i1} + 1}\left(M_{i1}^2 \sin^2 \beta - 1\right) \quad . \tag{2.52}$$

This completes the information necessary to compute the shock and interface angles. It may be summarized as follows:

a. Using Equations (2.41), (2.42) and (2.43) determine the acoustic velocity and the Mach number of the explosive and boundary gas.

b. Compute the value of β_{max} from Equation (2.45) and for a first trial assume $\beta \leq \beta_{max}$.

c. Compute θ, corresponding to the assumed value of β, using Equation (2.44).

d. Determine the value of γ_{e2}.

e. Since the interface angle equals the Prandtl-Meyer function (ν), the value of θ obtained from Equation (2.44) is used to determine the value of M_{e3} in Equation (2.46).

f. Using the value of γ_{e2} from Step (d) and M_{e3} from Step (e), solve Equation (2.49) to determine $(P_{et}/P_3)_3$.

g. Equations (2.47) and (2.50) can be solved and combined with Equation (2.49) to obtain P_{e3}/P_{e1}.

h. The value of P_{i2}/P_{i1} can be solved using Equation (2.52) and the assumed shock angle.

j) Since the static pressures ahead of the detonation wave are equal ($P_{e1} = P_{i1}$), the correct value of β has been determined when $(P_{12}/P_{i1}) = (P_{e3}/P_{e1})$.

k) If from Step (j), $(P_{e3}/P_{e1}) < (P_{i2}/P_{i1})$ the assumed value of β should be decreased whereas, if $(P_{e3}/P_{e1}) > (P_{i2}/P_{i1})$ then the assumed value of β should be increased. Steps (b) through (j) are repeated until $(P_{e3}/P_{e1}) = (P_{i2}/P_{i1})$.

A possible solution and the one which this study required was that for β assumed equal to β_{max}, P_{e3}/P_{e1} will be greater than P_{i2}/P_{i1}. This represents the case in which the shock is

detached, i.e., an oblique shock solution does not exist. This means that the turning angle, ν, required is larger than the boundary gas can achieve through an oblique shock. For flow over a wedge the shock wave becomes curved, is normal at the centerline of the wedge, and detaches from the wedge to a distance dependent on the wedge thickness. Such a condition cannot exist in the analogue and thus the analogue necessarily breaks down.

It is evident that the determination of the shock and interface angle is a trial and error process. To avoid tedious hand calculations, a computer program was written to compute these angles and is shown in Appendix A.

2.5.2a Determination of Shock and Interface Angles Using a Shock Tube Analogy.

It is also possible to determine the interface deflection angle of the induced shock in the boundary gas by using a shock tube analysis. This method was used by Dabora, et al. (18) where it was assumed that the gas behind the detonation was comparable to the driver gas and the boundary gas was equivalent to the driven gas. It is worthwhile to examine this method in order to determine its validity.

As was done in Reference 39, we can construct a shock tube analogue which is shown in Figure 9. The oblique shock wave is produced by a piston moving at a constant velocity

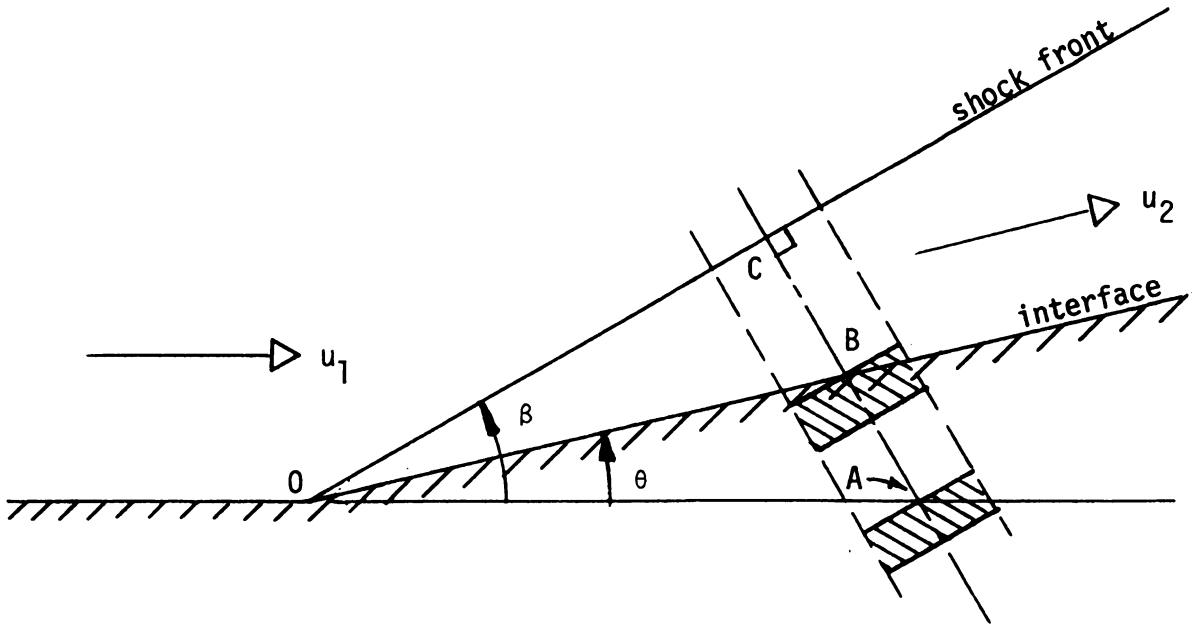

FIGURE 9. Shock Tube Analogy to the Interaction Process.

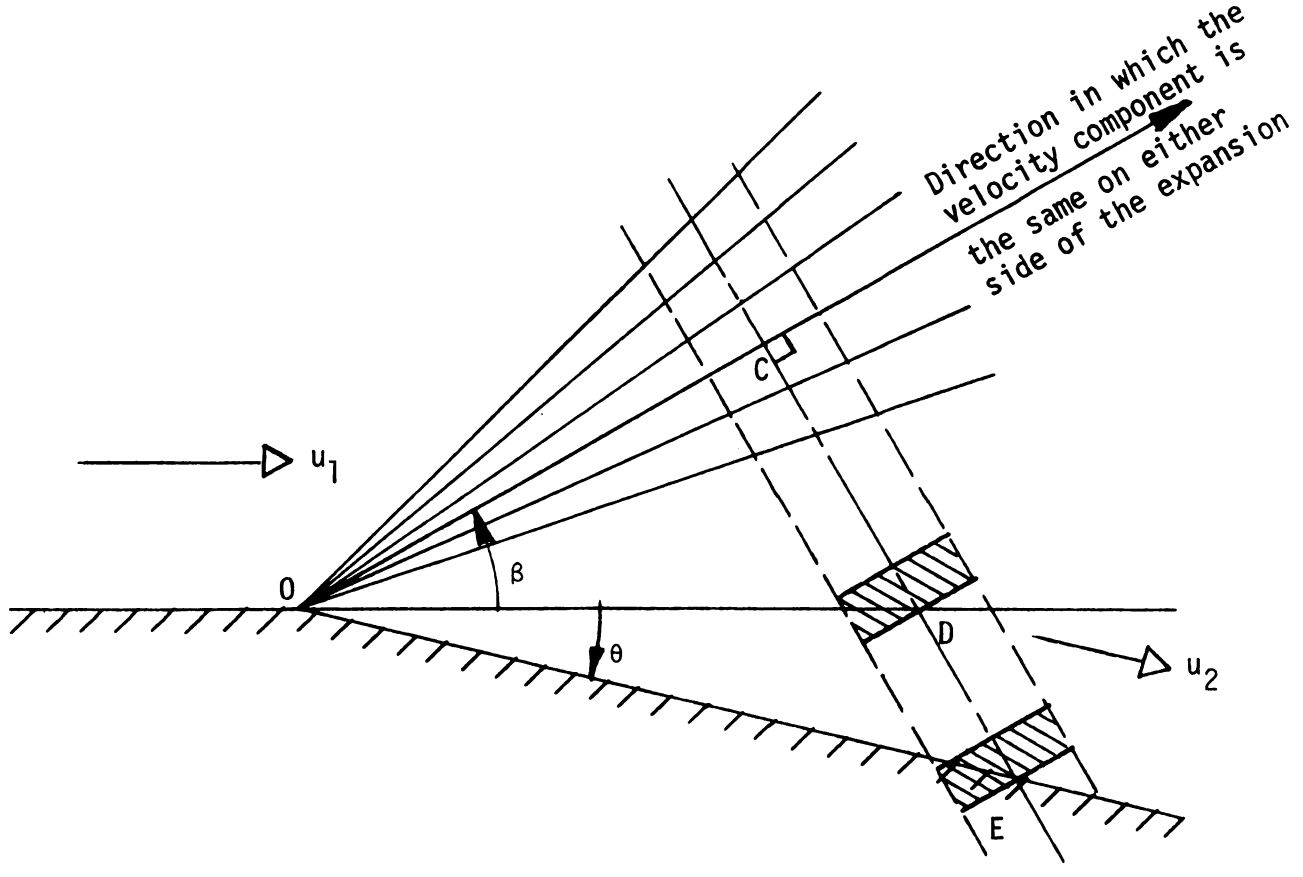

FIGURE 10. Shock Tube Analogy of a Prandtl-Meyer Expansion.

along the line AB and the boundary condition is satisfied if the ratio of piston velocity, w, to the free stream velocity, u_1, is made equal to the ratio of the length of AB to that of the length OA.

$$\frac{w}{u_1} = \frac{AB}{OA} = \frac{w}{a_1 M_1} \quad . \tag{2.53}$$

Since angle OCB is 90° and angle COB is equal to $(\beta - \theta)$, it follows that angle OBC is equal to $90° - (\beta - \theta)$ and angle OBA is $90° + (\beta - \theta)$. Using the law of sines:

$$\frac{AB}{\sin \theta} = \frac{OA}{\sin [90° + (\beta - \theta)]} \quad . \tag{2.54}$$

Combining Equations (2.53) and (2.54), yields

$$\frac{w}{\sin \theta} = \frac{u_1}{\sin[90° + (\beta - \theta)]}$$

or

$$\frac{w}{a_1} = \frac{M_1 \sin \theta}{\cos (\beta - \theta)} \quad . \tag{2.55}$$

A shock tube representation of a Prandtl-Meyer expansion is shown in Figure 10. If the convention is adopted that angles are positive when measured counterclockwise from the free stream direction, it will be found that the non-dimensional piston velocity will again be represented by Equation (2.55).

As was noted in the previous section, the pressure ratio on each side of the interface must be equal; therefore, for both cases the similarity law becomes:

$$\frac{P_2}{P_1} = f\left[\frac{M_1 \sin \theta}{\cos (\beta - \theta)}\right] \quad . \tag{2.56}$$

The angle β cannot be expressed as an explicit function of the free stream Mach number M_1, or of the turning angle θ. However, Bird (39) notes the angle of inclination of an oblique shock wave to the horizontal is very nearly equal to the free stream Mach angle, μ, so the replacement of $(\beta - \theta)$ by μ is a good approximation for oblique shock waves and a reasonable approximation for Prandtl-Meyer expansions. Thus, it must be concluded that a shock tube analogy for the determination of the shock and interface angles is, at best, a good approximation.

CHAPTER III

EXPERIMENTAL EQUIPMENT: ARRANGEMENT AND PROCEDURE

To study the interaction between a combustible gas and a low density boundary gas such as would exist in the combustion chamber described by Voitsekhovskii (12) would logically lead one to construct a similar combustion chamber. A review of the apparent expense and effort expended by Nicholls and Cullen (24) in an attempt to construct a rotating detonation wave engine and the subsequent failure by them to produce a system that would maintain a detonation wave was a significant factor in not trying to duplicate Voitsekhovskii's experiment. Instead, it was reasoned that a linear system would prove an acceptable model if the detonation wave could be made to propagate through a column of explosive gas bounded by an inert mixture. This would represent the detonation wave traveling in a circular track where it is bounded by the burned gas which, because of its temperature, would have a low density. The acoustic impedance (Reference 17, p. 138) of the light boundary gas would compare to that of the burned gas. Also, the burned gas would most likely not be subject to further oxidation; therefore, it would appear inert relative to the explosive mixture.

The studies of Sommers (17), Dabora, et al. (18), and Lu (19) involved the propagation of a gaseous detonation wave bounded by an inert gas. In addition, Dabora, et al., and Lu noted that for certain explosive-boundary combinations the detonation wave did appear to travel at half the Chapman-Jouget velocity. For this reason it was decided to construct a test section similar to that used by these experimenters but with some modifications as will be described.

3.1 Preparation of the Explosive Mixture and Method of Charging the System.

The extremely flammable nature of the explosive mixtures used necessitated the mixing and charging system to be constructed in such a manner as to minimize the possibility of any accidental ignition. To reduce the possibility of an accidental misfire, several safety features were installed in the system. These will be duly noted in the description of the system.

Figure 11 is a schematic diagram of the system. All connecting lines are 1/4 in. stainless steel with the exception of the detonation tube. The pre-mixed explosive storage tank was a Hoke, 5 gal., stainless-steel sampling cylinder. Another small steel tank (7 in. dia. × 12 in. high) was used for pre-mixing and storing some non-inert boundary gases which were used for investigating the propagation velocity of a detonation wave when bounded by a low density explosive gas. The butane was a C.P.

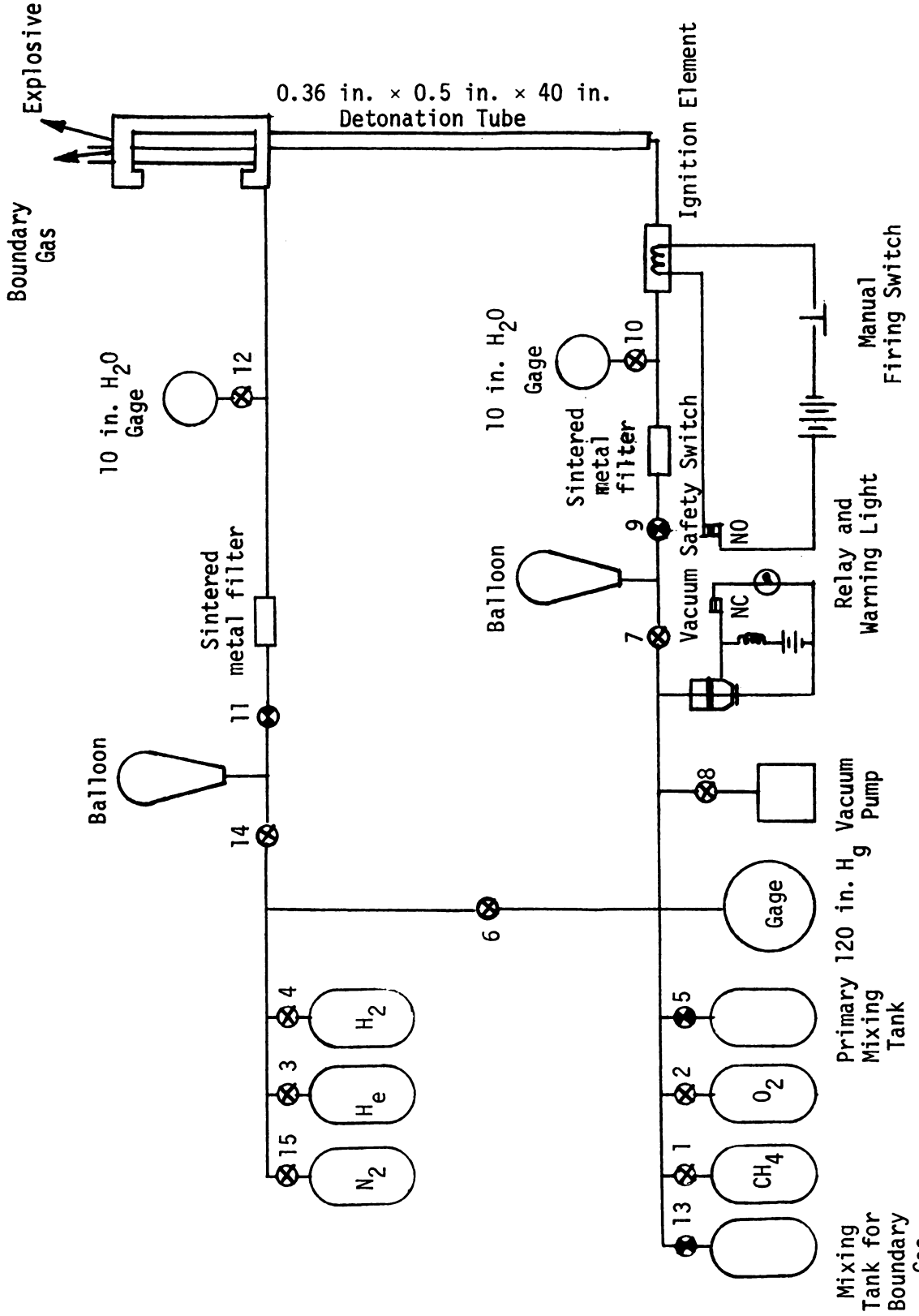

FIGURE 11. Schematic Diagram of Mixing and Charging System.

grade and stored in a 1-S cylinder; the other tanks were of the 1-A size and contained research grade gases.

To prepare the explosive mixture, the mixing tank and its related connecting lines were evacuated. The gases were then allowed to flow into the storage tank in order of their molecular weight, e.g., methane, then oxygen. The composition of the explosive mixture was obtained through the partial pressure method where the pressure was monitored by a Marsh test gauge, series 2100. The scale was subdivided into 0.1 in. of mercury increments which enable the operator to accurately control the partial pressure of each constituent. The mixing tank was generally charged to 120 inches of mercury (absolute) and the explosive mixture was allowed to stand for at least two hours, to insure adequate mixing, before being used. When the small boundary gas tank was used, it was charged in the same manner as described for the filling of the main system tank.

The detonation tube was a stainless steel welded assembly with 1/4 in. walls and a channel dimension of 0.36 × 0.5 × 40 in. Prior to assembly, the surfaces which were to comprise the channel walls were finished in order to minimize disturbances which might occur as a result of wall irregularities.

The explosive charging system was a flowing system in that the explosive mixture was flowing upwards through the detonation tube and the test section while the detonation was being formed.

This was done to minimize diffusion between the explosive and the boundary gas in the test section. To provide a flowing system of the pre-mixed explosive requires a storage chamber existing at a pressure somewhat above atmospheric pressure. Since there was always the possibility of the detonation flashing back into the storage area, a balloon was used as a temporary explosive reservoir. That way, if the detonation did flash back to the temporary storage area only a balloon would be exploded rather than a metal tank. However, this was still not a very safe system since the hazard posed by the exploding balloon, when nearly full (a volume of approximately 0.85 cu. ft.) could be sizeable. To prevent a flashback into the balloon a sintered metal filter was installed between the balloon and the ignition point. Egerton, et al. (40), and Lu (19) had both demonstrated the feasibility of using a sintered metal filter as a means of quenching a detonation wave. A Hoke 6312G4B micron filter with a 80410-5 filter element (40 to 55 micron range) was installed in the line. Although the filter did prevent the detonation wave from propagating back into the gas stored in the balloon, combustion of the explosive mixture does occur within the filter housing. This results in very high temperatures within the housing. If the combustible gas is allowed to flow for very long after the detonation has taken place the filter will be damaged to the extent that a flashback to the balloon could take place. The procedure

was then to immediately close the explosive gas metering valve after the detonation had occurred. This practice was also followed when using an explosive boundary gas since that supply line also contained a similar sintered metal filter.

To provide a means of isolating the temporary storage of the explosive gas in the balloon from the explosive gas mixing tanks, the lines between these storage areas were evacuated. The evacuated section of lines could then serve as buffer zones to insure that the detonation could not flash back to the main storage areas. To further insure that this section was evacuated prior to ignition, a vacuum switch (Figure 12) and a red warning light were installed in conjunction with a DPDT relay. The relay, two 6V. power sources, a red warning light and the vacuum switch were arranged as shown in Figure 11. The warning light was connected to the normally closed side of the relay to provide a positive visual indication, even in a darkened room, when the line was evacuated. The glow plug, which served as the ignition source, the firing switch and another 6V. battery were connected in series to the normally open side of the relay. To evacuate the line and close the vacuum switch, valves 1,2,5,6,7 and 13 were closed and valve 8 was opened. The line was then evacuated which resulted in the vacuum switch closing and the relay being energized to open the normally closed portion, thereby causing

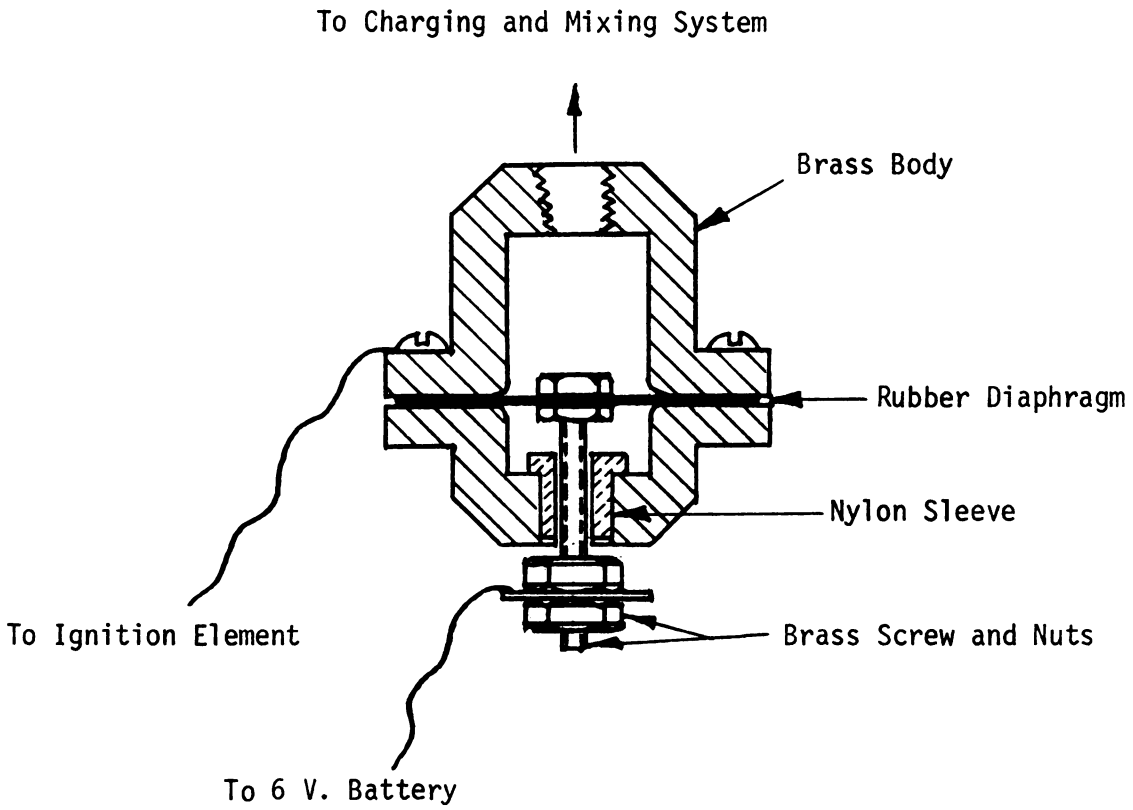

FIGURE 12. Vacuum Switch.

the red warning light to go out as well as closing the normally open side of the relay. This completed a circuit allowing the glow plug to be energized and ignite the explosive mixture.

3.2 Separation of the Explosive Gas from the Boundary Gas by a Thin Film.

The ideal configuration to investigate the interaction of a detonation wave with a boundary gas would be to have one gas bounded immediately by the other. Sommers' (17) investigation revealed that diffusion could be a governing factor in the ability of a detonation wave to propagate through an explosive mixture. He was also able to show that even the confinement provided by a .0005 inch thick cellophane wrap was sufficient to act as a solid wall as far as the detonation wave was concerned.

Gvozdeva (41) had observed that the presence of a nitrocellulose film with a thickness not greater than 1000Å had no effect on the refraction of a detonation wave in a methane oxygen mixture. Dabora, et al. (18), made use of thin nitrocellulose films and theoretically estimated the effect of the film in confing a detonation wave would be negligible when the film thickness, t_f, is

$$t_f \leq 0.1 \frac{\rho_e}{\rho_f} \overline{X} \quad .$$

Thin nitrocellulose films with thicknesses of less than 200Å have been successfully used in electron microscopy for

supporting specimens. These films are usually prepared by casting a single drop of a diluted collodion solution onto the surface of distilled water contained in a small Petrie dish. The solution spreads over the surface of the water, the solvent evaporates, and a thin film is left floating on the surface of the water. Various techniques have been used for removing the films from the surface of the water as described in a chapter on films in a book by Hall (42).

3.2.1. Preparation of Thin Films and Estimation of Their Thickness.

To provide what was hoped to be sufficient test section length, a thin film with a length over 17 in. was required. The initial attempts at producing a film with this dimension were performed by placing the film holder, with dimensions as shown in Figure 13, diagonally across the bottom of a 19-1/2 in. × 11-1/2 in. stainless steel utility tray which was partially filled with distilled water. Several drops of a dilute collodion solution were placed in rapid succession on the surface of the water near the center of the container. The collodion solution spread over the surface of the water until contact was made with the walls of the container. After several minutes the film holder was lifted, by hand, from the water and the surplus film trimmed from the film holder.

A great number of trials were made before a film was eventually removed from the water that completely covered the required area of the film holder. It was noticed upon drying

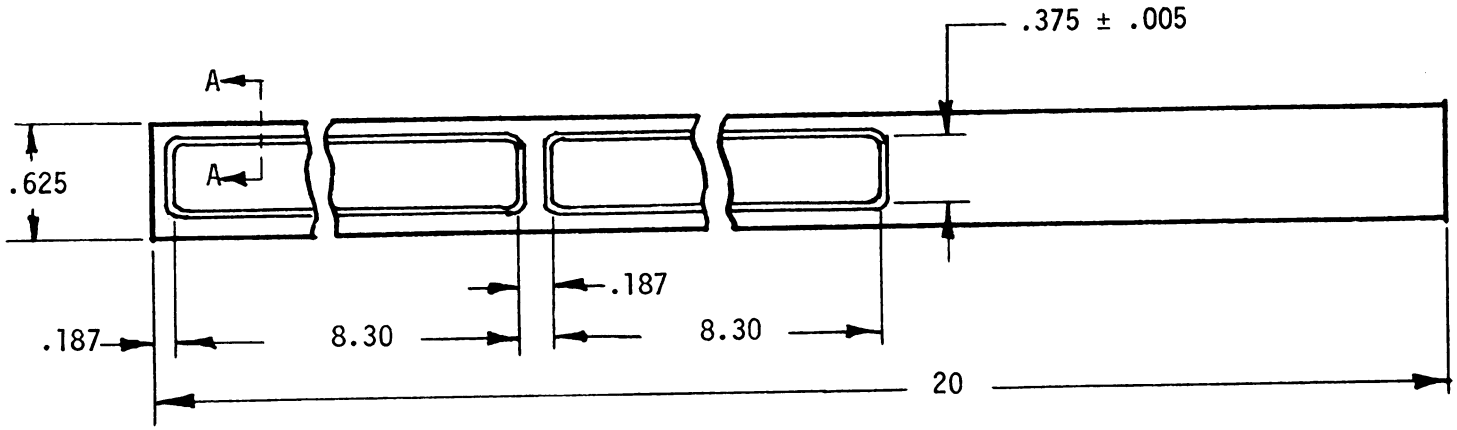

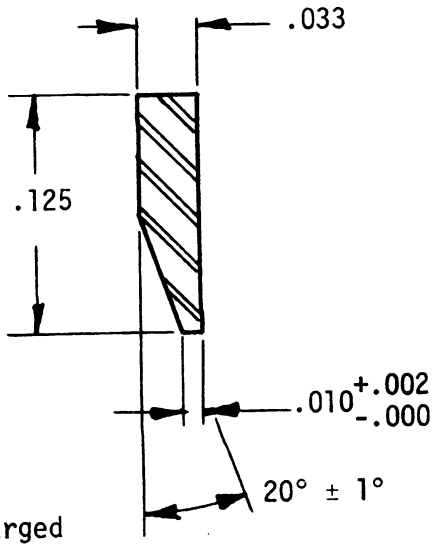

Section A-A, Enlarged

FIGURE 13. Thin Film Holder.

however, that the thickness of the film was not uniform. This determination was made based upon the results of a study by Peachy (43) who was able to make a correlation between the interference color of thin sections, when observed under white light, and their thickness. Table 2 shows the color-thickness correlation for films with an index of refraction = 1.5. The index of refraction of nitrocellulose is 1.514 which is close enough to 1.5 so that the values given in Table II can be considered applicable.

TABLE 2

COLOR THICKNESS CORRELATION FOR THIN FILMS
(Index of Refraction = 1.5)(43)

Thickness Range	Interference Color
< 600 Å	Gray
600 - 900	Silver
900 - 1500	Gold
1500 - 1900	Purple
1900 - 2400	Blue
2400 - 2800	Green
2800 - 3200	Yellow

Noting some gold and purple as well as silver and gray interference colors in the film, it was decided to try some other collodion solutions as well as different containers for the distilled water upon which the collodion solution was cast. Also, since a great deal of effort had been expended in getting the film off the water and onto the film holder without breaking, it seemed possible that a mechanical system could be designed to lift the film holder. This idea was finally abandoned after several unsuccessful attempts to construct a lifting system.

The eventual method of producing thin films was not significantly different from the method first tried. The container for the distilled water was a large elliptical shaped, aluminum serving tray measuring 25 × 21 in. along its major and minor axes, respectively and approximately 1-1/4 in. deep. The tray was partially filled with distilled water to a depth of approximately 3/4 inch. The film holder, which had been modified to remove the cross-piece from the center, was then placed in the water parallel to the major axis of the container. After the surface disturbances in the water had decayed, six drops of a 25% solution of collodion in amyl acetate were rapidly placed on the surface of the water along the longitudinal axis of the film holder. Care was taken that each drop was placed within the area covered by the spread of the preceding drop. This resulted in a film which spread in an

elliptical pattern and did not make contact with the sidewalls of the container. As the solvent evaporated, broad diffraction color bands appeared over the surface. When they disappeared, the film holder was gently lifted, by hand, at a slight angle. At the same time, the film holder was slightly rotated about its own longitudinal axis so that it initially made contact with the film only along an upper edge of the film holder. As the film holder was lifted further out of the water its upper edge usually began cutting the film although it was sometimes necessary to start the cut with a razor blade. The holder was slowly lifted out of the water with the film adhering to both the flat and chamfered parts, completely covering the opening. Any surplus film hanging from the lower portion of the film holder was trimmed off with a razor blade. The film holder was then hung so the excess water could drip and/or evaporate until the film was dry. The result was a smooth, evenly-colored silvery-gray film. Based on Peachy's (43) correlation it was evident that the film was less than 900Å thick. Before another film was made the surface of the water was "wiped" with a glass rod to pick up any film that was remaining. It was found also, that a piece of filter paper "wiped" over the surface was effective for picking up film residue.

It was also possible to make a determination of the film thickness by a method based on residue volume where it was assumed that the film was evenly distributed over the water

surface. From the uniform color of the film, this seemed a reasonable assumption. A relation for the calculation of film thickness can be written as

$$t_f = \frac{m_v V_c n}{A_f n_v \rho_f} \tag{3.2}$$

where m_v = mass of nitrocellulose per unit volume of collodion
= 0.12 gm/cc

V_c = volumetric concentration of collodion in amyl acetate
= 0.25

n = number of drops used = 6

A_f = area covered by the film = 1225 cm^2

n_v = number of drops per unit volume - 28/cc.

ρ_f = density of nitrocellulose = 1.58 gm/cc.

Using these values, the film thickness was determined to be 0.335×10^{-5} cm = 335Å. For an explosive (50% H_2 - 50% O_2) density $\triangleq 7.0 \times 10^{-4}$ gm/cc, at 70°F and 14.7 psia, and a conservative estimation of the reaction length of 2 mm, the maximum allowable film thickness from Equation (3.1) was found to be 8.90×10^{-6} cm or 890Å. For a mixture of 30% CH_4 - 70% O_2, the mixture density for the same pressure and temperature conditions as before is $\triangleq 1.11 \times 10^{-3}$ gms/cc and the maximum allowable film thickness was determined to be about 1.4×10^{-6} cm or 1400Å. Based

upon these values, the film thickness used was well below the allowable values and we can conclude that the effect of the film was negligible.

There are several disadvantages in working with such a thin film. The first and probably the most obvious is the difficulty in getting the film onto the film holder and off of the surface of the water without breaking. The second disadvantage is that the thinness of the films made them subject to breakage as the water was evapoated off their surface. Coupled with the frequent breakage encountered in positioning the films in the test section, which will be described shortly, it is estimated that only about one of every ten thin films made was useable.

3.3 Test Section

The detonation tube described earlier, terminated in the test section shown in both Figures 14 and 15. The original test section included two 1/2 in. glass plates which served as the front and back walls. Each glass plate had two grooves, 0.035 in. wide × 0.135 in. deep for the film holders to slide through. When the film holders were inserted into the test section from the top and slid into position, they formed two identical channels. The inner channel (the one next to the solid wall) formed a continuation of the detonation tube; whereas, the outer one could contain a column of inert or explosive boundary gas. The portion beyond the outermost thin film was open to the

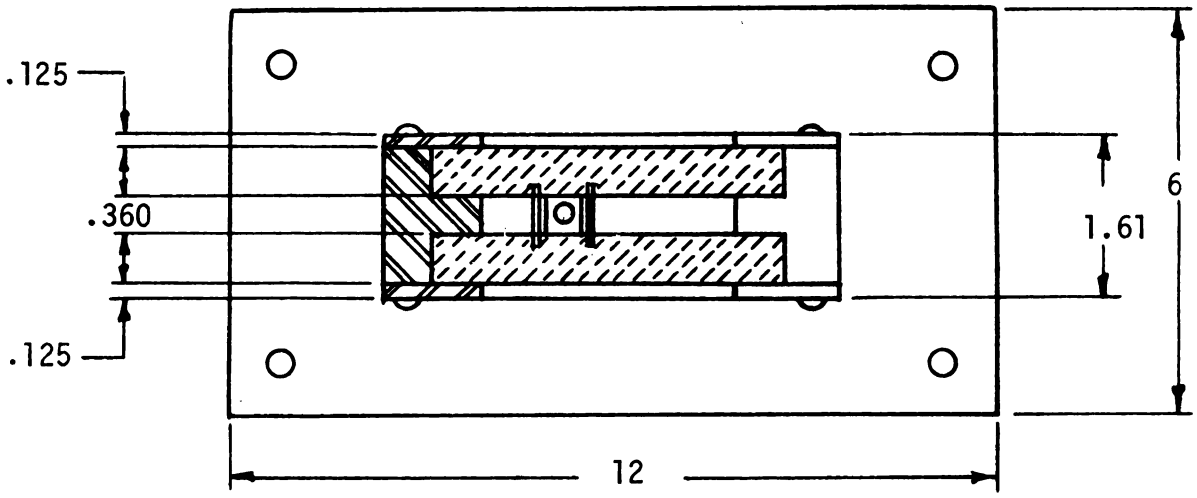

Section A - A

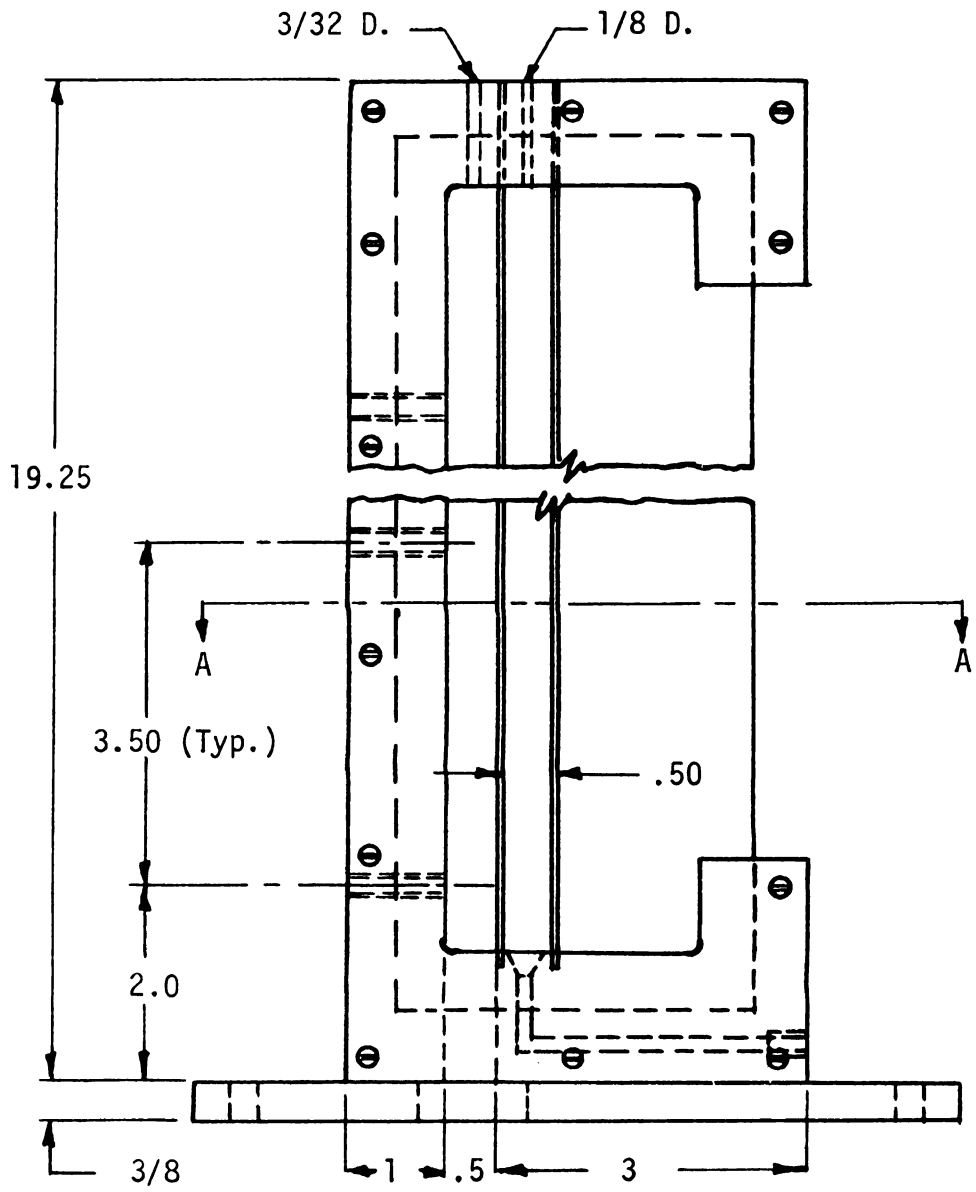

FIGURE 14. Test Section Assembly.

FIGURE 15. Photograph of Test Section.

atmosphere so as to provide minimum confinement of the detonation and try to reduce the pressure as rapidly as possible so as to prevent the breakage of the glass. The cross-sectional area selected for the channels was a compromise between size necessary to avoid quenching due to channel size and the size necessary to avoid the hazard posed by a large volume of explosive gas. Even so, several sets of glass plates were broken while running with only one column in the test section filled with an explosive mixture. The machined grooves in the glass plates served to raise the stress in these areas and all fractures were observed to have commenced at the groove. Experiments with an explosive mixture bounded by another explosive gas were limited because of the danger posed by flying glass particles.

As a result of the continual fracture of the glass plates it was decided to replace them with a clear acrylic. Although the optical characteristics of acrylics are usually not as good as glass satisfactory results were obtained by using 1/2 in. thick, Plexiglas II, UVA. After substituting the acrylic plates for the glass, only one set of plates was fractured when running a single column of explosive.

3.4 Equipment for Velocity Measurement.

Two electronic timers were utilized for most of this study: a type 1192/Z General Radio 32 MHz counter and a Model 5326A Hewlett-Packard 50 MHz counter. Both timers were capable of measuring time intervals down to 0.1 μsec with an accuracy of ± 0.1 μsec.

Both ionization probes and pressure transducers were used to detect the passage of the detonation wave. Two ionization probes were used in the detonation tube and positioned 16.000 in. apart. The probes were constructed by twisting two pieces of 18 gauge copper magnet wire together and inserting them through the center hole of a threaded stainless-steel housing. The wire was then sealed in place by filling the void portion of the center hole with an epoxy cement. After the epoxy dried, the portion of the wire extending from the end of the probe assembly which was to be threaded into the detonation tube was clipped off flush with the surface of the housing. This yielded what was considered to be an ideal ionization probe; viz, two bare copper wire ends that were electrically insulated from each other yet, separated by only two layers of varnish. The entire assembly was threaded into the detonation tube and comprised part of the smooth interior wall. A sketch of the assembled probe is shown in Figure 16.

Although the use of ionization probes offers an economical means of producing a signal to start and stop electronic counters, there are certain disadvantages associated with their use. It was found they are subject to fouling due to the water vapor produced in the detonation tube and the signal pulse produced was of such a duration that it was not suitable for use with all

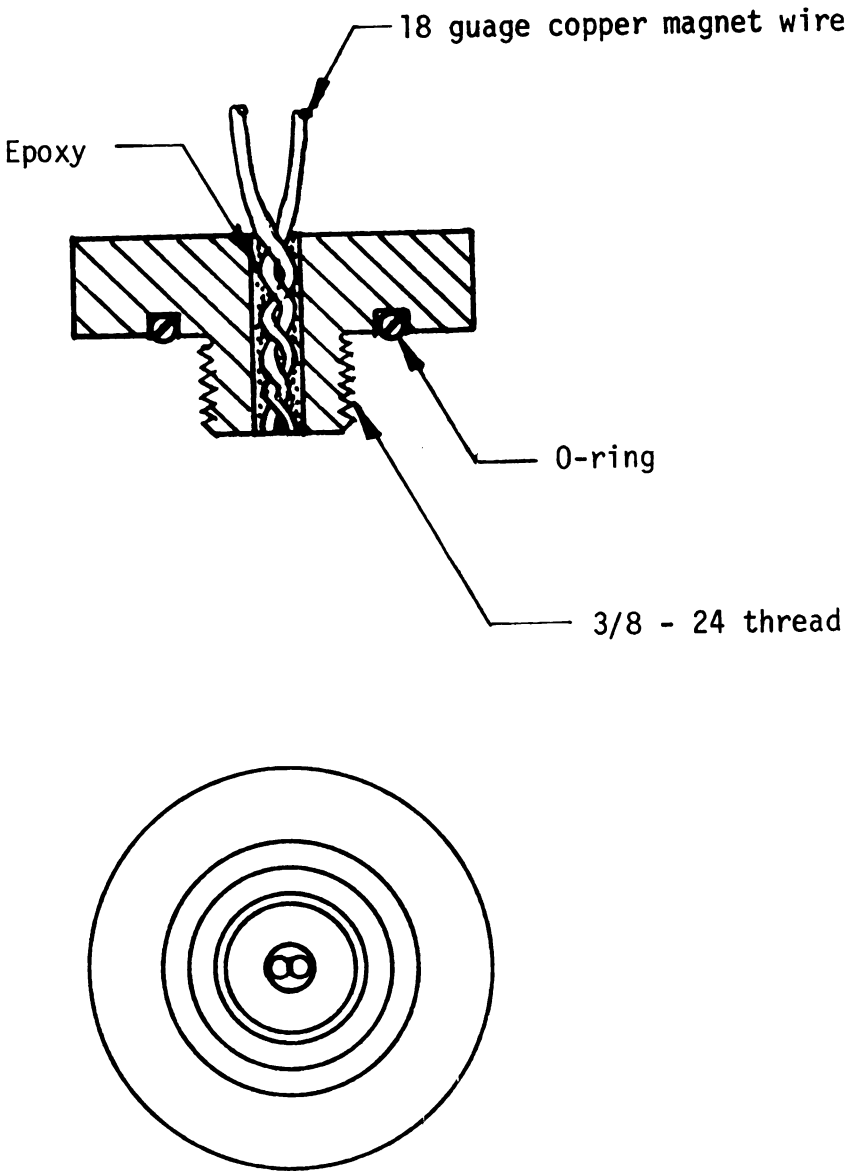

FIGURE 16. Ionization Probe Assembly.

electronic counters without the use of an additional circuit to shape their output pulse.

The fouling factor associated with the ionization probes was easily remedied by thoroughly cleaning them each day. This was accomplished by removing them from the detonation tube and lightly sanding the clipped ends with a fine grade emery paper to remove any oxides. It was found that a cleaning prior to the first run of the day was usually sufficient to prevent counter malfunction caused by probe contamination.

The problem associated with the required shaping of the output pulse of the ionization probes was not as easily remedied but once accomplished proved to be reliable. The probes were initially set up as shown in Figure 17. As the detonation passed the clipped ends of the probe it acted like a momentary closure of a switch and in effect put a -6V. pulse onto the input circuit of the General Radio Type 1192/Z counter. It was found that the counter would start as the detonation wave passed the probe but would not shut off as the wave passed the next probe which was connected to the stop channel of the counter. In order to determine the problem, the output of each probe was connected into a Tektronix Type 564 storage oscilloscope. The signal output of each probe was found to be satisfactory in magnitude, i.e., less than the -5V. necessary to overcome the bias on the start and stop channels and of a relatively long duration. Subsequent investigation of the counter characteristics disclosed

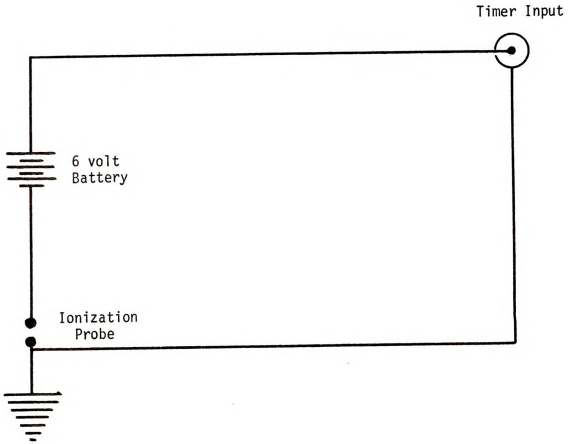

FIGURE 17. Circuit Diagram of Ionization Probe Installation.

that it was set up so that the pulse applied to the stop channel was ineffective as long as the start channel was still receiving an input signal. Because of the high velocity of the detonation wave, the resulting small time interval between pulses applied to the input channels of the counter and the relatively long time period during which the probes were in conduction, necessitated a circuit to shape the output pulse from the ionization probes. This circuit is shown in Figure 18 which is a one-shot multivibrator circuit.

The purpose of a one-shot multivibrator is to produce an output pulse of predetermined duration whenever a trigger pulse of sufficient amplitude is applied. In this circuit, the detonation wave passing the probe reduces the resistance across the exposed clipped ends which results in sufficient current flow to produce a trigger pulse in transistor T1 which is normally cut-off. Transister T2, which is normally saturated is now cut-off by the pulse that is coupled through the 56 pf. capacitor to its base. The output pulse width is governed by the value of this coupling capacitor and is taken from the collector of transitor T1. The input to the multivibrator is shown in Figure 19a and the resulting output pulse is shown in Figure 19b.

The battery voltage applied across the probe was increased from 6 to 90V. to insure an extremely rapid rise time to the

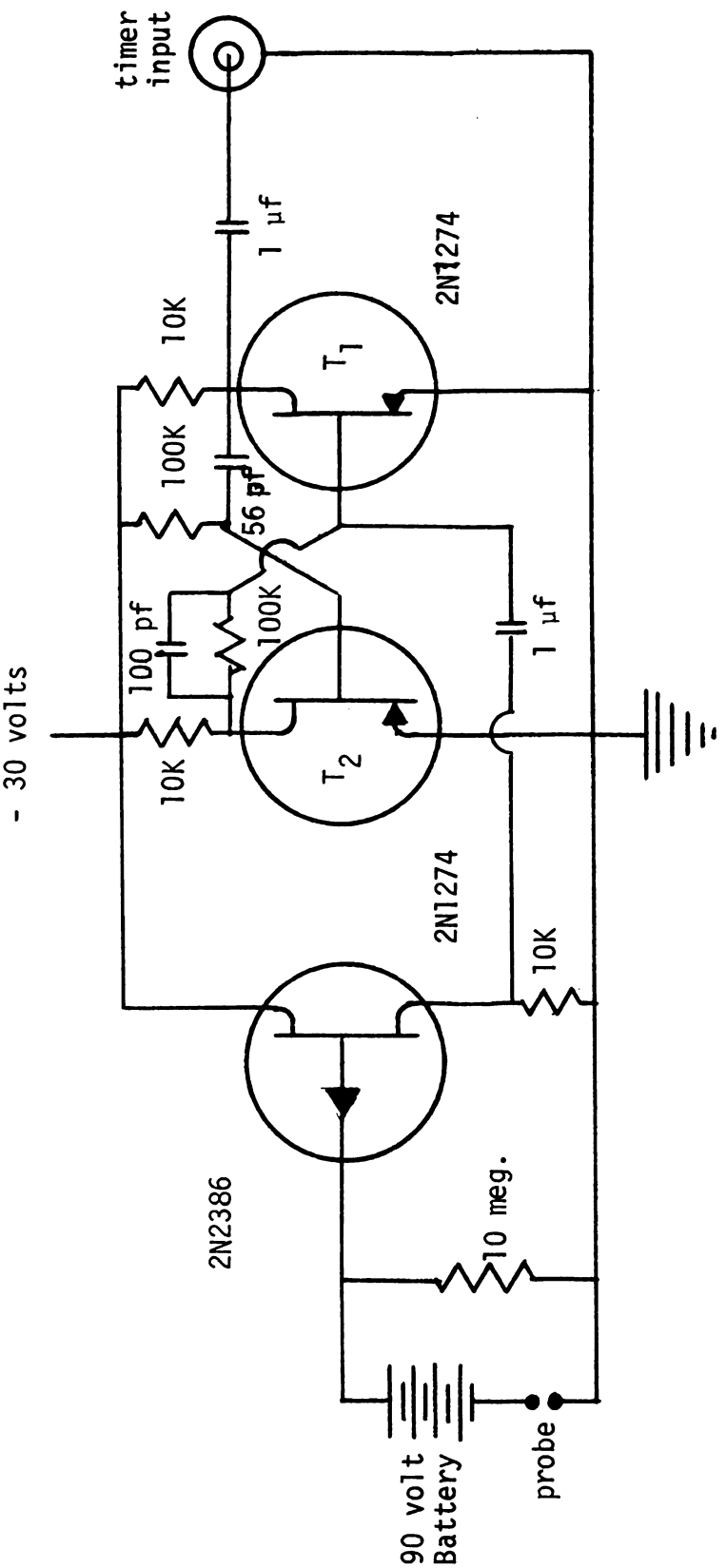

FIGURE 18. One-Shot Multivibrator Circuit.

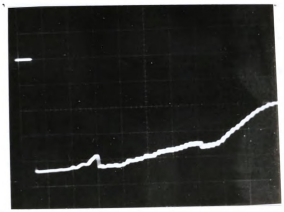

(a) Input to Multivibrator Circuit.
Scale: 0.2 msec/div. - horizontal
20 v/div. - vertical

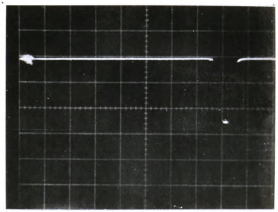

(b) Output of Multivibrator Circuit.
Scale: 5 sec/div. - horizontal
5 v/div. - vertical

FIGURE 19. Input and Output of Multivibrator Circuit.

necessary trigger level voltage. With the counter triggering on a pulse of - 5V. or less, it can be seen from Figure 19b that the effective rise time is approximately 1 μsec. Since this is also the delay incorporated in a similar circuit connected to the stop channel of the counter, the effect is self-cancelling and the correct time interval for the detonation wave to pass from one probe to the other is recorded.

The Hewlett-Packard time interval counter was of such a design that the stop channel could be activated even if the pulse applied to the input channel was still present. It was more suitable for use in the test arrangement at other positions rather than with the ionization probes, since the trigger voltages could be adjusted at the small values compatible with the pressure transducers.

Two pressure transducers, both manufactured by Celesco Industries, were used for the major portion of this study. An LD-25 blast pressure transducer was located in the detonation tube halfway between the two ionization probes. It was used to trigger the start channel of a time interval counter. The other transducer, an LD-107, was installed in the test section to generate a pulse to stop the time interval counter on arrival of the shock or detonation wave. The test section was machined so this transducer could be positioned at one of the five locations to detect velocity changes which might occur

as the detonation wave experienced side relief. The other four positions were normally fitted with screws which were flush with the sidewall. Both transducers were also used at one time or another to trigger the flash unit used for the photographic work which will be discussed shortly. The transducers incorportated a lead zirconate titanate sensing element, did not require an amplifier, and had a rise time of less than 1 μsec.

The velocity of the detonation wave passing through the detonation tube was determined by dividing the distance between the ionization probes by the time interval measured on the timer. The velocity of a detonation wave through various explosive mixtures is generally well documented. Thus, this measurement was only to verify that expected propagation velocity was achieved. Several runs were made with probes only 8 in. apart in the detonation tube. In every instance the sum of the time interval between two sets of probes 8 in. apart compared closely with measurements made when the probes were located 16 in. apart. The results were in accord with the experimental findings of other investigators and the propagation velocity of the detonation wave through the tube was noted as a constant.

The velocity of a detonation wave when subjected to side relief can vary depending upon the degree of confinement provided by the boundary gas. For this reason, the determination of the velocity through the test section was made by noting the time of arrival at the five distinct points in the test section and

plotting the data as distance versus time. Since only one transducer was available for use in the test section, several runs were made at each position to insure repeatability. Then the transducer was moved to a different location and the process repeated. The average velocity was determined at any point within the test section by computing the slope of the line on the time versus distance plot; the results of which will be discussed in the next chapter.

3.5 Photographic Equipment.

The photographic equipment made use of a simple schlieren system (44) using a pair of 18 in. diameter, bi-convex lenses of 60 in. focal length. These lenses were acrylic and were not of the finest optical grade; however, they were acceptable since only the major characteristics of the detonation wave were required to be observed. The collimating lens was located three feet from the test section which was as close as was deemed practical in an attempt to avoid damage to the lens should the test section windows shatter and flying fragments result. The focusing lens was located slightly over 9 ft. past the test section and the film plane located such that an image magnification of about 1.1 was achieved.

The light source was an EG & G 549 Microflash System that produced a peak light of 50×10^6 beam candlepower with

a duration of 0.5 μsec. Although the system incorporated a time delay (uncalibrated) it was generally set for zero delay and triggered by the passage of the detonation wave or shock wave over the face of the pressure transducer located in the test section. An iris diaphragm was located in front of the air-gap flash tube of the Microflash System to regulate the size of the source and was normally set for an opening of 4 mm.

The light produced by the spark in the air-gap flash tube was focused by the second lens of the schlieren system so that it passed through a "pin hole" and was concentrated at a horizontal knife edge so positioned that approximately half of the light was intercepted. The "pin hole" located in front of the knife edge was large enough so as not to interfere with the light to be cut-off by the knife edge and was installed to prevent fogging of the negative caused by the luminosity of the detonation process.

The film was either Polaroid Type 57, ASA 3000, or 4 × 5 Royal-X Pan ASA 1250. Depending on the type, the film was held by a Polaroid 4 × 5 Land Film Holder #545 or a 4 × 5 Graflex Sheet Film Holder. These holders, in turn, were positioned in a Graflex camera back. No shutter was used as extraneous light was prevented from reaching the film by the bellows, the pin hole and by operating in a darkened room. Figure 20 shows a schematic

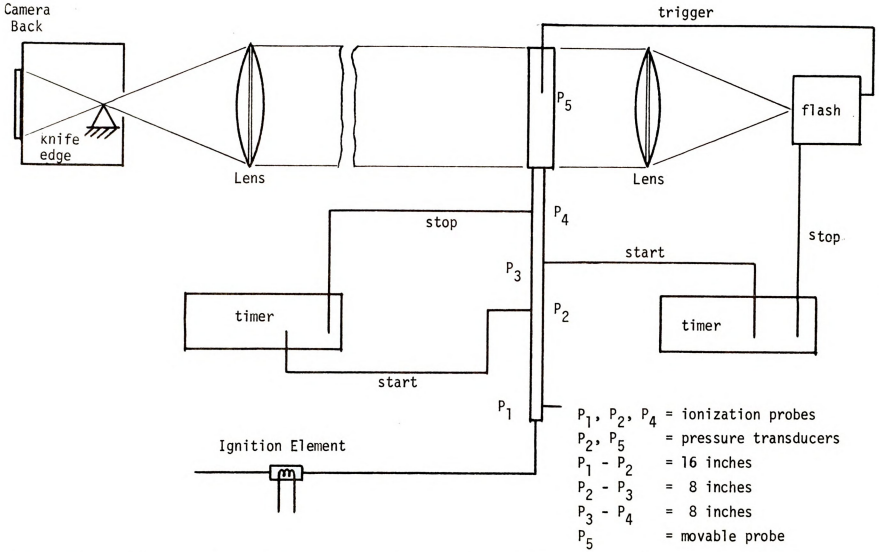

FIGURE 20. Schlieren System and Block Diagram of the Instrumentation Used for Obtaining Flash Pictures.

diagram of the schlieren system and a block diagram of the instrumentation used for obtaining spark pictures.

3.6 Experimental Procedure

All equipment was checked for proper settings and operating condition; the test section and connecting lines were inspected for possible damage and film was loaded into the camera back. Dry nitrogen was then passed through the detonation tube and test section to flush out any residual moisture from the previous run. Two film holders on which thin films had previously been mounted and with their edges coated with a light film of vacuum grease to provide a seal with the slots in the acrylic plates, were inserted into the test section. With valve 9 (Figure 11) closed, the balloon for the primary explosive was first evacuated and then filled with the explosive mixture. The balloon was charged until its volume was approximately 100 times the total internal volume of the charging tube and the detonation tube. Valves 5 and 7 were then closed and the section of the tube between them was evacuated.

To insure purity of the boundary gas, valve 11 was closed, valves 6 and 14 were opened and the balloon for the boundary was evacuated. If the balloon for the boundary gas was to contain an explosive, values 8 and 11 were then closed and valve 13 was opened, thereby charging the balloon with a premixed explosive.

Valves 13 and 14 were closed, valve 8 opened and then valve 6 was closed which then isolated the temporary explosive storage areas from each other as well as from the premixed explosive storage tanks by evacuated sections of line. The evacuation of the line caused an automatic closing of the vacuum switch which in turn caused the normally open side of the relay to close. This completed part of the circuit to the glow plug: the remaining portion of the ciruit was completed by manually depressing a firing switch. A glow plug rather than a spark plug was used since a spark discharge caused problems with some of the electronic equipment.

Generally, an inert mixture was used for a boundary gas. With valves 6 and 11 closed and valve 14 open, the inert gas was allowed to flow into the balloon located in the boundary gas supply line. Then valves 9 and 11 were opened simultaneously allowing both the boundary gas and the explosive mixture to flow into the test section. Care was taken to keep the pressures of the boundary and explosive gas the same at all times. Pressure gauges, Marshalltown, Figure 83C, measuring 10 inches of water full scale and with 1/8 in. of water increments, were located in the explosive and inert gas delivery lines. Valves 9 and 11 were adjusted so the delivery pressure was maintained at 1.5 in. of water. A double check that the pressures were the same on each side of the thin film separating the explosive and

inert gas was made by observing light reflection from the film. Should a pressure imbalance occur, the film bowed and the light reflection pattern was distorted.

When the balloon containing the explosive was almost exhausted, several minutes after opening the flow valves, the room lights were extinguished, the slide covering the photographic film was removed and valves 10 and 12 were closed. These protected the pressure gauges from damage due to high pressure pulses. The manual firing switch was then depressed momentarily initiating the detonation. Valves 9 and 11 were closed, the slide covering the photographic film was replaced and the room lights were turned on.

The major portion of the photographic work in this study was accomplished using Polaroid film so that the results of a particular run could be examined almost immediately. This was important since the very nature of this experiment involves a number of critical components and their adjustments and/or alignments. If the picture indicated a need for an adjustment of a component it was made prior to making any further runs. Also, the time intervals indicated by each of the electronic counters was recorded.

In order to obtain a complete sequence of photographs of any one explosive-boundary combination the light source, optical system,

knife edge and film holder were adjusted to new locations and the pressure transducer in the test section was installed at the proper position. The experiment was then repeated. This procedure was followed until sufficient photographic and distance-time data was collected.

CHAPTER IV

EXPERIMENTAL RESULTS AND DISCUSSION

The intent of this study was to determine the effect on the propagation velocity of a detonation wave when a gas much lighter than the explosive gas is used as a confining medium. Such a condition existed in the annular channel used by Voitseknovskii (12) where, after the first cycle, the burned gas is pushed radially outward by the fresh charge, thereby acting as the confining medium for the detonation wave in the next cycle. The burned gas is expanded from the Chapman-Jouget pressure to the lower pressure of the incoming charge. However, it would still be at a higher temperature than the incoming charge; consequently, its density would be much lower than the charge.

4.1 Effect on the Propagation Velocity of a Gaseous Detonation Wave When the Density of the Boundary is Much Lower Than That of the Explosive.

As shown in Chapter II, there is a possibility the required boundary gas pressure ratio, P_{i2}/P_{i1}, cannot be achieved through an oblique shock. For this case an oblique shock solution does not exist. Figure 8 shows that detachment will generally occur when the oblique shock wave is between 62° and

72°, depending upon the detonation Mach number and the specific heat ratio of the boundary gas.

Figure 21 shows the development of the detached shock when a detonation wave propagates through an explosive mixture composed of 30% CH_4 + 70% O_2 with a helium boundary. It is seen from this sequence of photographs that over approximately 15 inches of the test section through which the interaction has occurred a steady state condition has not been reached. This observation is based on the fact that the distance between the shock front at the solid wall and the leading shock in the boundary gas has continued to increase.

A minimum of five runs were made at each of the five available probe positions in the test section. From the data recorded it was possible to plot (see Figure 22) the position of the detonation wave versus the elapsed time from a fixed reference point (probe 3). Based upon what was considered to be the best line drawn from the point at which the detonation wave exited from the tube through the mean of the other five points it was found that the detonation wave exhibited a marked change in propagation velocity within the first inch of travel after experiencing side relief.

Another interesting feature was found when the slope of the line between probes 5 and 7 was measured and determined to correspond to a velocity that was almost exactly one-half

Y = .42 ft.
(a)

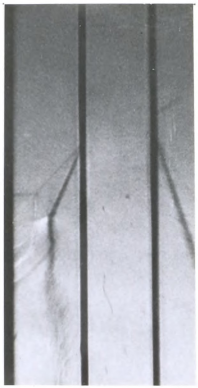

Y = .97 ft.
(b)

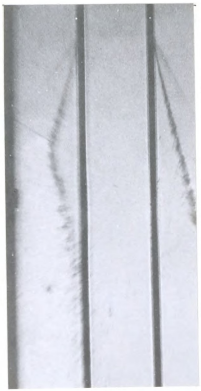

Y = 1.3 ft.
(c)

FIGURE 21. Schlieren Photographs of the Development of a Detached Wave. (30% Methane - 70% Oxygen, Helium Boundary).

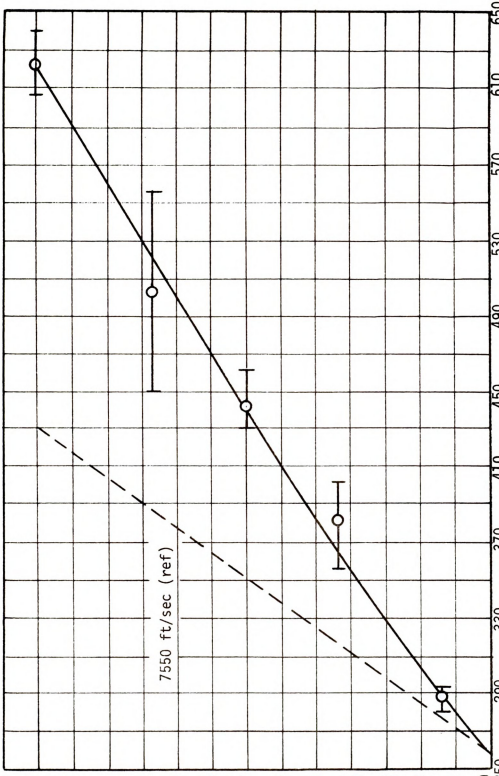

FIGURE 22. Position versus Time of a "Detonation" Wave in a 30% Methane - 70% Oxygen Mixture with a Helium Boundary.

the velocity exhibited by the detonation wave when confined by the solid tube. The indication is, therefore, that the wave velocity decreases rapidly over a length of slightly more than one inch when confined by a much lower density inert boundary gas. It appears to travel for approximately the next seven inches at an average velocity of half the Chapman-Jouget velocity (the result first reported by Voitsekhovskii and noted by Dabora, et al, and Lu). It might be concluded that the wave velocity was a constant at this point had not the additional length of the test section been available. As the detonation wave continued to propagate however, the velocity decreased slightly until it reached a seemingly constant velocity for the last 3.5 inches of measured travel. The velocity over this range corresponded to a value that was 44% of the Chapman-Jouget velocity.

Since the position of the line drawn through the data scatter of Figure 22 is subject to individual judgment, a further evaluation of the data seemed appropriate. Using the data of Figure 22, the equation corresponding to the least square parabola was calculated to be

$$Y = -.06 + 39.2 \times 10^{-4}t - 7.67 \times 10^{-7}t^2 \quad . \tag{5.1}$$

The curve corresponding to this equation is plotted in Figure 23 and shows some curvature for small values of t but appears to become linear for large values of t.

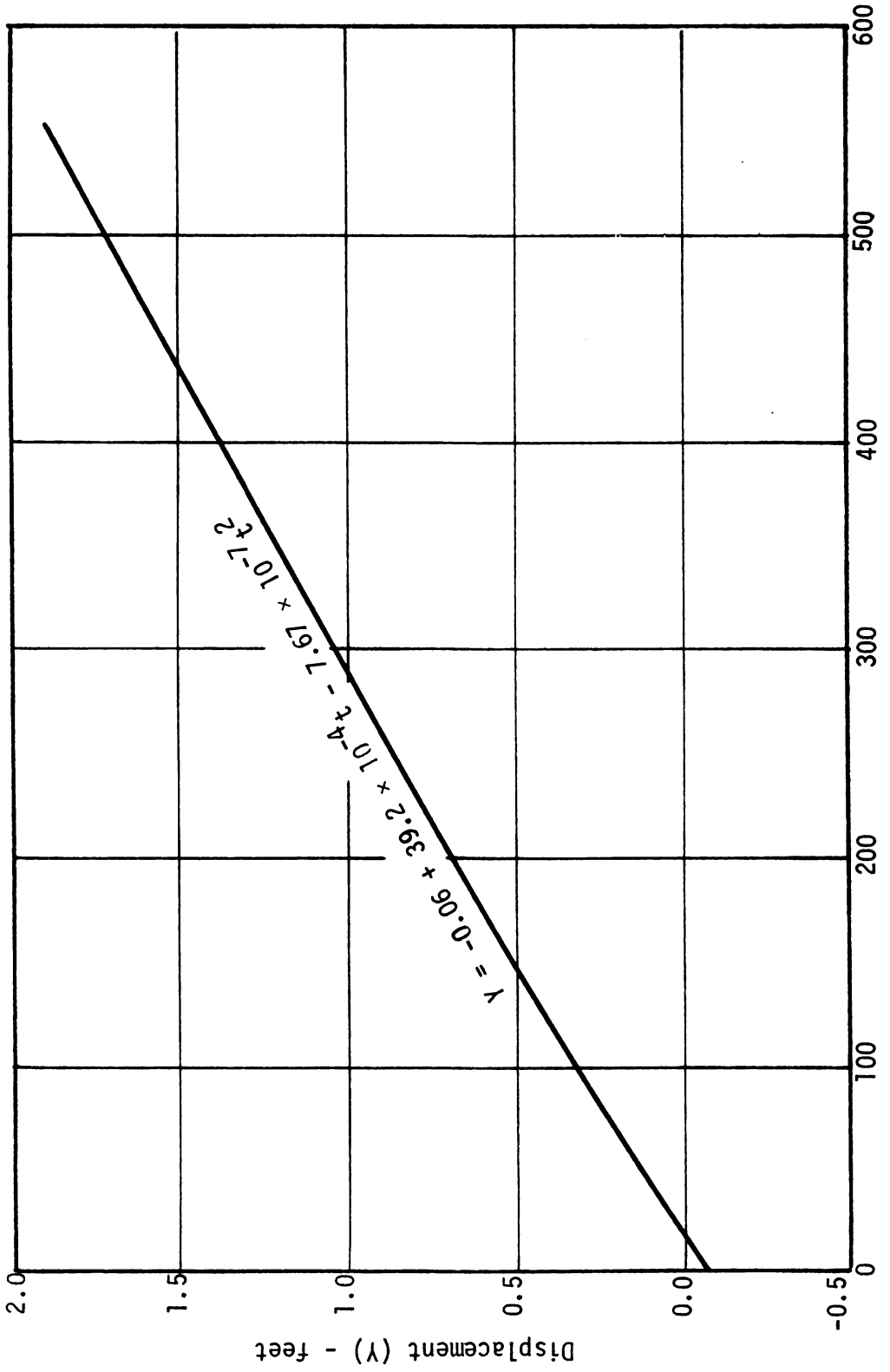

FIGURE 23. Least Squares Curve Fit of the Data Obtained from a "Detonation" Wave in a 30% Methane - 70% Oxygen Mixture with a Helium Boundary.

The questions that remained were (1) Is this wave that propagates at a low velocity a true detonation wave, and (2) Why did the velocity appear constant over portions of the test section?

To determine the possibility of the existence of a sub-Chapman-Jouget detonation wave it is necessary to examine several conditions that would lead to the required end state. These conditions will be discussed individually.

4.1.1 Degree of Completion of the Chemical Reaction and the Thickness of the Reaction Zone.

A detonation wave has been characterized as a shock wave followed by an exothermic chemical reaction initiated by the high local temperature and pressure. As was indicated in Chapter II, the chemical reaction cannot be instantaneous. Therefore, it must occur over some finite distance. The representation of a finite reaction zone by a family of Hugoniot curves corresponding to different extents of reaction is shown in Figure 24. If it is initially assumed that the detonation wave is a steady state phenomenon, all states through which the system passes must lie on a single Rayleigh line, thus corresponding to the same detonation velocity. When a detonation occurs in a channel of constant cross-sectional area, the initial transition must be to a point A (Figure 24) which lies on the unreacted Hugoniot or pure shock curve and corresponds to a simple shock

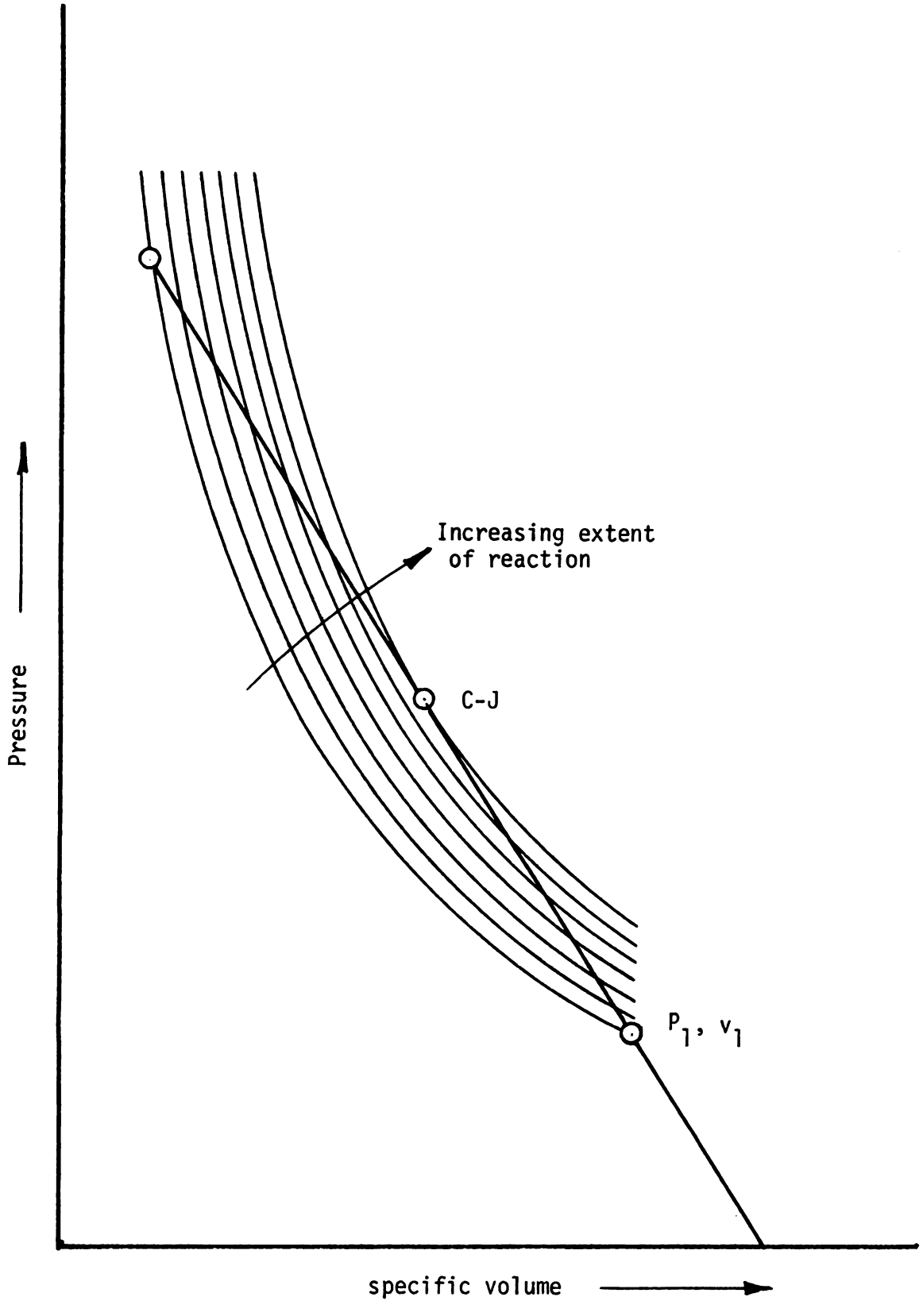

FIGURE 24. Representation of a Finite Reaction Zone by a Family of Hugoniot Curves Corresponding to Different Extents of Reaction.

transition. The state of the gas then changes along the Rayleigh line for progressively greater extent of reaction until the fully reacted Hugoniot is reached and which corresponds to the Chapman-Jouget point. The states covered by the Rayleigh line between the Point C-J and P_1,v_1 correspond to a weak detonation and when represented on the family of Hugoniot curves, it appear as an incomplete combustion process. A weak detonation wave has generally been considered unlikely to exist since it would seem the reaction would have to begin at point P_1v_1, corresponding to the initial conditions where no chemical reaction occurs, and move upward along the Rayleigh line toward the C-J point. Of interest, however, is the condition that a weak detonation wave would have a lower pressure and a larger specific volume than the state defined by a Chapman-Jouget wave.

Returning now to the experimental results and the configuration used for this study we see that the detonation wave in the detonation tube corresponds to the C-J point. As it passes out of the tube into the test section, the wave suddenly experiences side relief. The resulting effect is a decrease in pressure and an increase in specific volume as was suggested had to occur if a weak detonation wave was to exist. This state change would not occur as a result of partial chemical reaction as would seem necessary in a channel of

constant cross-sectional area but as the result of side relief. The properties corresponding to the end states would be the same in each case.

For the wave to propagate steadily at the low velocity commensurate with a weak detonation wave, it must be continually supplied with energy by the trailing exothermic chemical reaction. The criteria for the maintenance of a gaseous detonation wave propagating at the Chapman-Jouget velocity is that the reaction zone is relatively short, e.g., 0.3 to 1.9 cm (45), and is attached to the shock front (34, 35, 36). If the reaction zone begins to thicken, i.e., the distance over which the chemical reaction takes place increases, then the energy released by the combustion process cannot continue to drive the detonation wave (17). Based on the current level of understanding of gaseous detonation waves it appears that a weak detonation achieved through side relief would have basically the same configuration as a Chapman-Jouget wave. For the wave to steadily propagate at a reduced pressure and an increased specific volume the length of the reaction zone should probably show a very slight increase. This increase of length would result from the lower velocity of the detonation wave and consequently a lower local temperature immediately behind the shock wave and thereby an increase in induction time. It should be noted, however, that the increase in length of the reaction zone would be small since

it has been experimentally observed (17, 18, 26) that a marked increase in reaction zone length coupled with its separation from the shock are indicative of a quenched detonation or a deflagration wave.

The condition then for the existence of a weak detonation wave resulting from side relief is for the reaction zone to remain relatively thin. A close observation of Figure 21 indicates this is not the case for the methane-oxygen detonation wave interaction with helium. The reaction zone appears to thicken considerably. To further substantiate this observation, the time delay feature of the flash system was used to photograph the conditions some distance behind the induced oblique shock in the explosive mixture. The result is shown in Figure 25. The long turbulent region indicates the length of the reaction zone, is indicative of a deflagration (46).

Based on this observation and the results of previous studies (17, 18, 26) it appears that insufficient energy could be released to support a weak detonation wave. Thus, it is concluded that even the apparent steady state noted in Figure 22 is a transient condition. This conclusion supports the previously noted observation regarding Figure 21, from which it was determined a steady state condition had not been reached.

It was possible to determine the velocity of the shock in the boundary gas by measuring the oblique shock and interface

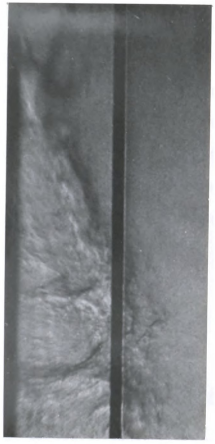

FIGURE 25. Schlieren Photograph of the Reaction Following the Intersection of a Reflected Shock Wave and the Gaseous Interface.

angles induced into the explosive mixture. Using the supersonic flow over a wedge analogue described in Chapter II, the propagation Mach number and consequently the velocity of the shock wave in the boundary gas was determined at several positions within the test section. The sequence of photographs shown in Figure 21 were used to obtain the data points at Y = 0.42, 0.97 and 1.31. The results are shown in Figure 26 and indicate a velocity decrease from a condition corresponding to an over-driven shock wave to a velocity of approximately 3300 ft/sec, the sound speed in the helium boundary. This speed found for the shock wave in the boundary gas near the top of the test section is the same apparently steady speed determined from the slope of the "best line" drawn through the data scatter of Figure 22. Thus, additional support is given to the conclusion that the detonation wave degenerates into a weak deflagration wave and a quasi-steady shock wave. This is typical of the quenching of a detonation wave (17).

4.1.2 Effect of Side Relief on Propagation and Quenching of a Gaseous Detonation Wave.

The criteria used to determine if a detonation wave is quenched are based on an examination of the wave itself. Figure 27a shows a "typical" detonation wave in that the combustion zone is "attached" to the shock front (35, 36, 37) whereas Figure 27b is "typical" of a quenched detonation wave (17). The quenched detonation wave has a shock front followed

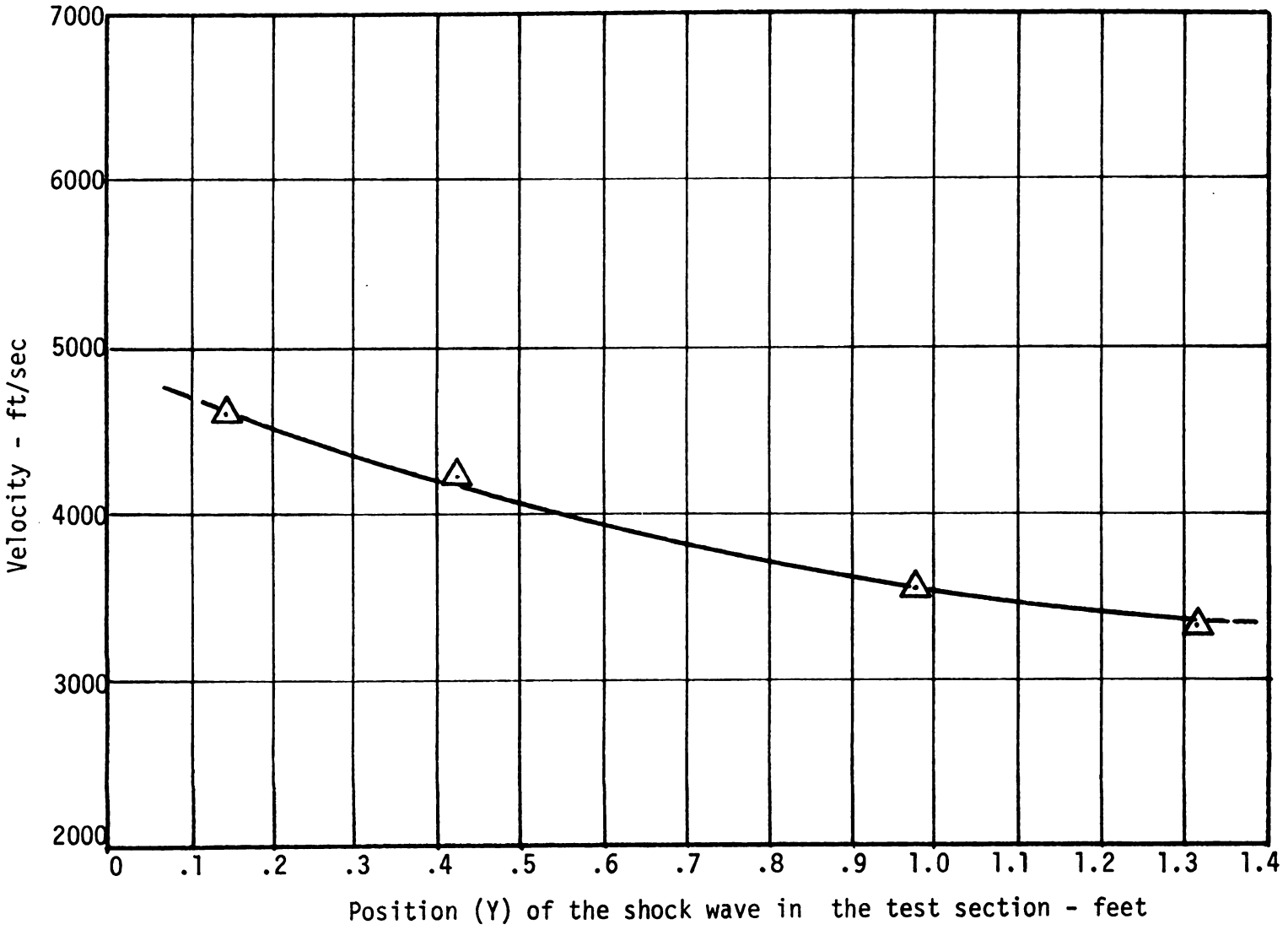

FIGURE 26. Shock Wave Velocity in the Helium Boundary with a "Detonation" Wave in a 30% Methane - 70% Oxygen Mixture.

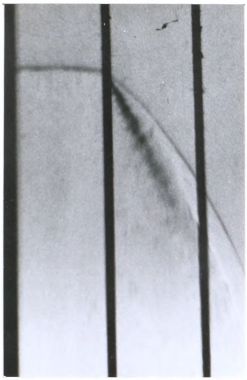

(a)

(b)

FIGURE 27. Typical Schlieren Photographs of a Quenched and Unquenched Detonation Wave.
(a) Unquenched: 50% H_2 - 50% O_2, Helium Boundary
(b) Quenched: 45% H_2 - 55% O_2, Helium Boundary

at an appreciable distance by a turbulent region. This turbulent region corresponds to the zone where the explosive either ceases to burn or is deflagrating. The greater distance behind the shock front over which the reaction occurs has been considered an indication that the energy released by the combustion process cannot continue to drive the detonation wave (17, 18, 26).

To determine the effect of side relief on the propagation of a gaseous detonation wave it is necessary to examine the work of Dabora, et al., from which it was concluded, "For H_2 - O_2 mixtures, a velocity decrement beyond 8% - 10% results in quenching of the detonation wave and its deterioration into a shock (18)." As can be seen from Figure 7, an area increase of only 17% would be sufficient to exceed a 10% velocity decrement and thereby quench an H_2 - O_2 mixture. It would appear that if the results of the previous section could be duplicated with a hydrogen-oxygen mixture, additional evidence would exist upon which to base a conclusion regarding the existence of weak detonation waves.

From the determination of shock and interface angles of Chapter II, it was found that an oblique shock solution did not exist for an explosive mixture of 50% H_2 - 50% O_2 with a helium boundary. This indicates that the area increase of 17% could probably be surpassed using this explosive-boundary

combination since it represents a lateral expansion of only 0.085 inches and quenching should result.

Figure 28 shows a sequence of photographs for the propagation of a detonation wave through a 50% H_2 - 50% O_2 mixture with a helium boundary. Although it was numerically determined that there is no oblique shock solution for this particular explosive-boundary combination, a detached shock similar to that observed in the 30% CH_4 - 70% O_2 mixture with helium boundary has not occurred. An examination of the sequence of photographs shows that the shock in the inert gas is essentially a normal shock at the explosive-boundary interface and the trailing portion of the oblique shock in the boundary gas is gradually overtaking the detonation wave. The data from this sequence of runs is plotted in Figure 29 which makes a comparison of the velocity of the detonation wave in the 50% H_2 - 50% O_2 mixture with a helium boundary to the velocity of the detonation wave through the same explosive mixture confined by a solid boundary. The detonation wave velocity has decreased as a result of side relief but the slope of the line indicates a velocity that is approximately 83% of the C-J velocity.

A series of runs were also made using hydrogen as the boundary gas for the 50% H_2 - 50% O_2 mixture. It was conceivable that a significant change might occur with the hydrogen being used as the boundary gas since its density is only

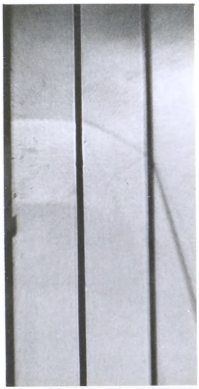

Y = 0.42 ft.

Y = 0.97 ft.

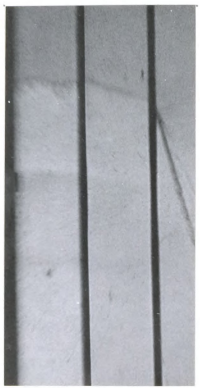

Y = 1.31 ft.

FIGURE 28. Schlieren Photographs of a Detonation Wave in a 50% Hydrogen - 50% Oxygen Mixture with a Helium Boundary.

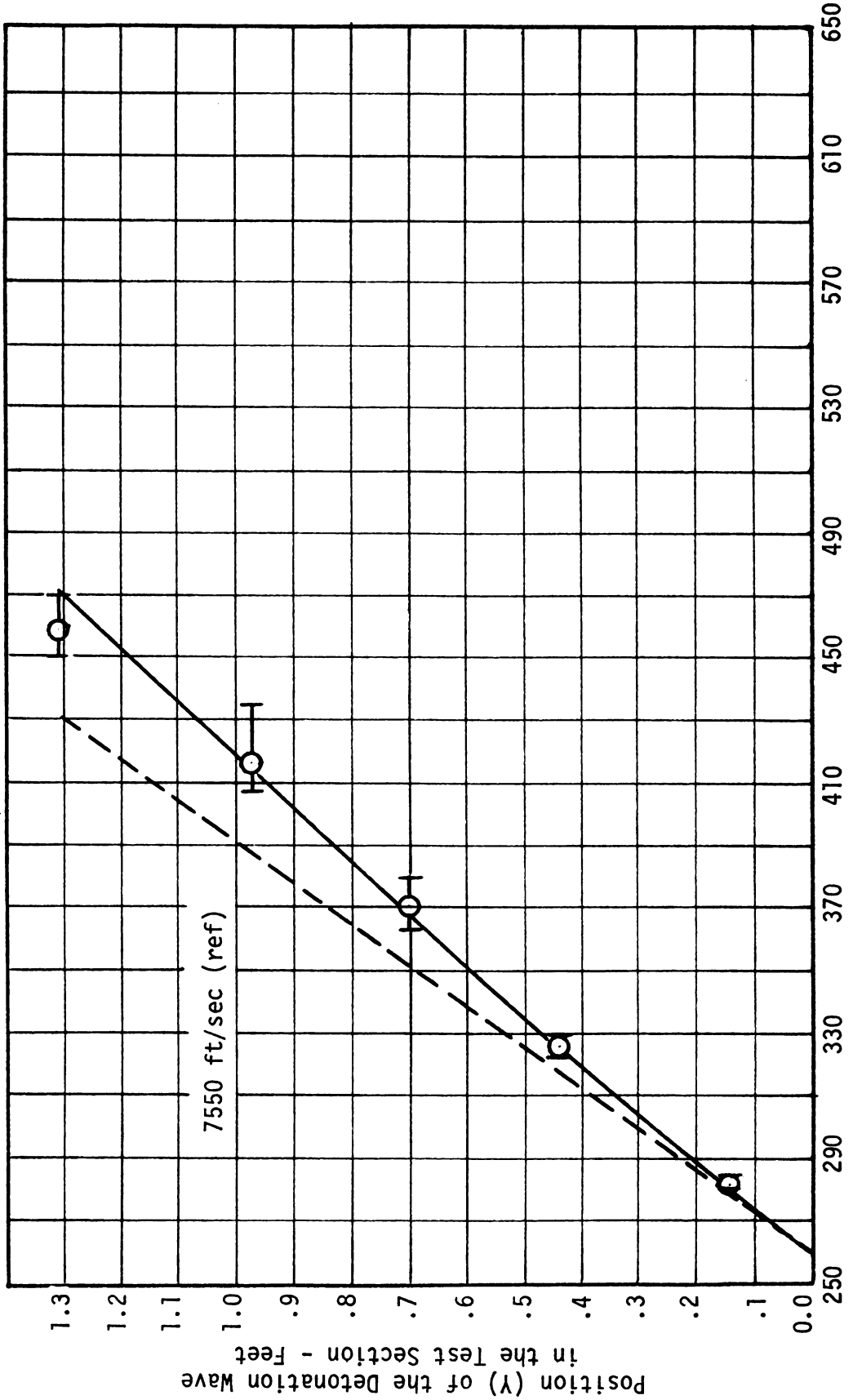

FIGURE 29. Position versus Time of a Detonation Wave in a 50% Hydrogen - 50% Oxygen Mixture with a Helium Boundary.

half that of helium and would therefore, provide even less confinement. The data obtained from these runs are shown in Figure 30. The results were surprisingly the same as obtained when helium was used as the boundary gas and the detonation velocity was about 83% of the C-J velocity. The distance-time plot for the 50% H_2 - 50% O_2 mixture bounded by hydrogen is shown in Figure 30. Also, no noticeable difference between the runs in which helium or hydrogen is used existed in the photographs taken of the detonation wave in the lower part of the test section. However, as the wave progressed further into the test section a detached shock did occur in the hydrogen boundary gas that moved ahead of the detonation wave. (See Figure 31.) It was also noted that even with the detached shock out in front of the detonation wave, the reaction zone was still thin and quenching was not apparent even though the velocity had decreased approximately 17%. A second feature can be seen in Figure 31 where the detonation wave has a very slight upward tilt toward the explosive-boundary interface, indicative of a slight diffusion of hydrogen into the explosive mixture. This diffusion through the thin film into the explosive mixture would, of course, increase the hydrogen content of the explosive mixture near the interface and thereby increase the detonation velocity (31). Although diffusion is

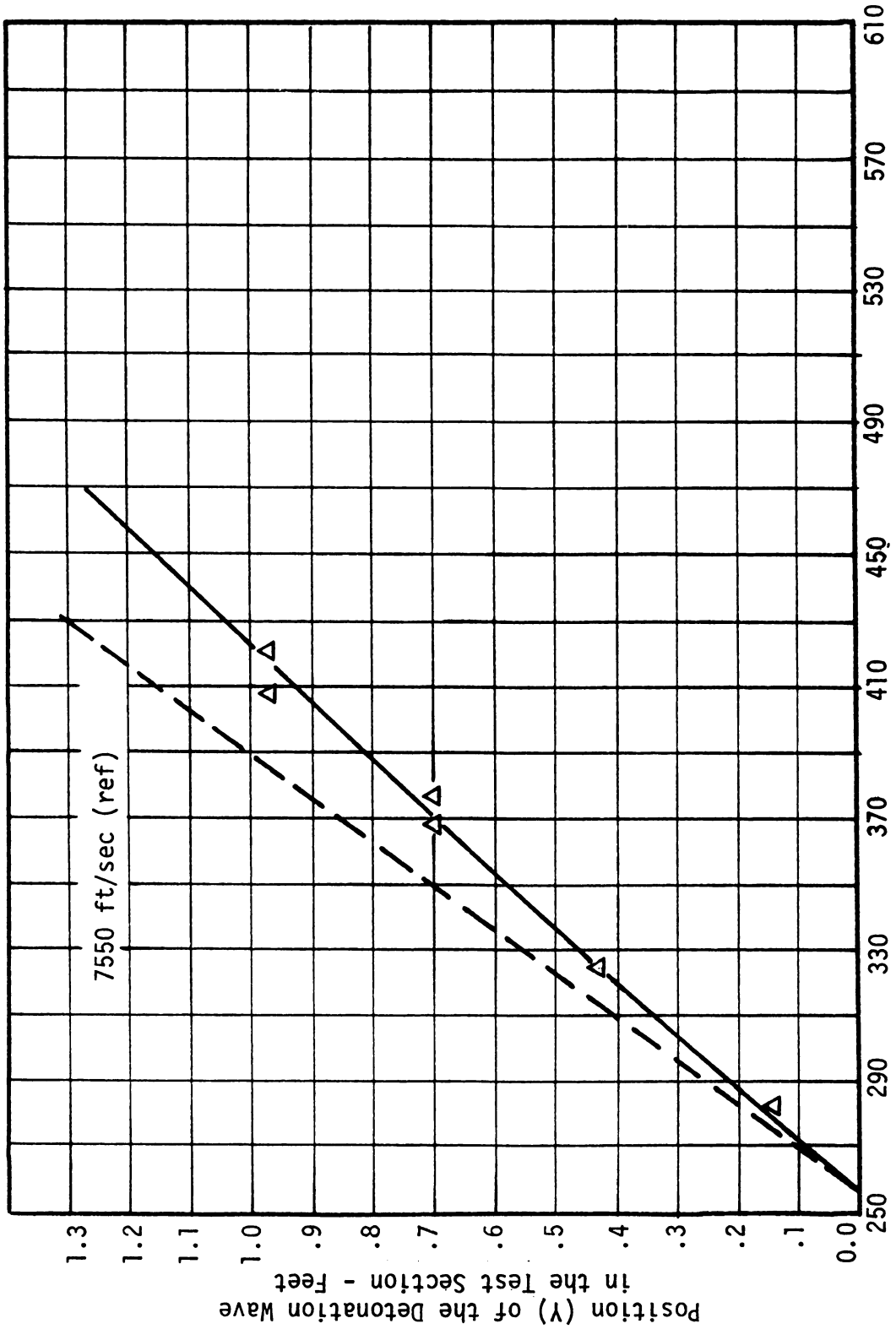

FIGURE 30. Position versus Time of a Detonation Wave in a 50% Hydrogen - 50% Oxygen Mixture with a Hydrogen Boundary.

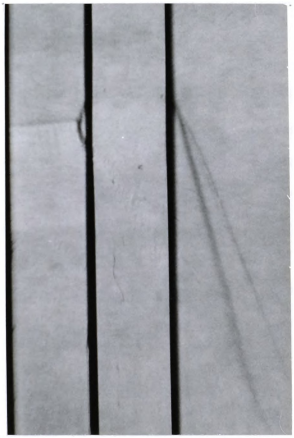

FIGURE 31. Schlieren Photograph of a Detonation Wave in a 50% Hydrogen - 50% Oxygen Mixture Showing an Oblique Shock in the Explosive Resulting from a Leading Shock in the Hydrogen Boundary (Y = 0.97 ft.).

obvious at the interface it is still small and does not appear to be a significant factor in the interaction of the detonation wave with the boundary gas.

When the explosive H_2 - O_2 mixture was "confined" by a much lower density inert boundary gas it was found that the velocity decreased only about 17% within the confines of the test section. This value is greater than the 10% previously noted as being indicative of quenching. If this is a detonation wave that is quenching then it should be noted that the velocity of propagation decreases rather slowly for the hydrogen-oxygen mixture and therefore, the quenching process itself must be rather slow.

Support for this conclusion can be found in the work of Lu who made soot track records of detonations with side relief. He observed:

> The side relief effect is gradually propagated across the channel as indicated by the gradual deformation of cells. After the side relief effect is felt across the whole channel width, most cells disappear and only two tracks are shown. This implies that the detonation wave is a two-headed spinning one. Finally the two tracks disappear also; this indicates the detonation quenches completely. From these records, it is clear that the quenching process of a detonation wave, unlike the abrupt onset of a detonation shown by Urtiew and Oppenheim, is a gradual process (19).

Due to the limited size of the test section it was not possible to extend the zone of interaction between the quenched detonation wave and the low density inert boundary gas without some external influence. One possibility would have

been to reduce the width of the explosive channel in the test section to the point where quenching would occur but this was not practical without redesigning the test section. A second possibility was to decrease the percentage of hydrogen in the explosive mixture and thereby create a mixture in which it would not be possible for the detonation wave to maintain itself (18). To investigate this condition a 35% H_2 - 65% O_2 mixture was used with a helium boundary. A detached shock condition developed and the shock was observed to run out ahead of the detonation wave in the explosive mixture but it was evident from previous results that a considerable length would still be required to achieve a substantial degeneration of the quenching detonation wave. Figure 32 shows the interaction of the detonation wave in the 35% H_2 - 65% O_2 mixture with a helium boundary.

The third possibility and the one used to achieve further quenching of the detonation wave so that further extrapolation to the end condition could be made, was to use an explosive mixture with a helium boundary and to bleed air into the flowing explosive mixture within the test section. The effect of introducing air into the test section would be to reduce the percentage of hydrogen in the explosive mixture which in turn would result in a mixture that could not sustain a detonation wave. This condition would also allow a fully developed detonation wave to experience quenching due to both mixture

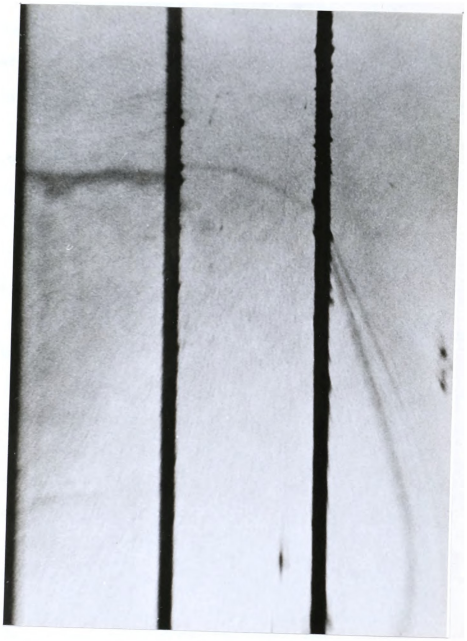

FIGURE 32. Schlieren Photograph of a Detonation Wave in a 35% Hydrogen - 65% Oxygen Mixture with a Helium Boundary. (Y = 0.16 ft.).

composition and side relief as it exited from the detonation tube into the test section.

A 50% H_2 - 50% O_2 mixture was used for these runs with bleed air since the initial mixture would sustain a detonation wave yet was not far removed from a composition that would allow the detonation wave to quench (18). The photographic sequence is shown in Figure 33. A comparison of the velocity of the quenched detonation wave "confined" by the much lower density inert boundary gas was made to the propagation velocity of the unquenched hydrogen-oxygen mixture confined by the detonation tube. This is shown in Figure 34. As might be expected, due to both the reduced composition of the mixture within the test section and the effect of side relief, the velocity of the detonation wave decreased rapidly as it exited from the detonation tube. Although fewer data points were used to obtain the curve shown in Figure 34 than were used for the methane-oxygen mixture, it was found that a marked similarity exists between the two curves. In fact, when the curves considered to be the best lines for both the methane-oxygen mixture and the hydrogen-oxygen-air mixture are compared very little difference exists. Not only do the propagation velocities over the first half of the test section correspond to half the Chapman-Jouget velocity but the sequence of photographs also show the same characteristics. In addition, the detonation wave in both the methane-oxygen mixture

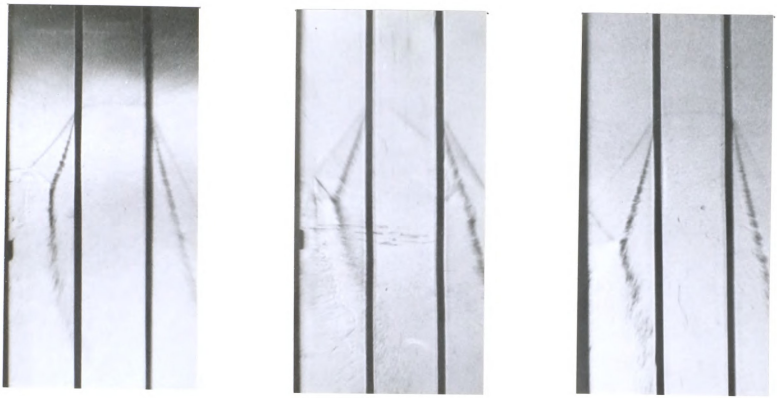

Y = 0.42 ft. Y = 0.7 ft. Y = 0.97 ft.

FIGURE 33. Schlieren Photographs of a Quenched Detonation Wave in a Hydrogen-Oxygen-Air Mixture with a Helium Boundary.

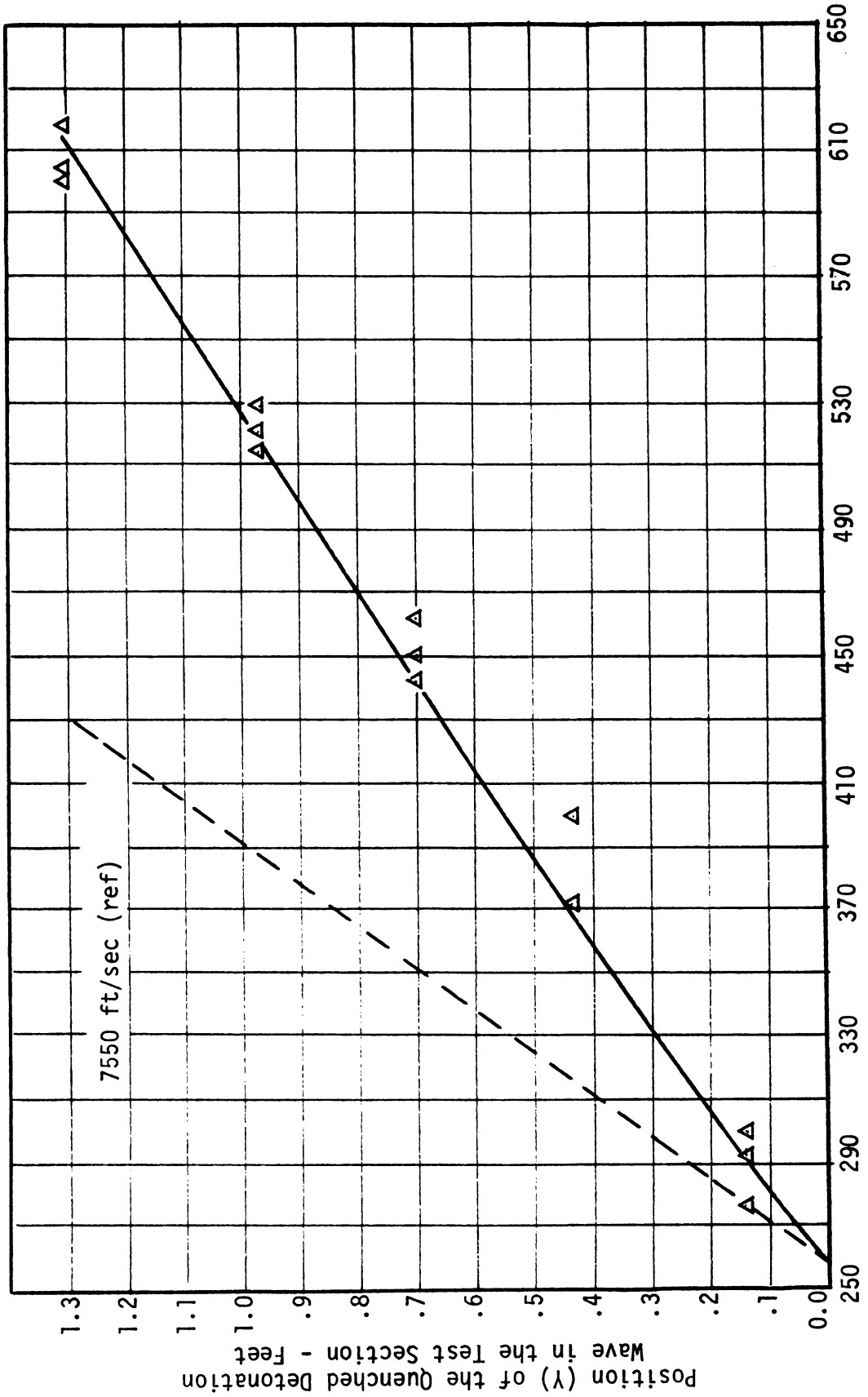

FIGRE 34. Position versus Time Plot of a Quenched Detonation Wave in a Hydrogen-Oxygen-Air Mixture with a Helium Boundary.

and the hydrogen-oxygen-air mixture appear to reach the same steady state velocity. This apparently steady state velocity was found to be about 3300 ft/sec and corresponds to the sound speed in the helium boundary gas. Hence, it is concluded that the methane-oxygen mixture bounded by helium experiences a large area increase due to side relief and this results in the quenching of the detonation wave. The detached shock in the boundary gas moves ahead as the pressures behind the shock try to establish an equilibrium condition. Eventually the shock in the boundary gas moves far enough out in front so that the refracted wave in the explosive is reflected from the solid wall of the test section. It is near this regime that the steady velocity observed is the result of a wave decaying to an acoustic pulse, traveling at the sound speed of the boundary gas.

4.1.3 Further considerations.

There are several other features regarding the propagation of a detonation wave through an explosive mixture, bounded by a much lower density inert gas, that bear consideration. The first of these is the possibility of the leading detached shock in the boundary gas inducing an oblique shock into the explosive mixture and forming a Mach stem at the wall. This would provide a high local temperature which might sustain a detonation. It would seem however, since the detonation wave is quenched at this point, that if a high local temperature was achieved behind the Mach stem, the detonation wave might

be re-established. However, there was no indication of a Mach stem forming at the wall.

For auto-ignition of the methane-oxygen mixture caused by a high local temperature created by a series of shocks, the temperature behind the refracted or reflected shock must exceed the minimum ignition temperature. A survey of the literature provided little in the way of what this temperature might actually be. In fact, for H_2 - O_2 mixtures, which is undoubtedly the most widely documented, Jost (5) notes a variation of over 500° C in the ignition temperature, based on the condition of the experiment. This indicates that only the ignition temperature achieved by an adiabatic compression process would be applicable for a determination of whether an auto-ignition could occur. A literature search failed to produce any applicable ignition temperature but as was previously noted, a Mach stem did not form and nothing in the data suggested that the detonation wave might propagate at a low velocity.

Another factor which might be partially responsible for the apparent constant velocity of the hydrogen-oxygen mixture bounded by helium is the configuration of the shock in the boundary gas. Although the shock angle in the boundary gas is approximately 90° at the interface, which is greater than the value of θ_{max} predicted by the oblique angle calculations and is therefore classed as a detached shock, it does not show the leading shock

characteristics that occurred with the heavier methane-oxygen mixture. This is, of course, a result of the still relatively high propagation velocity of the detonation wave in the mixture. It could be argued that the almost normal shock in the inert at the explosive-boundary interface produces a sufficient increase in the density behind the shock in the boundary gas so that what the detonation "sees" is this higher density gas. This would mean a lower deflection angle, for the interface streamline, a smaller area increase and therefore, a smaller change in velocity. This, of course, would result in very slow quenching. This same density increase in the helium when used as a boundary for the methane-oxygen mixture is not sufficient to offer suitable confinement for the reaction and the detonation wave quenches.

Another probably equally valid argument can be given for the relatively small velocity decrement shown by the detonation wave propagating through a 50% H_2 - 50% O_2 mixture bounded by helium by making a comparison of relative ignition energies of hydrogen-oxygen mixtures and methane-oxygen mixtures. Reference 6 gives some minimum spark ignition energies for both of these mixtures. Much less energy is required for ignition of hydrogen-oxygen mixtures. Since less energy is required for ignition achieved through an adiabatic compression as would occur across a normal shock wave. This would mean that the hydrogen-

oxygen mixture is able to sustain itself better than any other explosive mixture and thereby is less susceptible to the sudden lateral expansion and corresponding velocity decay exhibited by a hydrocarbon mixture.

4.1.4 Behavior of the Detonation Wave in the Explosive Mixture When the Boundary Gas is also an Explosive Mixture of Much Lower Density.

Only a limited number of runs were made to investigate the behavior of a detonation wave propagating through an explosive mixture that was bounded by another explosive of much lower density. With both of the channels in the test section filled with explosive mixtures, the total volume of explosive gas was quite large. When the detonation was initiated, the energy release was considerable and almost invariably some piece of the test section was damaged. Generally the damage was confined to the "windows" of the test section but in several instances the film holders were buckled by the explosion.

The procedure for running these experiments was identical to the tests conducted with an inert boundary gas except that an explosive was used as a boundary gas. Although the difference in the molecular weights of the respective mixtures was not sufficient to cause a shock detachment, the differences in the detonation velocities produced substantially the same results. For example, using a 35% H_2 - 65% O_2 mixture which has

a detonation velocity of approximately 6350 ft/sec as the primary mixture and a 78% H_2 - 22% O_2 mixture with a detonation velocity of about 10,800 ft/sec as the boundary mixture, it is obvious that the detonation should run out ahead in the boundary gas. There is always a delay time between the ignition and the development of the detonation wave but it was thought that the induced shock into the boundary mixture and the ignition caused by the lateral expansion of the reaction zone of the primary mixture would reduce the time required for the development of a detonation wave.

Figure 35 shows the interaction between a primary mixture of 35% H_2 - 65% O_2 and a boundary mixture of 78% H_2 - 22% O_2 approximately 2.25 inches into the test section. The wave front in the primary mixture exhibits a slightly curved shock which is attributed to the divergence of the streamlines in the reaction zone when subjected to side relief. Also, the reaction zone of the primary mixture shows a thickening and some separation from the shock front. This is indicative of the onset of quenching and is in accordance with the findings in Reference 18. The shock in the boundary mixture is slightly behind the shock in the primary mixture and it has the appearance of a discontinuity at the film separating the two explosive mixtures. This condition is presently not understood. The structure behind the oblique shock in the boundary gas also

FIGURE 35. Schlieren Photograph of a Quenching Detonation Wave in a 35% Hydrogen - 65% Oxygen Mixture with a 78% Hydrogen - 22% Oxygen Boundary. (Y = 0.188 ft.).

exhibits a somewhat turbulent structure and it is not possible to tell if a detonation has actually formed. Outboard from the boundary mixture, an oblique shock and the interface angle are clearly visible in the air boundary.

The interaction of an explosive mixture composed of 30% CH_4 - 70% O_2 and a boundary mixture made up of 78% H_2 - 22% O_2 is shown in Figure 36. This photograph was taken approximately 8 in. into the test section and the detonation wave in the hydrogen-oxygen mixture appears to be well established and beginnning to move out ahead of the shock front in the methane-oxygen mixture. Based on the results of a previous study (18), the detonation wave in the hydrogen-oxygen mixture should continue to propagate through the length of the test section since both the air on the outboard side and the methane-oxygen mixture on the inboard side will provide suitable confinement.

FIGURE 36: Schlieren Photograph of a Detonation Wave in a 35% Methane - 70% Oxygen Mixture with a 78% Hydrogen - 22% Oxygen Boundary. (Y = 0.75 ft.).

CHAPTER V

CONCLUSIONS

The interaction of a gaseous detonation wave with an inert boundary gas results in a lateral shock wave moving into the boundary. This shock wave may be a weak oblique shock or a detached shock, depending upon the Mach number of the detonation and the properties of the explosive and boundary gases. The prediction of the transition from the oblique shock can be obtained by using the explosive-boundary interface angle as an analogue to a wedge placed in a supersonic stream. It was calculated that shock detachment would occur when the shock angle required exceeded a value between 62° and 72°, depending on the explosive-boundary combination.

A thin nitrocellulose film proved to be an acceptable means of minimizing diffusion between two different flowing gases over a fairly long distance. Although it was evident from some runs in which hydrogen was used as the boundary gas that diffusion was taking place, it was not considered to be sufficient to influence the results. The making and positioning of films, long enough to provide a reasonable interaction length and yet thin enough so as to not influence the lateral

expansion of the reaction zone, is very difficult. It is so difficult, in fact, that alternate methods should be investigated as a means of separating two gases. If a suitable alternative could be found it would afford one the possibility of extending the zone of interaction.

A velocity corresponding to that predicted by the Chapman-Jouget theory was found when a detonation wave was formed in a column of gas composed of 30% CH_4 - 70% O_2. However, when this detonation wave experienced side relief to a boundary gas of much lower density, the velocity of the detonation wave decreased by 50% almost immediately and the shock in the boundary gas ran out ahead of the detonation wave. The length of the reaction zone continued to increase behind the detonation wave and the detonation appeared to decay to a weak deflagration wave. The removal of the energy supply from immediately behind the shock wave in the explosive mixture allowed the velocity to decrease and the whole system degenerated into a shock moving at the sound speed in the boundary gas.

The use of 50% H_2 - 50% O_2 explosive mixture bounded by a much lower density inert gas demonstrated the resistance to quenching offered by a hydrogen-oxygen mixture. The velocity of the detonation wave decreased approximately 17% in the test section when propagating next to a hydrogen or a helium boundary. This was not considered to be steady state since the configuration

of the detonation wave and the induced shock wave in the boundary gas appeared to be gradually changing. The reason for this slow decay is not understood. It is plausible that the increase of density of the boundary gas behind the shock wave is almost sufficient to provide suitable confienment for the reaction zone and/or the low ignition temperature and the high reaction rate of the H_2 - O_2 mixture is almost sufficient to sustain the detonation. The results of this research suggest additional studies into the quenching mechanism of a hydrogen-oxygen reaction bounded by a much lower density boundary gas.

The percentage of hydrogen in a hydrogen-oxygen mixture, bounded by helium, was decreased by bleeding air into the test section. When a stable detonation wave was propagated into this hydrogen-oxygen-air mixture and simultaneously experienced side relief the decrease in the velocity and the interaction of the shock waves in the boundary and explosive gas columns were strikingly similar to those observed for the methane oxygen mixture. The velocity of the shock wave in the explosive mixture initially decreased to half of the original value and then gradually decayed to a quasi-steady value corresponding to the sound speed in the boundary gas. Hence, it is concluded that a quenched detonation wave will degenerate into a pure shock traveling at a speed commensurate with the sound speed of the lowest density gas which it can "see."

The lateral expansion of a detonation wave into an explosive boundary gas will result in the rapid formation of a detonation wave in the boundary mixture. When the composition of the boundary mixture is such that its detonation velocity is higher than that in the primary mixture, the detonation wave formed in the boundary gas runs out ahead of the wave in the primary mixture. This produces an oblique shock in the primary mixture similar to that resulting from a shock detachment, during the interaction of a detonation wave and a much lighter inert boundary gas. Further studies into the interaction of various explosive mixtures would prove interesting.

No supporting evidence was found in this study for suppositions relative to the existence of a weak detonation wave. It was found that a quenched detonation wave "confined" by a much lighter inert boundary gas would exhibit a transient velocity corresponding to 50% of the Chapman-Jouget velocity. Since this velocity occurred in the first 8 inches of the test section, which was longer than the test section used by Dabora, et al., and approximately equal to length of the longest interaction observed by Lu, it is concluded that this condition is the "apparently steady" velocity they observed. As the interaction progressed, the velocity of the shock wave was observed to decay to a quasi-steady value corresponding to the acoustical velocity in the inert boundary gas.

Insufficient information is given in the results of the studies by Voitsekhovskii so that a determination can be made as to why a detonation velocity was observed corresponding to half the Chapman-Jouget velocity or why the detonation was maintained for only 1 to 1.5 seconds. The results of the present research indicate that probably a slowly quenching detonation wave was observed.

Although the results of this research do not disprove the existence of weak detonation waves it appears unlikely that a sub-Chapman-Jouget wave occurred in the present study. The results are not as conclusive as desired because of the relatively long times for large changes to occur in some of the detonation configurations and because a major criterion for quenching is rather qualitative, i.e., thickening of the reaction zone. It is evident that considerable effort and care are required to determine the existence and nature of steady state detonation wave configurations with compressible side relief.

BIBLIOGRAPHY

BIBLIOGRAPHY

1. Berthelot, M. and Vielle, P. "Sur la Vitesse de Propagation des Phenomenes Explosifs dans les gas." Comptes Rendus de l'Academie des Sciences, Paris, 93, (1881), pp. 18-22.

2. Mallard, E. and LeChatelier, H. L. "Sur la Vitesse de Propagation de L'inflammation dans les Melanges Explosifs." Comptes Rendus de l'Academie des Sciences, Paris, 93, (1881), pp. 145-148.

3. Chapman, D. L. "On the Rate of Explosions in Gases," Phil. Magazine, 47 (1899), 90.

4. Jouget, E.,"Sur la Propagation des Reaction Chimiques dans les Gas." J. Mathematique. 6, No. 1 (1905), 347; 6, No. 2 (1906), 6.

5. Jost, W. and Croft, H. O. Explosion and Combustion Processes in Gases, McGraw-Hill Book Co., Inc. 1946.

6. Lewis, B. and von Elbe, G. Combustion, Flames and Explosion of Gases. Academic Press Inc., New York, 1951.

7. Morrison, R. B., Adamson, T. C., Jr. and Weir, A., Jr. Detonative and Deflagrative Combustion." Advances in Chemistry Series No. 20, American Chemical Society, 1958.

8. Evans, M. W. and Ablow, C. M. "Theories of Detonation." Chemical Review (April, 1961), 129.

9. Oppenheim, A. K., Manson, H. and Wagner, H. Gg. "Recent Progress in Detonation Research." AIAA Journal, 1, (October, 1963), 2243-2252.

10. Strehlow, R. A. Fundamentals of Combustion. International Textbook Co., Scranton, 1968.

11. Nichols, J. A. and Dabora, E. K. "Recent Results on Standing Detonation Waves" AFOSR Report No. TN 60-441, May, 1960.

12. Voitsekhovskii, B. V., "Maintained Detonations," Soviet Physics Doklady, 4, No. 6, Translated from Dokaldy Akad. Nauk SSSR, Vol. 129, No. 6, pp. 1254-1256, November-December, 1959.

13. Voitsekhovskii, B. V. "Spinning Maintained Detonation," Zh. Prik. Mekhan. i Tekhn. Fiz. (Journal of Applied Mechanics and Technical Physics) No. 3, 147-164 (1960).

14. Brochet, Ch., Leyer, J. C. and Manson, N. "Phenomenes vibratoires dans les detonations dissociees." Compt. Rend. 253 (1960), p. 621.

15. Brochet, Ch. and Manson, N. "Ondes explosives et detonations instables dans les melanges propane-oxygene-azote." Les Ondes de Detonation CNRS, Paris (1962), pp. 209-222.

16. Manson, N., Brochet, Ch., Brossard, J. and Pujol, T. "Vibratory Phenomena and Instability of Self-Sustained Detonations in Gases." Ninth Symposium (International) on Combustion, Academic Press, New York (1963), pp. 461-469.

17. Sommers, W. P. The Interaction of a Detonation Wave with an Inert Boundary. Ph.D. Thesis, The University of Michigan, 1961.

18. Dabora, E. K., Nichols, J.A., and Morrison, R.B. "The Influence of a Compressible Boundary on the Propagation of Gaseous Detonations." Tenth Symposium (International) on Combustion. The Combustion Institute, Pittsburgh, Pennsylvania (1965), pp. 817-830.

19. Lu, Pai-Lien. The Structure and Kinetics of H_2-CO-O_2 Detonations. Ph.D. Thesis, The University of Michigan, 1968.

20. Taki, S. and Fujiwara, T. "One Dimensional Non Steady Processes Accompanied by the Establishment of Self-Sustained Detonation." Thirteenth Symposium (International) on Combustion. The Combustion Institute, Pittsburgh, Pennsylvania (1971), pp. 1119-1128.

21. Lee, J. H., Lee, B. H. K. and Shanfield, I. "Two-Dimensional Unconfined Gaseous Detonation Waves." Tenth Symposium (International) on Combustion. The Combustion Institute, Pittsburgh, Pennsylvania (1965), pp. 805-815.

22. Levin. V. A. "On the Transition of a Plane overdriven Detonation Wave to the Chapman-Jouget Mode." Translated into English from Izv. Akad. Nauk SSSR, Mekhan Zhedkosti i Gazu (Moscow) No. 2 (March-April, 1968), pp. 50-55.

23. Ubbeholde, A. R. "The Possibility of Weak Detonation Waves." Fourth Symposium (International) on Combustion. Williams and Wilkins, Baltimore (1953), pp. 464-467.

24. Nicholls, J. A. and Cullen R. E., "The Feasibility of a Rotating Detonation Wave Rocket Motor." Technical Documentary Report No. RPL-TDR 64-113, April, 1964.

25. Lange, O. H., Stein, R. J. and Tubbs, H. E. Inventors, Continuous Detonation Reaction Engine Patent, U.S. Patent 3,336,754. Issued August 22, 1967.

26. Sichel, A. "A Hydrodynamic Theory for the Interaction of a Gaseous Detonation Wave with a Compressible Boundary." The University of Michigan Tech. Report. ORA Project 05170. February, 1965.

27. Edwards. D. H., "A Survey of Recent Work on the Structure of Detonation Waves." Twelfth Symposium (International) on Combustion. The Combustion Institute, Pittsburgh, Pennsylvania (1969), pp. 819-828.

28. Dunn, R. and Wolfson, B. T. Generalized Equations and Procedures for the Calculations of Detonation Parameters. WADC TN 54-B, March 1956.

29. Eisen, C. L., Gross, R. A. and Rivlin, T. J. Theoretical Calculations in Gaseous Detonations. AFOSR Report No. TN-58-326, March, 1958.

30. Gealer, R. L. and Churchill, S. W. "Detonation Characteristics of Hydrogen-Oxygen Mixtures at High Initial Pressures." A.I.Ch.E. Journal, 6 (September, 1960), 501-505.

31. Moyle, M. P. The Effect of Temperature on the Detonation Characteristics of Hydrogen-Oxygen Mixtures. Ph.D. Thesis. The University of Michigan, December, 1956.

32. Zeleznik, F. S. and Gordon, S. A General IBM 704 and 7090 Computer Program for Computation of Chemical Equilibrium Compositions, Rocket Performance and Chapman-Jouget Detonations. NASA TN D-1737, (October, 1963).

33. Personal communication from Professor T. C. Admanson, Department of Aeronautical and Astronautical Engineering, The University of Michigan, Ann Arbor, Michigan.

34. Doering W. and Burkhardt, G. Contribution to the Theory of Detonation (translated from German). Technical Report No. F-TS-1227-IA (GDAM A9-T-46), Wright-Patterson Air Force Base, Dayton, Ohio (May, 1949), pp. 209-219.

35. Zeldovich, Y. B. "Theory of Propagations of Detonations in Gaseous Systems." J. Exper. and Theoret. Phys.(USSR), 10 (1940), p. 542.

36. von Neumann, J. Theory of Detonation Waves. Progress Report 238, to April 1, 1942, OSRD Report 549, 1942, Ballistic Research Lab. File No. X-122, Inst. for Adv. Study, May 4, 1942.

37. Doering, W. "Uder den Detonationsvorgang in Gases." Annalen de Physik. 43 (1943), p. 421.

38. Liepman, H. W. and Roshko, A. Elements of Gasdynamics. John Wiley and Sons, Inc., New York, 1957.

39. Bird, G. A. "Some Remarks on the Foundations of Piston Theory and Supersonic-Hypersonic Similarity." Journal of the Aero. Sciences, 25, No. 2, February, 1958, pp. 138-139.

40. Egerton, A. C., Everett, A. J. and Moore, N. P. W. "Sintered Metals as Flame Traps." Fourth Symposium (International) on Combustion. Williams and Wilkins, Baltimore (1953), pp. 689-695.

41. Gvozdeva, L. G. "The Refraction of Detonation Waves Incident on the Boundary Between Two Gas Mixtures." Soviet Physics, Tech. Phys. 6, No. 6, December, 1961.

42. Hall, C. E. Introduction to Electron Microscopy. McGraw-Hill Book Co., Inc., New York, 1953, Chapter 11.

43. Peachy, L . D. "Thin Sections I. A Study of Section Thickness and Physical Distortion Produced During Microtomy." J. Biophysics and Biochem. Cytol., 4 (1958), p. 233.

44. Holder D. W. and North, R. J. "Schlieren Methods," Notes on Applied Science, No. 31. National Physical Laboratory, Her Majesty's Stationary Office, London (1963).

45. Fay, J. A. "Two-Dimensional Gaseous Detonations: Velocity Deficit." Phys. of Fluids, 2 (1959), p. 283.

46. Schmidt, D. H. W., Steinicke, H. and Neubert, U. "Flame and Schlieren Photographs of Combustion Waves in Tubes." Fourth Symposium (International) on Combustion. Williams and Wilkins, Baltimore (1953), pp. 658-666.

47. Wilson, E. B., Jr. An Introduction to Scientific Research. McGraw-Hill Book Co., Inc., New York (1952), p. 272.

APPENDICES

APPENDIX A

COMPUTER PROGRAM FOR CALCULATION OF SHOCK AND INTERFACE ANGLES

The computer program is designed to compute the oblique shock angle by a convergence on the angle Beta. The maximum shock angle is found using Equation (2.45) whereas the minimum angle, Beta, will occur when the exit Mach number, M_{e3}, is equal to unity. Using these limiting values of Beta as starting points, the difference in the pressure ratios across the interface is determined. When the absolute value of the difference in the aforementioned pressure ratios is less than 0.01, the program is terminated.

A brief explanation of the convergence process is given in Figure 37.

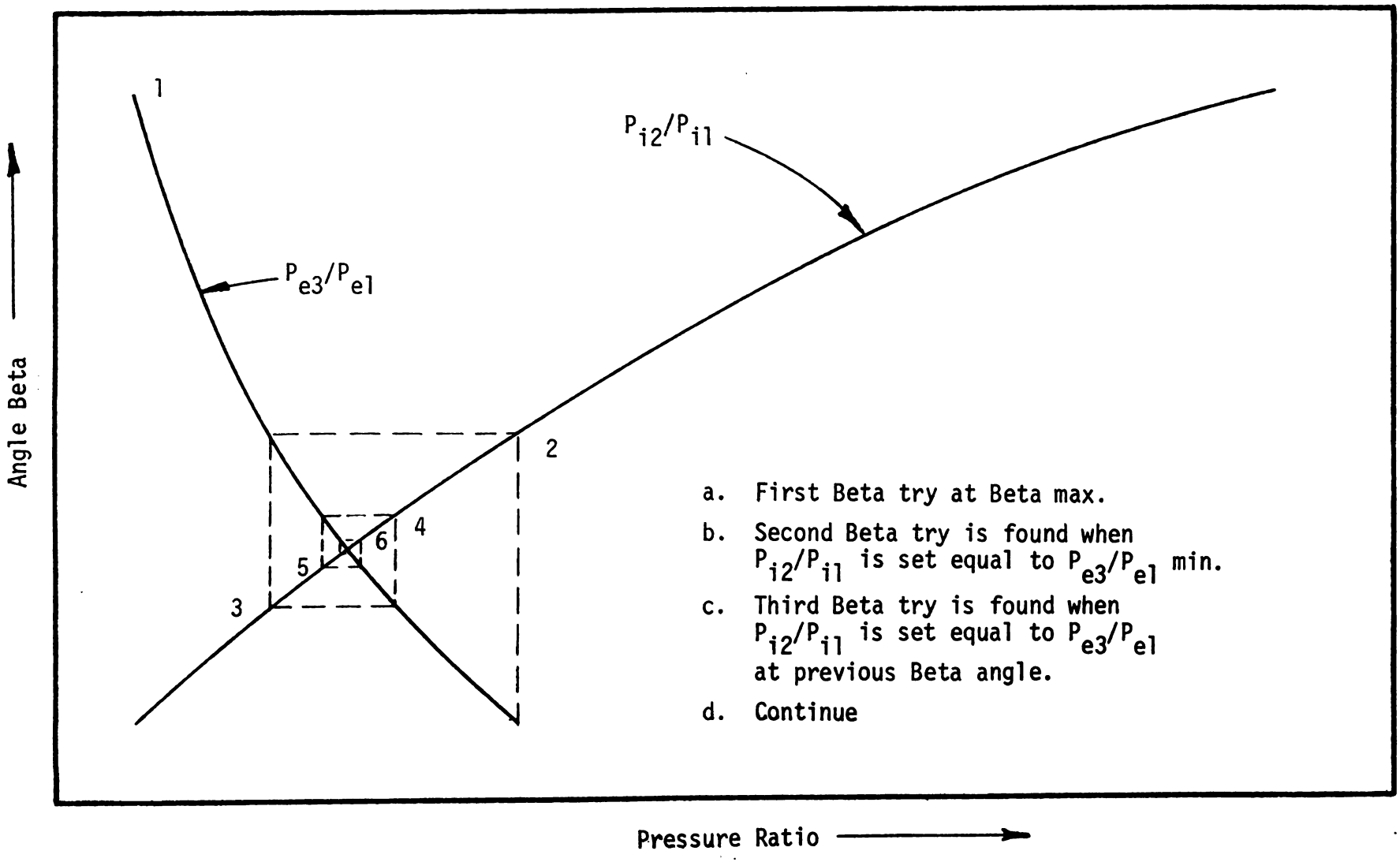

FIGURE 37. Convergence Process for Determination of the Oblique Shock Angle.

```
// FOR
*LIST SOURCE PROGRAM
*ONE WORD INTEGERS
      SUBROUTINE XMTRE(PHI,GE2,I,K,J,XME3)
      J=0
      IF(I-1)40,30,40
   30 XME3=1.0
   31 XME3=XME3+0.1
   32 X=(XME3**2.0)-1.0
      Y=(GE2+1.0)/(GE2-1.0)
      Z=(GE2-1.0)/(GE2+1.0)
      Q=((SQRT(Y)*ATAN(SQRT(Z*X)))-ATAN(SQRT(X)))-PHI
      IF(IFIX(Q))31,60,31
   33 XME3=XME3-0.09
      IF(XME3-0.99)59,59,32
   59 J=1
      GO TO 60
   40 X=2.0
      Y=(GE2+1.0)/(GE2-1.0)
      Z=(GE2-1.0)/(GE2+1.0)
   10 Q=((SQRT(Y))*(ATAN(SQRT(Z*((X**2.0)-1.0)))))-(ATAN(SQRT((X**2.0)-1
     C.0)))-PHI
      DQ=((SQRT(Y))*Z*X)/((1.0+((Z*(X**2.0)))-Z)*(SQRT((Z*(X**2.0))-Z)))
     C-(X/((X**2.0)*(SQRT((X**2.0)-1.0))))
      ONE=(X-(Q/DQ))
      DIVS=ABS(ONE-X)
      IF(DIVS-0.005)44,44,20
   20 X=ONE
      GO TO 10
   44 XME3=ONE
      IF(XME3-0.99)59,59,60
   60 RETURN
      END
// DUP
*STORE       WS  UA  XMTRE
// FOR
*LIST SOURCE PROGRAM
*ONE WORD INTEGERS
C     ANGLE BETA MAXIMUM AND MINIMUM
      SUBROUTINE BETA(GI,XMI,I,BMIN,BMAX)
      IF(I-1)20,30,20
   30 S=SQRT(1.0/(XMI**2.0))
      S1=S
      Q=1.0
      DO 35 MM=2,50,2
      Q=Q*(FLOAT(MM-1)/FLOAT(MM))
   35 S=S+(Q*((S1**FLOAT(MM+1))/(FLOAT(MM+1))))
      BMIN=S
      GO TO 50
   20 A=GI
      B=XMI**2.0
      Z=SQRT((A+1.0)*(1.0+(((A-1.0)/2.0)*B)+(((A+1.0)/16.0)*(B**2.0))))
      Z1=((A+1.0)/4.0)*B
      Z2=A*B
      S=SQRT((1.0/Z2)*(Z1-1.0+Z))
      S1=S
      Q=1.0
      DO 25 MM=2,20,2
```

```
      A1=FLOAT(MM-1)
      A2=FLOAT(MM)
      A3=FLOAT(MM+1)
      Q=Q*(A1/A2)
   25 S=S+(Q*((S1**A3)/A3))
      BMAX=S
   50 RETURN
      END
// DUP
*STORE      WS  UA  BETA
// FOR
*IOCS(CARD,1132 PRINTER)
*LIST SOURCE PROGRAM
*ONE WORD INTEGERS
      DIMENSION B(120),PHI(120),R(120)
 2050 READ(2,1)T,GI,GE,V,YMI,YME,VR,RBAR,GRAV
      WRITE(3,17)
C     CALCULATE THE VELOCITY OF SOUND
      AE=SQRT((GE*RBAR*T*GRAV)/YME)
      AI=SQRT((GI*RBAR*T*GRAV)/YMI)
      WRITE(3,1)T,GI,GE,V,YMI,YME,VR,RBAR,GRAV
      WRITE(3,2)AE,AI
C     CALCULATE THE MACH NUMBERS
      XME=V/AE
      XMI=V/AI
      WRITE(3,3)XME,XMI
C     CALCULATE THE VALUES WHEN THETA IS EQUAL TO ZERO DEGREES OR BETA
C     IS A MINIMUM.
      K=0
      I=1
      CALL BETA(GI,XMI,I,  BMIN,BMAX)
      B(I)=BMIN
      GNA=(B(I)*180.0)/3.1416
      QZ=((2.0*COS(B(I)))/(SIN(B(I))))*(((XMI**2.0)*(SIN(B(I))**2.0))-1.
     CO)
      QZ1=(2.0+((XMI**2.0)*(GI+COS(2.0*B(I)))))
      PHI(I)=ATAN(QZ/QZ1)
      ANG=(PHI(I)*180.0)/3.1416
      PQ=1.0+((GE*(XME**2.0))*(1.0-(1.0/VR)))
      GE2=((1.0/PQ)*(1.0+((GE*(XME**2.0))))-1.0)
      CALL XMTRE(PHI(I),GE2,I,K,J,XME3)
      IF(J)8001,24,8001
   24 PV=((1.0+(((GE2-1.0)/2.0)*(XME3**2.0)))**(GE2/(GE2-1.0)))
      PT=(1.0+((GE2-1.0)/2.0))**(GE2/(GE2-1.0))
      PRATI=((PQ)*(PT)*(1.0/PV))
      PI=1.0+(((2.0*GI)/(GI+1.0))*((XMI**2.0)*(SIN(B(I))**2.0)-1.0))
      R(I)=PI-PRATI
      Q1=PRATI
      WRITE(3,18)
      WRITE(3,1800)ANG,GNA,PQ,GE2,XME3,PV,PT,PRATI,PI,R(I)
C     THE ABOVE VALUES MUST BE NEGATIVE SO THAT BETA MUST BE INCREASED
C     CALCULATIONS FOR ANGLE WILL FOLLOW.  CALCULATE BETA MAXIMUM
      I=2
      CALL BETA(GI,XMI,I,BMIN,BMAX)
      B(100)=BMAX
      I=1
      B(I+1)=BMAX
      KK=0
```

```
 6000 I=I+1
      IF(I-20)105,105,8000
C     CALCULATIONS OF PHI CORRESPONDING TO ANGLE BETA
  105 QZ=((2.0*COS(B(I)))/(SIN(B(I))))*(((XMI**2.0)*(SIN(B(I))**2.0))-1.
     CO)
      QZ1=(2.0+((XMI**2.0)*(GI+COS(2.0*B(I)))))
      PHI(I)=ATAN(QZ/QZ1)
      WRITE(3,7)
      L=I-1
      GNA=(B(I)*180.0)/3.1416
      ANG=(PHI(I)*180.0)/3.1416
      WRITE(3,5)L,GNA,ANG
      PQ=1.0+((GE*(XME**2.0))*(1.0-(1.0/VR)))
      GE2=((1.0/PQ)*(1.0+((GE*(XME**2.0)))))-1.0)
      CALL XMTRE(PHI(I),GE2,I,K,J,XME3)
      K=1
      IF(J)8001,25,8001
   25 PV=((1.0+(((GE2-1.0)/2.0)*(XME3**2.0)))**(GE2/(GE2-1.0)))
      PT=(1.0+((GE2-1.0)/2.0))**(GE2/(GE2-1.0))
      PRATI=((PQ)*(PT)*(1.0/PV))
      PI=1.0+(((2.0*GI)/(GI+1.0))*((XMI**2.0)*(SIN(B(I))**2.0)-1.0))
      R(I)=PI-PRATI
      Q2=PRATI
      QZ=Q1+Q2
      WRITE(3,1900)
      WRITE(3,19)PQ,GE2,XME3,PV,PT,PRATI,PI,R(I)
      IF(I-2)5000,5001,5000
 5001 R(100)=R(I)
 5000 IF(IFIX(R(I)*100.0))180,30,40
  180 P=PRATI
  181 ZFQ=(SQRT((((P-1.0)*(GI+1.0))/(2.0*GI))+1.0))/XMI
      S=ZFQ
      ZZQ=1.0
      DO 182 MXN=2,50,2
      A21=FLOAT(MXN-1)
      A22=FLOAT(MXN)
      A31=FLOAT(MXN+1)
      ZZQ=ZZQ*(A21/A22)
  182 S=S+(ZZQ*((ZFQ**A31)/A31))
      B(I+1)=S
      IF(B(I+1)-BMAX)5600,5600,8000
 5600 IF(B(I+1))8000,6000,6000
   40 IF(XME-XMI)160,170,180
  160 IF(KK-1)183,180,180
  183 KK=KK+1
      P=QZ-PRATI
      GO TO 181
  170 B(I+1)=(BMAX-BMIN)/2.0
      GO TO 6000
   30 IF(B(I)-BMAX)7999,31,8000
 7999 IF(B(I))8000,31,31
 8001 WRITE(3,8002)
 8000 WRITE(3,15)
      GO TO 9000
   31 QZ=((2.0*COS(B(I)))/(SIN(B(I))))*(((XMI**2.0)*(SIN(B(I))**2.0))-1.
     CO)
      QZ1=(2.0+((XMI**2.0)*(GI+COS(2.0*B(I)))))
      PHI(I)=ATAN(QZ/QZ1)
```

```
      ANG=(PHI(I)*180.0)/3.1416
      CALL XMTRE(PHI(I),GE2,I,K,J,XME3)
      BANG=(B(I)*180.0)/3.1416
      WRITE(3,16)ANG,BANG,XME3,GE2,R(I)
 9000 READ(2,1) XEE
      IF(XEE)2050,9500,2050
    1 FORMAT(3F22.10)
    2 FORMAT(10X,'SPEED OF SOUND',/,15X,'AE=',F15.5,/,15X,'AI=',F15.5)
    3 FORMAT(10X,'MACH NUMBERS',/,15X,'XME=',F15.5,/,15X,'XMI=',F15.5)
   18 FORMAT(30X,'VARIOUS VALUES FOR MINIMUM BETA')
 1800 FORMAT(1X,'PHI=',F8.4,8X,'BETA=',F8.4,8X,'PE2/PE1=',F8.4,8X,'GAMMA
     C E2=',F8.4,/,1X,'MACH E3=',F8.4,8X,'PET/PE3=',F8.4,8X,'PET/PE2=',F
     C8.4,/,1X,'PE3/PE1=',F8.4,8X,'PI2/PI1=',F8.4,8X,'PI2/PI1-PE3/PE1=',
     CF8.4)
    7 FORMAT(/////)
    5 FORMAT(1X,'THE ANGLE BETA UNDER THE',1X,I2,1X,  ' ITERATION WAS FO
     CUND TO BE EQUAL TO TO',F7.3,1X,'DEGREES.  THE ANGLE PHI IS',F7.3)
 1900 FORMAT(6X,'PE2/PE1',5X,'GAMMA E2',4X,'MACH E3',5X,'PET/PE3',6X,'PE
     CT/PE2',6X,'PE3/PE1',4X,'PI2/PI1',2X,'PI2/PI1-PE3/PE1')
   19 FORMAT(1X,8F12.4)
 8002 FORMAT(40X,'**********EXIT MACH NUMBER LESS THEN ONE**********',/,
     C40X,'**********OBLIQUE ANGLE BETA CAN NOT EXIST**********')
   15 FORMAT(40X,'**********UNDER THE DEFINED CONDITIONS**********',//,5
     COX,'NO OBLIQUE SOLUTION ANGLE BETA EXISTS')
   16   FORMAT(40X,'----------AN OBLIQUE SOLUTION DOES EXISTS----------',/
     C/,40X,'----------THE FOLLOWING VALUES CORRESPOND TO THIS SOLUTION-
     C---------',//,50X,'ANGLE PHI=',F10.3,/,50X,'ANGLE BETA=',F10.3,/,5
     COX,'EXIT MACH NUMBER=',F10.3,/,50X,'GAMMA E2=',F10.3,/,50X,'THE PR
     CESSURE RATIO PI2/PI1 - PE3/PE1 =',F10.5)
   17 FORMAT(1H1)
 9500 CALL EXIT
      END
// XEQ
```

Program Symbol	Equivalent Engineering Symbol
T	T
GI	γ_i
GE	γ_e
V	u
YMI	m_i
YME	m_e
VR	v_1/v_2
RBAR	$\bar{R}$
GRAV	g_c
AE	a_e
AI	a_i
XME	M_e
XMI	M_i
BMIN	β_{min}
BMAX	β_{max}
GNA	β°
PQ	P_{e2}/P_{e1}
PV	P_{et}/P_{e3}
PT	P_{et}/P_{e2}
PI	P_{i2}/P_{i1}
ZFQ	$\sin^{-1}\beta$
PHI	ν or θ

APPENDIX B

ERROR ANALYSIS

The determination of the wave velocity in the test section is subject to error due to measurements as well as explosive composition. It is therefore, necessary to assess the accuracy of the measurements.

According to Reference 47, the error in a quantity y, where

$$y = F(X_1, X_2, \ldots, X_n) \tag{B-1}$$

can be calculated by the following equation:

$$(\overline{dy})^2 = \sum_{i=1}^{n} \left(\frac{\partial F}{\partial X_i}\right)^2 (\overline{dx_i})^2 \tag{B-2}$$

which will be used below.

B.1 Error in Velocity Measurement from Measurement by Pressure Transducer.

The velocity of the wave is calculated by dividing the distance the wave travels by the measured elapsed time. This may be written as

$$u = \frac{\ell_{35}}{t_{35}} \tag{B-3}$$

where ℓ_{35} is the distance between probe 3 and probe 5 and t_{35} is the time, measured by the Hewlett-Packard timer, it takes the wave to travel from probe 3 to probe 5.

Applying Equation (B-2) to (B-3), one obtains

$$\sqrt{\left(\frac{\overline{du}}{u}\right)^2} = \left(\frac{d\ell_{35}}{\ell_{35}}\right)^2 + \left(\frac{dt_{35}}{t_{35}}\right)^2 \quad . \tag{B-4}$$

The distance between ℓ_{35} can be estimated to within 1/32 in. in ~ 16 in., and t_{35} is measured to an accuracy of 0.1 μsec in ~ 180 μsec. Therefore,

$$\frac{d\ell_{35}}{\ell_{35}} = \frac{.03125}{16} = .0019 \quad \text{and} \quad \frac{dt_{35}}{t_{35}} = \frac{0.1}{180} = .000566$$

which gives

$$\sqrt{\left(\frac{\overline{du}}{u}\right)^2} = 0.2\% \quad . \tag{B-5}$$

B.2 Error Due to Composition

The explosive mixture is prepared by the partial pressure method. The accuracy of the gauge used, combined with the accuracy of reading it is about 0.6 in. of mercury. A total pressure of 120 in. of mercury (absolute) is usually attained during the preparation of each mixture.

The mole fraction of the gas is

$$x = \frac{P_{partial}}{P_{total}} \quad . \tag{B-6}$$

For a 30% Methane - 70% Oxygen mixture, then

$$\left(\frac{dP}{P}\right)_{CH_4} = \frac{0.6}{120 \times .3} = 0.0167$$

and a 50% Hydrogen - 50% Oxygen mixture

$$\left(\frac{dP}{P}\right)_{H_2} = \frac{0.6}{120 \times .5} = 0.01 \quad . \tag{B-8}$$

But,

$$\left(\frac{dP}{P}\right)_{total} = \frac{0.6}{120} = 0.005 \quad . \tag{B-9}$$

So that

$$\sqrt{\left(\frac{\overline{dx}}{x}\right)^2_{CH_4}} = 1.75\% \tag{B-10}$$

and

$$\sqrt{\left(\frac{\overline{dx}}{x}\right)_{H_2}} = 1.12\% \quad . \tag{B-11}$$

Obviously, the small percentage errors determined here are insufficient to explain the data spread. Although care was taken in flushing the detonation tube and the explosive mixture was allowed to flow for several minutes prior to ignition it seems probable that a variation in mixture composition within the test section is the cause of the variation in the measured time intervals.